Sede Amministrativa: Università degli Studi di Padova
Dipartimento di Scienze Biomediche

SCUOLA DI DOTTORATO IN SCIENZE BIOMEDICHE

CICLO XXXII

Channel formation from F-ATP synthase: Role of subunit f

Tesi redatta con il contributo finanziario della Fondazione Cariparo

Coordinatore: Ch.mo Prof. Paolo Bernardi

Supervisore: Ch.mo Prof. Paolo Bernardi

Co-Supervisore: Dr.ssa Valentina Giorgio

Dottoranda: Chiara Galber

December 2019

Table of Content

SUMMARY / SOMMARIO

SUMMARY

The mitochondrial F-ATP synthase is a large multisubunit complex of 600 kDa, organized into a catalytic portion (F_1) and a membranous moiety (F_O) linked by central and peripheral stalks. Besides its established functions of catalyzing ATP production and of promoting *cristae* formation, it has been proposed that this enzyme may be the key constituent of the mitochondrial permeability transition pore (PTP). PTP opening mediates the permeability transition (PT), a Ca^{2+}- and ROS-dependent increase of the inner membrane permeability that may trigger cell death. Our laboratory is investigating how F-ATP synthase could switch from a key enzyme for the aerobic synthesis of ATP into a channel with the potential to trigger cell death.

Our working hypothesis is that the channel forms from F-ATP synthase dimers following Ca^{2+}-binding to the catalytic site and causing conformational changes that are transmitted through the peripheral stalk, to the subunits located within the inner mitochondrial membrane. The subunits involved in pore formation and regulation are still undefined, although current data point to the e, g and f "accessory" subunits.

The goal of my PhD thesis has been to assess the role of subunit f, which is located at the end of the peripheral stalk at the dimer interface. We have defined its role in F-ATP synthase function, mitochondrial morphology, PTP modulation and viability in human cells.

The full knock out of the f protein, achieved through the CRISPR/Cas9 system, showed a severe phenotype, comparable to the one described in yeast or human HAP1 cells. This phenotype included impaired mitochondrial respiration due to a drastic decrease of respiratory chain complexes, as well as of the level of other subunits of the F-ATP synthase enzyme (like the a, c, e and g subunits), resulting in lack of sensitivity to oligomycin. Electrophysiological studies on f-null cells demonstrated that the PTP was no longer present, while currents of lower conductance were observed.

Decreased expression of f subunit, achieved through the RNA interference approach, instead did not affect mitochondrial respiration, respiratory chain

complexes content, or F-ATP synthase subunit stoichiometry. In line with these results, the catalytic activity of the enzyme was maintained, together with its sensitivity to oligomycin. The down regulation of the f subunit expression level, altered *cristae* morphology and decreased the number of *cristae* junctions. A fraction of mitochondria no longer underwent Ca^{2+}-dependent swelling in sucrose media, while swelling in KCl was indistinguishable from that of wild type mitochondria, suggesting that mitochondrial lacking subunit f, but otherwise normal, have smaller pores.

Given the f subunit localization in the F_O domain, our results suggest that the PTP forms at the interface between F-ATP synthase monomers and it involves subunit f.

SOMMARIO

L'enzima F-ATP sintasi è un complesso multi-proteico mitocondriale di 600 kDa, organizzato in due porzioni funzionalmente e strutturalmente distinte: una catalitica (F_1) e una di membrana (F_O). Questi due domini interagiscono tra loro attraverso due "ponti", un ponte è localizzato centralmente e l'altro lateralmente. Oltre alle consolidate funzioni di catalizzare la produzione di ATP e di favorire la formazione di *cristae*, recentemente è stata proposta una terza funzione. Si pensa che questo enzima possa essere anche il componente chiave del poro di transizione della permeabilità (PTP) mitocondriale. L'apertura del PTP, mediata da Ca^{2+} e ROS, causa un aumento della permeabilità della membrana interna e attiva la morte cellulare. Nel nostro laboratorio stiamo cerando di capire come la F-ATP sintasi riesca ad avere questo duplice ruolo, i.e. essere sia un enzima chiave per la sintesi aerobica di ATP, sia un canale in grado di innescare la morte cellulare.

La nostra ipotesi è che la formazione del poro avvenga nella regione di dimerizzazione della F-ATP sintasi in seguito al legame del Ca^{2+} sul sito catalitico dell'enzima. Il legame del Ca^{2+}infatti, induce dei cambiamenti conformazionali che vengono trasmessi, attraverso il "ponte" laterale, alle subunità situate nella membrana mitocondriale interna. Le subunità della F-ATP sintasi direttamente coinvolte nella formazione e nella regolazione del poro però non sono ancora state identificate e, attualmente, l'attenzione è riposta sulle subunità "accessorie" e, g, f.

L'obiettivo della mia tesi di dottorato è stato quello di analizzare il ruolo della subunità f, situata alla fine del "ponte" laterale e sull'interfaccia del dimero, in cellule umane. Abbiamo identificato il suo ruolo nella funzione catalitica della F-ATP sintasi, nella morfologia mitocondriale, nella modulazione del PTP e nella crescita cellulare.

L'eliminazione (knock out) stabile dell'espressione della subunità f, ottenuta attraverso il sistema CRISPR/Cas9, ha mostrato un fenotipo grave, paragonabile a quello già descritto per le cellule di lievito o per cellule umane HAP1. Le cellule knock out erano infatti caratterizzate da una diminuzione (i) della respirazione

mitocondriale, (ii) dei complessi della catena respiratoria e (iii) dei livelli di altre subunità della F-ATP sintasi (come le subunità a, c, e e g) con conseguente insensibilità all'oligomicina. Studi elettrofisiologici su cellule knock out per la subunità f, hanno dimostrato che il PTP non era più presente e solo correnti di bassa conduttanza sono state rilevate.

La diminuzione dell'espressione della subunità f (down regolazione), ottenuta attraverso la tecnica dell'interferenza dell'RNA, non ha invece influenzato la respirazione mitocondriale, il contenuto dei complessi della catena respiratoria o la stechiometria delle diverse subunità della F-ATP sintasi. In linea con questi risultati, l'attività catalitica dell'enzima è rimasta inalterata, come anche la sua sensibilità all'oligomicina. Una diminuzione della quantità della subunità f ha però alterato la morfologia delle *cristae* e, ha causato una diminuzione del numero di giunzioni delle *cristae*. Per quanto riguarda la formazione del PTP, abbiamo osservato che mitocondri con una down regolazione della subunità f, se risospesi in un buffer contenente saccarosio, erano parzialmente resistenti al rigonfiamento della matrice mitocondriale causato dal Ca^{2+}, mentre se risospesi in un buffer contenente KCl, il rigonfiamento era indistinguibile rispetto ai controlli. Questo suggerisce che i mitocondri con una minore quantità di subunità f hanno dei pori più piccoli, che non lasciano passare molecole grandi di saccarosio.

Data la localizzazione della subunità f nel dominio F_O, i nostri risultati suggeriscono che il PTP si forma all'interfaccia tra i monomeri della F-ATP sintasi e coinvolge la subunità f.

List of publications

- Giorgio V., Schiavone M., Galber C., et al. The idebenone metabolite QS10 restores electron transfer in complex I and coenzyme Q defects. Biochim. Biophys. Acta. (BBA) 1859:901-908 (2018).

- Galber C., et al. Purification of Functional F-ATP Synthase from Blue Native PAGE. Methods Mol Biol. 1925:233-243 (2019).

List of Abbreviations

6.8PL: 6.8 kD proteolipid

AA: amino acid

AA: antimycin A

ACS: acyl CoA synthetase

ADP: adenosine diphosphate

Ala: alamethicin

ANT: Adenine nucleotide translocator

ATP: adenosine triphosphate

BAX: BCL-2-associated-X-protein

Bcl2: B-cell lymphoma 2

BN-PAGE: Blue Native-Polyacrylamide Gel Electrophoresis

BSA: bovine serum albumin

Cas9: CRISPR associated protein 9

CJ: *cristae* junctions

CoQ or Q10: ubiquinone

CRC: Calcium Retention Capacity

CRISPR: Clustered Regularly Interspaced Short Palindromic Repeats

CsA: Cyclosporin A

CTR: control

CyPD: Cyclophilin D

Cyt *c*: Cytochrome *c*

Da: Dalton

DAPIT: Diabetes Associated Protein in Insulin sensitive Tissue

DMEM: Dulbecco's Modified Eagle Medium

DPC: Diethyl Pyrocarbonate

ECAR: Extracellular Acidification Rate

EDTA: Ethylene Diamine Tetraacetic Acid

EGTA: Ethylene glyol-bis (β-aminoethyl ether) N,N,N’tetracetic acid

EM: Electron Microscopy

ER: Endoplasmic Reticulum

ETC: Electron Transfer Chain

FAD: Flavin Adenine Dinucleotide

FADH2: Flavin Adenine Dinucleotide (reduced form)

FCCP: Carbonyl cyanide 4-(trifluoromethoxy) phenylhydrazone

GBAS: Glioblastoma Amplified Sequence

gRNA: guide RNA

HAP1: near-haploid human cell line

HEK293T: Human embryonic kidney 293T cell line

HeLa: Henrietta Lacks cells

HKII: Hexokinase II

IDH2: Isocitrate Dehydrogenase 2

IF1: Inhibitor Factor 1

IMM: Inner Mitochondrial Membrane

IMS: Intermembrane Space

KD: knockdown

KO: knockout

LOHN: Leber Hereditary Optic Neuropathy

LS: Leigh Syndrome

MCU: Mitochondrial Ca^{2+} Uniporter

MGO: Methylglyoxal

MICOS: Mitochondrial Contact Site and *Cristae* Organization System

MMC: Mitochondrial Mega Channel

mtCK: Mitochondrial Creatine Kinase

mtDNA: mitochondrial DNA

NAD: Nicotinamide Adenine Dinucleotide

NADH: Nicotinamide Adenine Dinucleotide (reduced form)

NAO: Nonyl Acridine Orange

nDNA: nuclear DNA

OCR: Oxygen Consumption Rate

OGDH: α-ketoglutarate dehydrogenase

Oligo: oligomycin

OMM: Outer Mitochondrial Membrane

OPA: Optic Atrophy Protein

ORF: Open Reading Frame

OSCP: Oligomycin Sensitivity Conferral Protein

OXPHOS: Oxidative Phosphorylation

PBR: Peripheral Benzodiazepine Receptor

PGO: Phenylglyoxal

PhAsO: Phenylarsine Oxide

P_i: Inorganic Phosphate

P_iC: Phosphate Carrier

PKA: Protein Kinase A

PT: Permeability Transition

PTM: Post-Translational Modification

PTP: Permeability Transition Pore

RC: Respiratory Chain

RCC: respiratory chain complexes

ROS: Reactive Oxygen Species

Rot: Rotenone

SCs: supercomplexes

SDH: Succinate Dehydrogenase

SDS: Sodium Dodecyl Sulfate

SDS-PAGE: Sodium Dodecyl Sulfate-Polyacrylamide Gel Electrophoresis

shRNA: short hairpin RNA

SIRT3: Sirtuin3

SPG7: Spastic Paraplegia 7 protein

TEM: Transmission Electron Microscopy

TSPO: Translocator protein

VDAC: Voltage-Dependent Anion Channel

ρ0: rho zero cells

List of Figures

1 *INTRODUCTION*

1.1 Mitochondria

Mitochondria are intracellular organelles present in the cytoplasm of almost all eukaryotic cells where they are essential for cell survival. They are denominated as "the powerhouse of the cell" because their primary function is to support respiration and to provide high-energy substrates (such as ATP) for intracellular metabolic pathways (Figure 1). This is possible through oxidative phosphorylation, the process that couples respiration to ATP synthesis. Beyond their crucial role in cellular bioenergetics, mitochondria are involved in other important functions. For example, they are key players in signalling, particularly in programmed cell death (apoptosis), calcium homeostasis, thermogenesis, immunity, and they are involved also in cell cycle control and cell growth (McBride, Neuspiel & Wasiak, 2006, Tait, Green, 2012). Furthermore, several metabolic pathways take place within mitochondria, including pyruvate decarboxylation, Krebs cycle, fatty acid β-oxidation, amino acid oxidation, lipid and cholesterol synthesis, oxidative phosphorylation and ATP production (Spinelli, Haigis, 2018) (Figure 1).

Considering the multiple fundamental roles in cell homeostasis, mitochondrial dysfunction may give rise to a wide set of defects in all tissues (Nunnari, Suomalainen, 2012). Mitochondrial respiratory chain dysfunction has been reported after both genetic and acquired mutations, and can be a key player in a variety of different conditions, such as aging (Balaban, Nemoto & Finkel, 2005), cancer (Chandra, Singh, 2011), diabetes (Szendroedi, Phielix & Roden, 2011), and degenerative disorders including muscular dystrophies (Zulian et al., 2016), Parkinson's disease (Winklhofer, Haass, 2010), and Alzheimer's disease (Hauptmann et al., 2009).

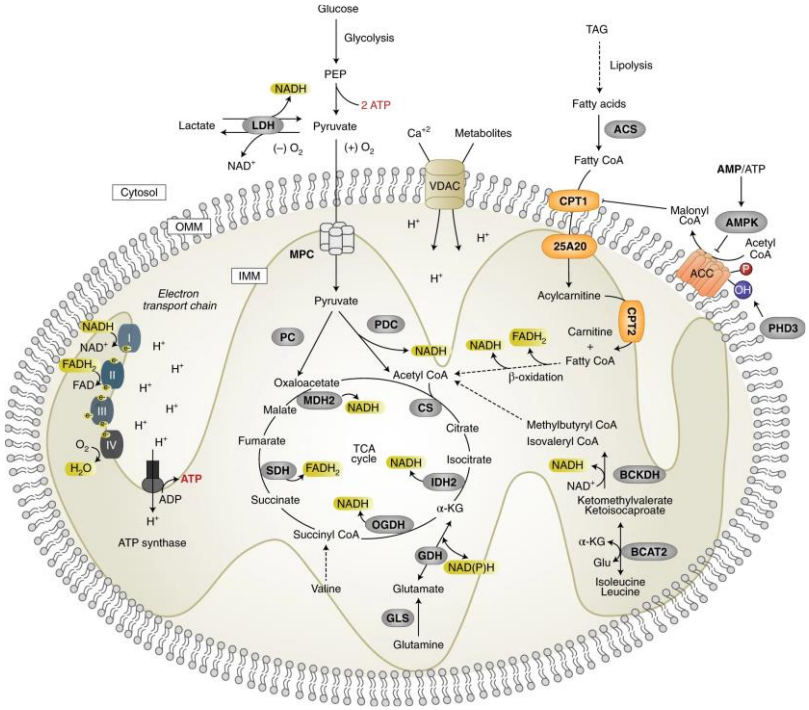

Figure 1. Mitochondria are the powerhouse of the cell. Different metabolic pathways localize within mitochondria. Inside this organelle, pyruvate (derived from glucose or lactate), fatty acids and amino acids are oxidized to harness electrons onto the two NADH and $FADH_2$ carriers. NADH and $FADH_2$ transport electrons to the electron transport chain, leading to ATP production through oxidative phosphorylation. VDAC, voltage-dependent anion channel; IDH2, isocitrate dehydrogenase 2; OGDH, α-ketoglutarate dehydrogenase; SDH, succinate dehydrogenase; BCAT2, branched-chain amino transferase 2; ACS, acyl CoA synthetase. Electrons and reducing equivalents are shown in yellow. From (Spinelli, Haigis, 2018).

1.1.1 Mitochondrial structure and dynamics

Mitochondria have a cylindrical shape and a diameter between 0.5 and 5 μm, but they can vary considerably in size and structure. According to the endosymbiotic theory, mitochondria evolved from a bacterial progenitor that survived endocytosis from an eukaryotic host cell, and then became permanently incorporated into the cytoplasm (Sagan, 1967, Gray, 2012). Bacteria were maintained because of an evolutionary advantage, since they could provide to cells the ability to use oxygen; ATP production through oxidative phosphorylation indeed is much more efficient than glycolysis. The result was the establishment of a relationship of interdependence during evolution. Mitochondria share with bacteria many other features: the presence of cardiolipin molecules and the absence of cholesterol in the inner mitochondrial membrane, as well as the

presence of their own ribosomes, which are similar to bacterial ones both in size and structure (O'Brien, 2003). A peculiar feature of these organelles is the presence of a double lipid membrane (other organelles have just one membrane) that creates four different compartments, each carrying out specialized functions (Figure 2). The outer membrane (OMM) is permeable to small molecules (molecular weight < 5.000 daltons) and ions, which freely move through non-selective transmembrane channels formed by porins (a family of integral membrane proteins). The OMM represents also the site of interaction with other cellular components such as endoplasmic reticulum, ribosomes, nucleus and cytoskeleton filaments.

The inner membrane (IMM) instead is impermeable to most small molecules and ions including H^+, although highly specific transporters allow selected species to cross this membrane. The inner membrane is folded into *cristae*, where the components of the respiratory chain as well as F_1F_O-ATP synthase (F-ATP synthase) are located. This structural organization expands the surface area, thus enhancing the ability to produce ATP. *Cristae* have a remarkably variable structure depending on the cell type and the physiological conditions of the cell (Pernas, Scorrano, 2016); for example, cells with a high ATP requirement, such as muscle cells, have mitochondria with a larger amount of *cristae* compared to other cells. The two membranes are separated by an intermembrane space (IMS), while the IMM delimits the mitochondrial matrix that contains the mitochondrial DNA, and the enzymes required for all the metabolic processes occurring inside the mitochondrion (e.g. Krebs cycle and β-oxidation enzymes).

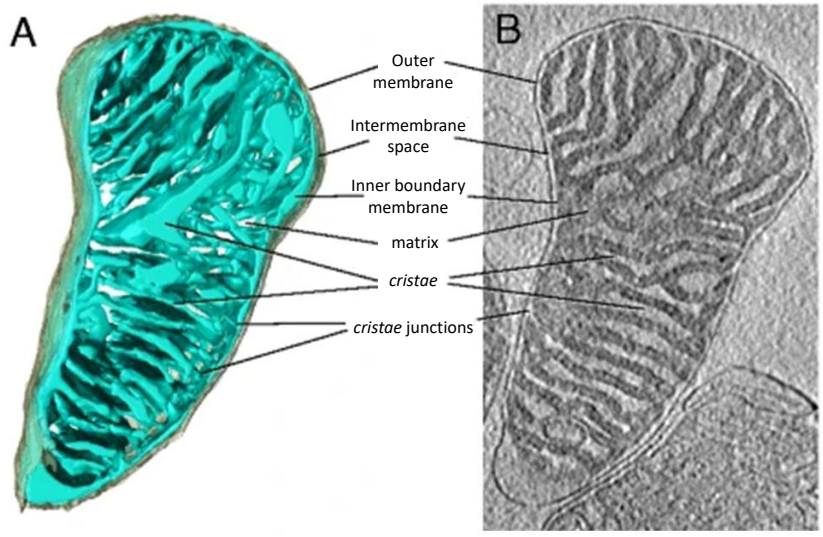

Figure 2. Structure of a mouse heart mitochondrion. (A) Three-dimensional volume of a mouse heart mitochondrion determined by cryo-ET. The outer membrane (grey) envelops the inner membrane (light blue) which is folded into cristae. (B) Tomographic slice through the map volume. From (Kuhlbrandt, 2015).

As already mentioned, mitochondria are highly dynamic cellular components, constantly changing their size, shape and position in response to various external stimuli as well as to physiological processes (Pernas, Scorrano, 2016). Moreover, within a cell the number of organelles is extremely variable; it changes according to the organ, tissue or cell type. Many of these changes are correlated to the ability of mitochondria to undergo a highly coordinated process of fission (division of a single organelle into two or more independent structures) or fusion (the opposing reaction). Both are active (i.e. energy-requiring) processes, they require specialized proteins that physically modify the mitochondrial membranes, and adaptor proteins that regulate the interaction of these proteins with organelles (Scott, Youle, 2010). Since mitochondria are semi-autonomous and can divide independently from cell cycle by binary fission, their number can display a large variation during cell life. The balance between the two processes of fission and fusion regulates the overall morphology of mitochondria within any given cell. When the energy needs are high, they can grow and divide, while when the energy used is low, they are destroyed or they become inactive.

Another important feature that differentiates mitochondria from other organelles, is that they possess their own genome, the mitochondrial DNA (mtDNA), consisting of a double-stranded DNA molecule present in several copies in each mitochondrion. The mitochondrial genome varies significantly in its molecular

architecture among different species. Two main molecular architectures have been identified for the mtDNA: the most known and abundant is the circular form while the other, less characterized, is linear. These linear molecules were found in mitochondria from a variety of organisms including fungi, apicomplexan parasites and plants (Nosek, Tomaska, 2003).

The mitochondrial genome size is approximately 16 Kb long and was successfully sequenced in the 1980s (Anderson et al., 1981). The human mitochondrial genome (Figure 3) is composed of two chains, the light and the heavy chains. The genes are 37, 28 encoded by the heavy and 9 by the light strand. Thirteen genes encode polypeptides that are synthesized on mitochondrial ribosomes and are all subunits of the respiratory chain. The remaining 24 genes encode 22 tRNAs and 2 rRNAs necessary for protein synthesis. All the other ~1200 proteins present in the organelle are encoded by nuclear DNA (nDNA), synthesized in the cytosol and then actively imported through specific membrane transporters into the mitochondrion (Anderson et al., 1981, Milenkovic et al., 2007, Calvo, Clauser & Mootha, 2016). Therefore, the mitochondrial proteome must be finely and dynamically regulated between the two different genomes and an adequate crosstalk is required to get a final functional mitochondrion (Garesse, Vallejo, 2001).

Mitochondrial genome has fewer genes compared to that of the ancestor bacteria, as some genes were lost during evolution, while others were transferred to the nucleus, such as those encoding for the subunits of Complex II of the respiratory chain (Chan, 2006). Like that of bacteria, the genome of mitochondria is extremely compact, contains overlapping genes, does not have histones and with very few exceptions does not have introns too (Anderson et al., 1981). These group II introns were described in yeast, algae and plants and their splicing reaction is assisted by proteins either encoded by the introns themselves, or encoded by other genes of the host organisms (Luban et al., 2005, Lehmann, Schmidt, 2003).

Although mitochondria of many eukaryotes, including most plants, use the standard genetic code, mammalian mitochondria use an alternative code (Barrell, Bankier & Drouin, 1979).

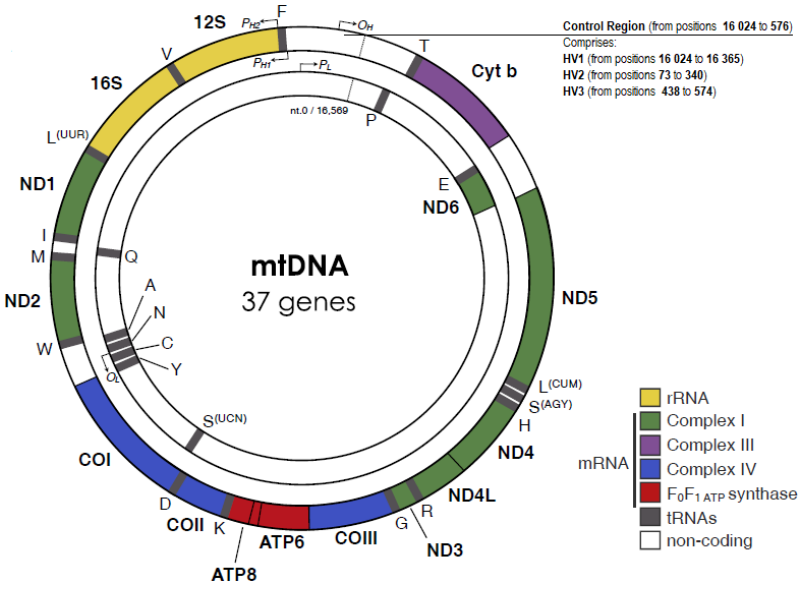

Figure 3. Map of a human mitochondrial DNA. The human mitochondrial DNA genome contains proteins, ribosomal RNA, and transfer RNA genes. The genes that encode the subunits of complex I (ND1–ND6 and ND4L) are shown in green; cytochrome c oxidase (COI–COIII) are shown in blue; cytochrome b of complex III is shown in purple; and the subunits of the F-ATP synthase (ATP6 and 8) are shown in red. The two ribosomal RNAs (rRNAs; 12S and 16S) are shown in yellow and 22 tRNAs are shown by black lines and denoted by their single letter code. From (Amorim, Fernandes & Taveira, 2019).

1.1.2 Mitochondrial diseases

Mitochondrial diseases represent a highly heterogeneous group of disorders characterized by an impairment of mitochondrial function, and particularly a dysfunction of the mitochondrial respiratory chain (DiMauro, 2004). When this occurs, less ATP can be produced within the cell, and consequences range from cell injury to cell death. The mitochondrial respiratory chain is the final pathway for aerobic metabolism, and this means that tissues and organs that are highly dependent on aerobic metabolism are those preferentially involved in these disorders.

The mitochondrial respiratory chain is under a dual genetic control. It is therefore possible to distinguish respiratory chain defects caused by mtDNA mutations, that show maternal inheritance, and by nuclear DNA (nDNA) mutations, which are inherited as Mendelian disorders. Mitochondrial genetics differs from the classical Mendelian genetics for three different aspects: maternal inheritance, heteroplasmy and mitotic segregation (DiMauro, 2004, Amorim, Fernandes & Taveira, 2019).

Maternal inheritance

All mitochondria and thereby all mtDNA of the zygote derive from the egg. Therefore, because of this uniparental inheritance, a mother carrying a mtDNA mutation may transmit it to her sons and daughters, but only her daughters will transmit the same mutation to their progeny.

Heteroplasmy and threshold effect

In each cell, there are multiple mtDNA molecules (on average 103-104 copies), which at cell division distribute randomly among daughter cells. In normal tissues, all mtDNA molecules show the same sequence (homoplasmy), while when pathogenic mutations occur, they can affect only a proportion of the mtDNAs molecules within a cell or tissue. The coexistence of this mixed population of normal and mutant genomes is known as heteroplasmy. As a result, the biochemical and/or clinical phenotype can occur only once a threshold of mutated genomes is reached. This threshold is not fixed, but rather can vary in different tissues, according to the type of mutation and to the relative dependence of each organ on oxidative metabolism. Usually, this value is 70% but it can be lower, for example in those tissues (nervous system, cardiac tissue, skeletal muscle) that highly depend on oxidative metabolism and have high energetic requirements. This is why mitochondrial diseases can appear at any time during development, or just in some tissues of the body and not in others, only when and where the threshold of mutated mitochondria is reached.

Mitotic segregation

During cell division, mitochondria segregate randomly between the two daughter cells. Consequently, the proportion of mutant mtDNA in cells can change in subsequent generations and the phenotype may change accordingly. This phenomenon is called mitotic segregation and may explain the highly variable clinical course of a disease during the patient's life. In fact, over time, the mutated mtDNAs can either surpass or fall below the pathogenetic threshold (Lightowlers et al., 1997).

Mammalian mtDNA accumulates mutations more frequently than nDNA. Two explanations of this phenomenon are (i) less efficient DNA repair mechanisms,

and (ii) the fact that mtDNA is not coated by protective histones. The mtDNA is close to the respiratory chain, where it is exposed to high levels of oxygen free radicals that can damage mtDNA molecules and therefore cause mutations.

As already mentioned, mitochondrial diseases can be due to mutations in the mtDNA or nDNA. Mutations in mtDNA can be divided in two main groups: those that impair mitochondrial synthesis *in toto* (e.g. affecting tRNA or rRNA genes) and those impairing protein-coding genes (e.g. affecting one of the 13 respiratory chain subunits). Mutations in nDNA are more frequent because they can affect not only the synthesis of respiratory chain subunits, but also all the steps required for the correct assembly and functioning of respiratory chain complexes. There can be mutations in genes encoding subunits or assembly factors, genes required for mtDNA maintenance and replication, genes required for proteins import into mitochondria or for the synthesis of mitochondrial membrane phospholipids.

Although mitochondrial disorders can be so variable and affect different organs and tissues, some symptoms are quite common. These include muscle weakness and cramps, visual problems, learning disabilities, neurological problems, heart diseases and gastro-intestinal disorders (DiMauro, 2004).

1.1.3 Mitochondrial oxidative phosphorylation

Mitochondria are the site where energy is conserved and where most of cellular ATP synthesis takes place. The mammalian system of oxidative phosphorylation is based on electron transport from a set of electron donors to electron acceptors.

Electrons derive from oxidation of different carbon sources introduced with food, i.e. sugars, fats, and amino acids, and their final acceptor is molecular oxygen, which is then reduced to form water. In 1948, Eugene Kennedy and Albert Lehninger discovered that mitochondria are the site of oxidative phosphorylation in eukaryotes. Since then, a series of studies lead to the identification of the electron carriers of the mitochondrial respiratory chain (also called electron transfer chain, ETC). These carriers are organized into four membrane-embedded complexes (I to IV, Figure 4) and two lipid-diffusible electron transporters, cytochrome *c* (cyt *c*) and ubiquinone (coenzyme Q10 or CoQ). These enzymatic complexes couple NADH and $FADH_2$ oxidation and electron transfer to proton transport across the inner mitochondrial membrane. F-ATP synthase (complex V)

then uses the resulting electrochemical potential to synthesize ATP (Adenosine triphosphate) from ADP and phosphate.

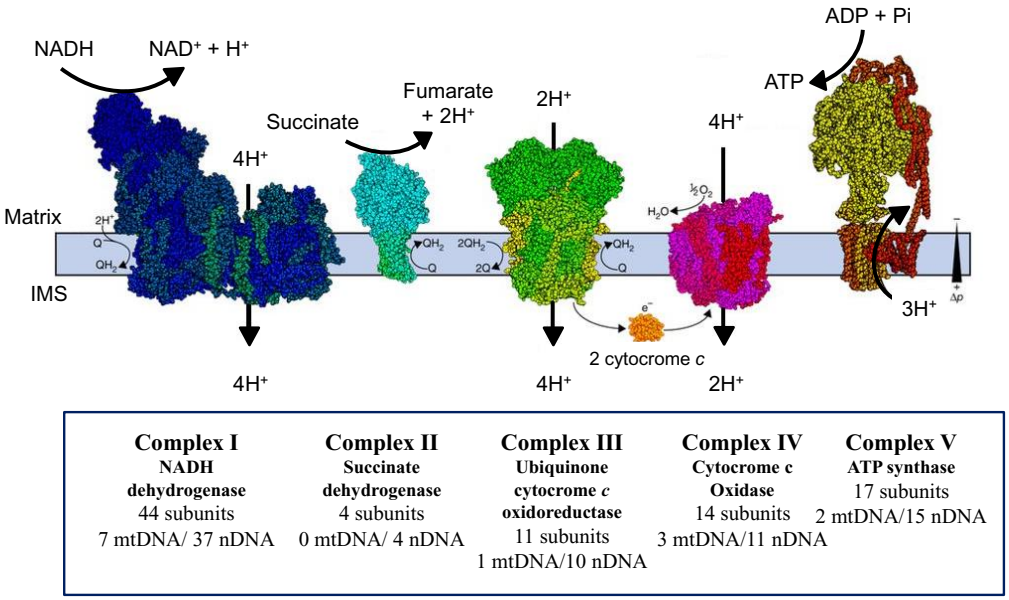

Figure4. Schematic representation of the mammalian OXPHOS system composed of complex I-IV and the F-ATP synthase (complex V). The structural models of the mammalian mitochondrial OXPHOS complexes are shown. Electrons transfer from reduced cofactors (NADH or FADH2) to oxygen, finally yielding water, is marked with black curved arrows. Electron flow is accompanied by H^+ pumping from matrix to the IMS at the level of complex I-III and IV (marked with black straight arrows), producing both a chemical and an electrical gradient across the IMM. This electrochemical gradient ($\Delta\mu H$) is then used to produce ATP via the reentering of protons into the matrix through the F_O domain of the F-ATP synthase enzyme. For each complex the subunit composition is presented. Adapted from (Letts, Sazanov, 2017).

Briefly, (Figure 5) complex I and complex II catalyse electron transfer to ubiquinone from two different electrons donors: NADH and succinate, respectively. Complex III transports electrons from reduced ubiquinone to cytochrome *c*, and complex IV completes the process by transferring electrons from cytochrome *c* to molecular oxygen.

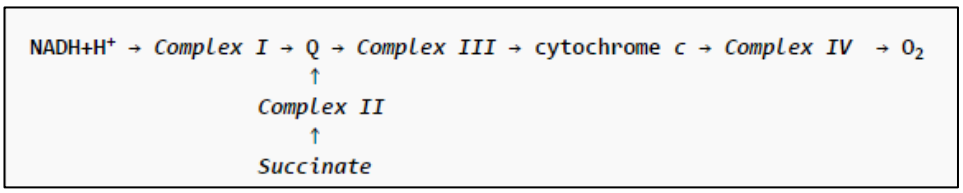

Figure 5. Summary of the electron flux in the mitochondrial respiratory chain. Electrons coming from the two reducing equivalents NADH (Complex I) and $FADH_2$ (complex II), flow to CoQ and subsequently to complex III, cyt *c*, and complex IV, which passes them to oxygen as final acceptor.

1. Complex I: NADH dehydrogenase. It is a large enzyme with an L-shape, in which the long arm is integrated into the membrane and the short arm is extended into the matrix surface. These complex catalyses two coupled processes: the exergonic transfer of electrons from the Krebs Cycle electron carrier NADH to the ubiquinone carrier, and the endergonic transfer of four protons from the matrix (i) to the intermembrane space (o).
   Rx: $NADH + 5H^+i + Q \rightarrow NAD+ + QH_2 + 4H^+o$
2. Complex II: succinate dehydrogenase-ubiquinone oxidoreductase. This is the simplest complex which is also part of the Krebs cycle; electrons originated from the oxidation of succinate to fumarate, are delivered through this complex and through $FADH_2$ to ubiquinone. It is a parallel electron transport pathway to complex I, but during the process no protons are pumped in the intermembrane space, therefore it does not contribute to generation of the proton-motive force. Complex II is also peculiar because it does not assemble into higher structures like the other complexes do, as I will discuss below.
   Rx: succinate + $Q \rightarrow$ fumarate + QH_2
3. Complex III: ubiquinone cytochrome *c* oxidoreductase or cytochrome bc_1 complex. Similarly to complex I, the oxidation of a substrate (QH_2) and the transfer of electrons to a mobile carrier (cytochrome *c*) is coupled to the transport of protons across the inner mitochondrial membrane. Once cytochrome *c* is reduced, it moves towards complex IV and here it donates its electrons.
   Rx: QH_2+ 2 cyt c (oxidised) + $2H^+_i \rightarrow Q$ + 2 cyt c (reduced) + $4H^+_o$
4. Complex IV: cytochrome *c* oxidase. This is the final step of the respiratory chain, in which two different events occur. First, four electrons are removed from four molecules of cytochrome *c* and then used to convert/reduce molecular oxygen into water. Second, eight protons are removed from the matrix, but just four of them translocate across the inner mitochondrial membrane, while the others are used for oxygen reduction (4 H^+ are consumed, while 4 H^+ are used to create the electrochemical gradient).
   Rx: 4 cyt *c* (reduced) + $8H^+_i + O_2 \rightarrow$ 4 cyt *c* (oxidised) + $4H^+_o$ + 2 H_2O

The free energy resulting from these redox reactions is used to pump protons out of the matrix, creating the so-called proton-motive force, which is composed by the chemical potential (difference in H^+ concentration, ΔpH) and the electrical potential (difference in charge distribution across the inner mitochondrial membrane, negative inside). The chemiosmotic model, proposed by Peter Mitchell, explains the mechanism that couples electron transport with oxidative phosphorylation. According to this model, the engine that drives the synthesis of ATP is the protonmotive force: when protons flow back into the matrix through the proton channel of the F-ATP synthase, they allow ATP production from ADP and Pi (Mitchell, 1961). This process is known as oxidative phosphorylation (OXPHOS). Since the inner mitochondrial membrane is largely impermeable to ions, protons preferentially pass through this proton channel down their electrochemical gradient. Since the F-ATP synthase is one of the main topics of my Thesis, I will describe its structure and properties in more detail in chapter 1.2.
Rx: $ADP + P_i + nH^+_o \rightarrow ATP + H_2O + nH^+_i$

The complexes of the respiratory chain are composed by more than 80 protein subunits, but only 13 are encoded by mtDNA: 7 subunits of complex I, 1 of complex III, 3 of complex IV and 2 of complex V. Complex II is the only one that has no mtDNA-encoded subunits, like cytochrome *c* and all the enzymes required for coenzyme Q biosynthesis (Figure 4) (DiMauro, 2004).
The nuclear genome encodes for all the remaining subunits of the respiratory chain complexes, as well as for all the proteins necessary for the synthesis of prosthetic groups, the transport and inclusion of metal cofactors on protein subunits, and for the correct assembly of the respiratory complexes.

1.1.3.1 Supercomplex organization

Mitochondria are important organelles not only as ATP generators but also in controlling and regulating many cellular functions. This regulation occurs through: (i) long-term responses at the level of expression, transcription and translation (ii) short-term posttranscriptional responses and (iii) regulation of the supra-organization of the respiratory chain complexes (RCC) in the IMM. Two different models have been proposed to explain the arrangement of the RCC

within the inner mitochondrial membrane (Figure 6). According to the fluid model (Figure 6A) proposed by Hackenbrock and co-workers (Hackenbrock, Chazotte & Gupte, 1986), all the components can diffuse randomly in the membrane; they exist as independent entities, with Coenzyme Q and cytochrome *c* acting as mobile electrons carriers that freely diffuse in the lipid membrane.

In the plasticity model (Figure 6B), RCC exist in a dynamic equilibrium: they can either be individual entities (like complex II or V) or form regulated complexes with variable copy number and stoichiometry (like complex I, III and IV). With the latter arrangement, the substrate is channelled directly from one enzyme to the next (Lobo-Jarne, Ugalde, 2018).

The first evidence supporting the plasticity model was the BN-PAGE isolation of supercomplexes (SCs) in bovine heart and yeast mitochondria (Acin-Perez et al., 2008, Schagger, Pfeiffer, 2000). However, their existence was initially questioned and respiratory chain SCs have been considered to be BN-PAGE- and detergent-induced artefacts. Indeed, the comigration of complexes depends on the type and amount of detergent used to solubilize the mitochondrial membranes. Nevertheless, now the plasticity model has been validated by other findings, i.e. the observation that SCs cannot form when one of their component complexes is absent (Acin-Perez et al., 2008), the high resolution cryo-electron microscopy (Cryo-EM) analysis showing the detailed structural architecture of mammalian SCs (Letts, Fiedorczuk & Sazanov, 2016), and studies done in lymphocytes from patients with Barth syndrome, a mitochondrial disorder in which cardiolipin levels are drastically reduced. These studies reveal a destabilization of SCs with matching mitochondrial dysfunction (McKenzie et al., 2006). Moreover, SCs formation, stabilization and function is not only influenced by the lipid composition of the IMM, but also by *cristae* morphology. Indeed genetic manipulation of *cristae* structure (for example ablation of OPA1, which is the master *cristae* shape regulator) affects assembly and activity of SCs *in vitro* and *in vivo*, and reveals a role in mitochondrial respiratory efficiency (Cogliati et al., 2013).

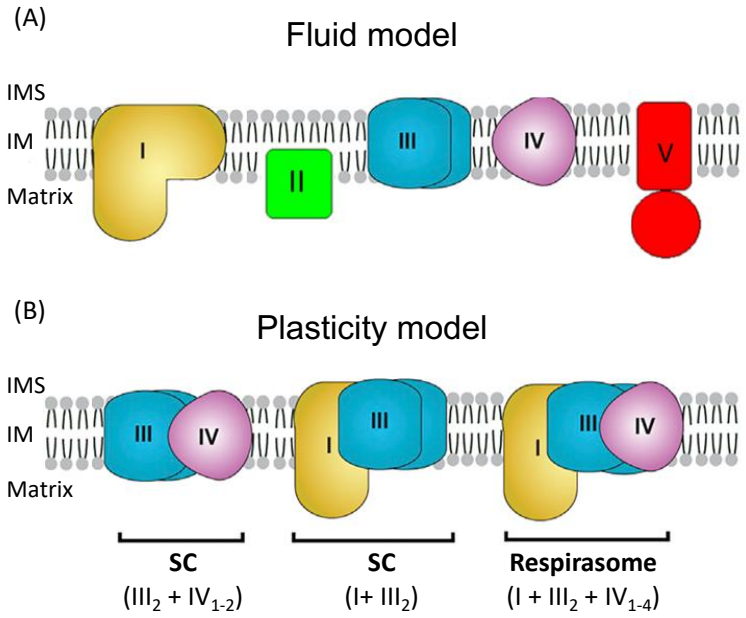

Figure 6. Schematic representation of the two models explaining complexes organization within the inner mitochondrial membrane. (A) The classical fluid and (B) plasticity models for the organization of the OXPHOS system. In (B) the mitochondrial respirosome ($I + III_2 + IV_{1-4}$) and the two supercomplexes ($III_2 + IV_{1-2}$ and $I + III_2$) are shown as a cartoon, with representative stoichiometry and nomenclature. Adapted from (Milenkovic et al., 2017).

Three different SCs have been reported (Figure 6B). The most abundant and stable supercomplex contains Complex I/III, while other SCs contain Complex III/IV, or I/III/IV. The last one is considered a "respirasome", as it contains the components required to transfer electrons from NADH to molecular oxygen, and is able to perform this function *in vitro* (Acin-Perez et al., 2008). This can occur because complexes are arranged into a functional structure within the inner membrane. The functional role of SCs is still not well known, but the organization in supercomplexes, may be required to stabilize individual complexes. Indeed, Complex I needs the interaction with the other complexes for its stability and correct functioning. For instance, loss of function of Complex III abolishes respirasome formation, and causes a secondary Complex I defect (Schagger et al., 2004, Acin-Perez et al., 2004).

Importantly, SCs appear to provide a kinetic advantage, by maximizing electron flow through the respiratory chain, thus increasing metabolic efficiency (Schagger, Pfeiffer, 2000, Greggio et al., 2017) while minimizing damage by oxygen radicals (Maranzana et al., 2013).

1.2 The F-ATP synthase

The F-ATP synthase is a complex molecular machine found in membranes of mitochondria, eubacteria and chloroplasts. It uses the proton electrochemical gradient to drive the synthesis of ATP from ADP and phosphate by a rotary mechanism that will be explained in a paragraph below. The F-ATP synthase is a close relative of V-ATPases (vacuolar ATPases) that use ATP hydrolysis to generate proton gradients across membranes, and of the A-ATPases (archeal ATPases) that synthesize ATP in archea (Walker, 2013). Its molecular structure and catalytic mechanism were understood thanks to the coordinate work of many Scientists, among which three stand out: Sir Peter Mitchell, who conceived the chemiosmotic theory and proposed that the proton motive force is the driving energy for ATP production (Mitchell, 1979); Sir John E. Walker, who resolved the structure of the catalytic part of mammalian F-ATP synthase (Abrahams et al., 1994); and Paul Boyer, who proposed and elucidated the three-step mechanism of rotational catalysis (Boyer, 1993).

Here, the focus will be on the mitochondrial F-ATP synthase, highlighting its central role in producing ATP, as well as its potential role in directly forming a high-conductance channel, as proposed by our laboratory (Giorgio et al., 2013, Urbani et al., 2019).

1.2.1 Mitochondrial F-ATP synthase structure

The overall structure of F-ATP synthases is highly conserved among species, as summarized in figure 7. I will present the structure of the bovine mitochondrial F-ATP synthase underlining relevant differences with other species.

The mitochondrial enzyme is a large multisubunit complex of 600 kDa localized in the IMM and composed of about 30 subunits. It is organized into a catalytic portion (F_1) where the ATP is formed from ADP + P_i, and a membrane moiety (F_O) through which protons flow. These sectors are linked by central and peripheral stalks (Figure 7, model on the left). The full assembly process is complex and still under investigation, since subunits are encoded by both nuclear and mitochondrial genes. The mtDNA-encoded subunits are subunits a, A6L and c (named also subunits 6, 8, 9 respectively) for the yeast complex, and only subunits a and A6L for the mammalian enzyme.

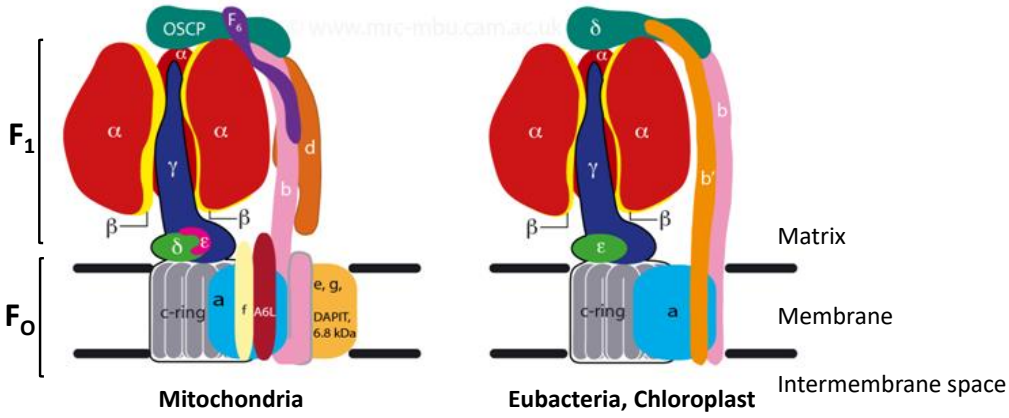

Figure 7. Structure and protein subunit organization in F-ATP synthases. The mitochondrial, bacterial, and chloroplast ATP synthases are shown. The upper part of each model contains the subunits of the F_1 catalytic domain: the two catalytic subunits α and β, and the three central stalk subunits, γ, δ and ε for the mitochondrial enzyme, γ and ε for the other two models. The γ subunit is in contact with the lower part of the enzyme: the F_O domain. This domain contains the c-ring and the a subunit, plus a number of subunits with transmembrane α-helices embedded in the mitochondrial membrane. These supernumerary subunits are: subunits e, f, g, A6L, DAPIT and 6.8PL. The peripheral stalk instead is on the right of each model. In the bacterial and chloroplast enzyme it consists of δ subunit, and two b subunits (or single copies of homologous subunits b and b'), while in the mitochondrial enzyme it contains single copies of subunits OSCP, b, d and F_6 (adapted from (Walker, 2013)**.**

- The **F_1 domain** is the membrane-extrinsic sector containing the catalytic region. It consists of a globular assembly of five subunits (α, β, γ, δ and ε) with the stoichiometry 3:3:1:1:1 respectively (Walker et al., 1985) and with a combined molecular mass of about 370 kDa.

  The three α and three β subunits form an orange-shape structure, and alternate around the coiled-coil structure of the γ subunit. The γ subunit occupies the central axis of this sector, but it also protrudes beyond the $\alpha_3\beta_3$-subcomplex forming, together with the δ and ε subunits, a "foot" that anchors the soluble region to the hydrophobic domain of the enzyme (Walker 2013). This foot interacts with a ring of c subunits located in the IMM. All together, the γ, δ and ε subunits form the so-called central stalk (Gibbons et al., 2000). The ε subunit is reported to be essential for oxidative phosphorylation, indeed its down-regulation leads to lethal uncoupling of mitochondria and loss of stability of F-ATP synthase (Tetaud et al., 2014).
- The **Fo domain** is the membrane-intrinsic sector, the site of proton flow across the IMM, and "O" is meant to denote its interaction with the specific

inhibitor oligomycin. This is the region that during evolution has undergone the highest variations in its subunits composition. The mitochondrial enzyme consists of a single subunit a (also called ATP6) and a number of c subunits, this number varies across species, i.e. 10 copies in yeast or 8 copies in vertebrates. The c subunits form a ring structure within the IMM, the ring is connected to F_1 by the central stalk, and peripherally to the a subunit. At the c ring-a subunit interface two semichannels are formed through which the H^+ flow by protonation/deprotonation of conserved carboxylic residues present in each c subunit (Guo, Bueler & Rubinstein, 2017, Pogoryelov et al., 2009, Symersky et al., 2012). Subunit a also associates with other two regions of the F_O domain: the membrane-embedded part and the peripheral stalk. The first one consists of single copies of "accessory" subunits named A6L (or ATP8), e, g, and f (Collinson et al., 1994), and of two or three additional supernumerary subunits: DAPIT (diabetes associated protein in insulin sensitive tissue) and 6.8 PL (6.8 kD proteolipid) in vertebrates (Chen et al., 2007); i/j, k, and l in yeast (Guo, Bueler & Rubinstein, 2017). Subunits j and k are considered the orthologs of 6.8PL and DAPIT, respectively, and subunit l is closely related to subunit k (He et al., 2018). The peripheral stalk is composed by one copy of subunits b, d, F6, and oligomycin sensitivity conferral protein (OSCP), the latter being located on top of F_1. More recently, also the N-terminal domain of subunit A6L (Lee et al., 2015) has been found at the base of the peripheral stalk.

In yeast the C-terminal domain of subunit A6L, the N-terminal domain of subunit f (Guo, Bueler & Rubinstein, 2017) and subunit i/j (Srivastava et al., 2018) have been identified as component of the peripheral stalk.

The subunit a, the peripheral stalk, and the associated supernumerary subunits constitute the enzyme's "stator", against which the rotor, made of the c ring and the central stalk, turns. Proton flow at the c ring-a interface releases energy allowing the clockwise rotation of the rotor (as viewed from the matrix) during ATP synthesis.

The subunit composition of **bacterial** (Guo, Suzuki & Rubinstein, 2019) **and chloroplast** (Hahn et al., 2018) ATP synthases is simpler than that of

mitochondria, and the complexes are monomeric (Figure 7, model on the right). The F_1 catalytic domain is highly conserved, it consists of the $\alpha_3\beta_3$ subcomplex plus the central stalk made of single copies of subunits γ and ε (Walker, 2013). The bacterial or chloroplast ε subunit is the ortholog of the mitochondrial δ subunit, while the bacterial δ subunit is the orthologue of the mitochondrial OSCP (Walker et al., 1982). The ε subunit is known to be a catalytic regulator of the F-ATP synthase, and to be essential for oxidative phosphorylation (Watanabe et al., 2018, Cingolani, Duncan, 2011, Hara et al., 2001).

Together with the δ subunit, the bacterial peripheral stalk contains also two b subunits (or single copies of homologous subunits b and b'). Mitochondrial and bacterial peripheral stalk subunits display no sequence conservation, even though the overall structure is similar. Other differences between the two variants involve (i) the number of c subunits (8 in mammals and variable between 9 and 17 in bacteria) and (ii) the absence/presence of the supernumerary subunits in the F_O domain as in bacteria or mammals, respectively.

1.2.1.1 Subunit f

The presence of this subunit was originally demonstrated in the bovine enzyme (Collinson et al., 1994) and subsequently also found in the enzyme from *Saccharomyces cerevisiae* (Spannagel et al., 1997).

In the **bovine** enzyme the protein is oriented with the N-terminal region exposed to the matrix side, and the highly hydrophobic C-terminus in the intermembrane space suggesting that the protein spans the membrane with an α-helix once only (Belogrudov, Tomich & Hatefi, 1996, Lee et al., 2015). Furthermore, it does not have functional domains homologous to other known proteins that could provide information about its function. Crosslinking studies showed a close proximity of subunit f and A6L (Belogrudov, Tomich & Hatefi, 1996), and later on that subunits f cross links with subunit e, 6.8PL and g (Belogrudov, Tomich & Hatefi, 1996, Lee et al., 2015).

Since its discovery, the physiological role of the f subunit has been studied much more extensively in yeast than in mammals.

In **yeast** the protein has the same orientation as the bovine species (Velours et al., 1998, Guo, Bueler & Rubinstein, 2017, Stephens, Nagley & Devenish, 2003), and the predicted secondary structures of the two proteins are similar but not identical, as well as their amino acid sequence (34% of identity). At variance from subunits e and g, the f subunit is required for the formation of an enzymatically active complex. Indeed, *ATP17*-deleted yeast strains are respiration-deficient, they are unable to grow by oxidative phosphorylation, and show no oligomycin-sensitive ATPase activity, although the F_1 sector displays high levels of ATPase activity. This is a nuclear recessive mutation, indeed if the disrupted strain is mated with a ρ_0 strain, the diploids recover the ability to grow on a glycerol medium (Spannagel et al., 1997). Furthermore, complementation is also possible using a shorter version of subunit f devoid of the last 28 amino acid (AA) residues, i.e. of the transmembrane domain. However, in this case, (i) there is a two-fold decrease in the ATP synthase activity and (ii) a decrease in the stability of the complex even if the N-terminal domain is still able to tightly interact with the other components of the F_O sector (Roudeau et al., 1999).

Immunoprecipitation of the yeast F-ATP-synthase enzyme from the null mutant strain reveals that the f protein is also important for the assembly of the full enzyme: the f-null complex lacks subunits 6 and 8 (homologs of subunit a and A6L), and it contains a decreased amount of other F_O subunits like subunit 4 and 9 (homologs of subunit b and c) compared to wild-type mitochondrial extracts (Spannagel et al., 1997).

Crosslinking experiments performed in yeast have indicated a close proximity between the N-terminal portions of subunit f and 4 (Velours et al., 1998, Spannagel et al., 1997) and between subunit f and 8 in the matrix and intermembrane space (Stephens, Nagley & Devenish, 2003). This set of data was also confirmed by Cryo-EM structures obtained in *Yarrowia lipolytica* (Hahn et al., 2016) and *Saccharomyces cerevisiae* (Guo, Bueler & Rubinstein, 2017). Summarizing, gene disruption have demonstrated that the yeast f protein is necessary for assembly and function of the F-ATP synthase complex.

In **human** cells, the f subunit is encoded by the *ATP5J2* gene. It is a small hydrophobic protein of 94 amino acid residues and a mass of 10.9 kDa. It has several interesting features, i.e. the expression of four different isoforms due to

alternative splicing, the presence of two predicted acetylated and one phosphorylated amino acid residue, and a hydrophobic and charged transmembrane C-terminal region that is highly conserved among species. Recently, it has been shown that the f subunit is fundamental also for enzyme assembly in human mitochondria of the haploid HAP1 cell line. Indeed, f subunit removal in these cells caused alterations in F-ATP synthase assembly and subunit composition, and it affected dimer/oligomer stability besides having a severe effect on respiration with decreased levels of several respiratory complexes (He et al., 2018).

1.2.2 F-ATP synthase functions

The F-ATP synthase is essential for cell survival since it has important functions: it catalyses ATP synthesis or ATP hydrolysis according to the membrane potential (Walker, 2013); and it is important for mitochondrial morphology (Davies et al., 2011). Indeed, the F-ATP synthase is organized in dimers and oligomers in different species, with the exception of bacteria in which the enzyme is only present as a monomer. Our working hypothesis is that this enzyme can have another important function, i.e. be the key constituent of the mitochondrial permeability transition pore (PTP) (Giorgio et al., 2013, Bernardi et al., 2015, Carraro et al., 2019), an issue that is still the matter of debate. This last topic will be discussed in depth in the 1.3 paragraph.

Due to its essential role in cellular metabolism, malfunctioning of the enzyme has been associated to a variety of pathological conditions (cardiovascular and neurodegenerative diseases, obesity and cancer), and is now a promising drug target for multiple diseases (Lippe et al., 2019, Nesci et al., 2019).

1.2.2.1 F-ATP synthase catalytic activity

The F-ATP synthase can synthesize or hydrolyze ATP depending on substrate availability and on the magnitude of the proton electrochemical gradient. This catalytic mechanism requires Mg^{2+} as essential cofactor (Frasch, 2000), indeed kinetic studies with *Escherichia coli* F_1 mutants, showed that in the absence of Mg^{2+}, ATP binds the three catalytic sites of the F_1 domain, with the same low affinity (Weber, Senior, 1996). Residue T163 in the β subunit of the mammalian

F-ATP synthase is essential for binding of Mg^{2+} to the catalytic site (Rees et al., 2012). Mg^{2+} can be replaced by other divalent cations, including Ca^{2+}. Intriguingly, Ca^{2+} ions, differently from other divalent cations with similar ionic radius, only support ATP hydrolysis, but not H^+ translocation, both in bacteria (Nathanson, Gromet-Elhanan, 2000), mammals (Papageorgiou, Melandri & Solaini, 1998) and plants (De Col et al., 2018).

Based on detailed kinetic binding studies, in the 1990s Paul Boyer proposed the so-called rotational catalysis mechanism, in which the three active sites localized in the β subunit take turns in the catalysis of ATP synthesis (Boyer, 1993). His proposal was then supported and validated by many other pieces of evidence, such as high-resolution structures determined by X-ray crystallography in the bovine (Abrahams et al., 1994, Orriss et al., 1998, Menz, Walker & Leslie, 2001, Bowler et al., 2007) and yeast (Stock, Leslie & Walker, 1999, Kabaleeswaran et al., 2006) enzymes. One of these structures is summarized in Figure 8.

In the catalytic core of the F_1 domain, the three non-catalytic α subunits and the three catalytic β subunits alternate and are arranged around the asymmetric α-helical structure of the γ subunit. Because the γ subunit is asymmetrical, F-ATP synthase is an asymmetrical enzyme too. All of these six subunits contain a nucleotide binding site, but only those of the three β subunits carry out the ATP synthesis process. The nucleotides in the α subunits have no known direct role in the formation of ATP (Walker, 2013). Although the amino acid sequences of the β subunits are identical, their conformations during the catalytic cycle differ, partly due to the association of the γ subunit with only one of them at a time during rotation. The conformational differences are also reflected at the level of their binding sites for ATP and ADP; and named according to the presence of the adenine nucleotide: β_{TP} when ATP is bound, β_{DP} when ADP in bound and β_E when the site is empty. During the catalytic cycle of ATP hydrolysis or synthesis, the rotation of the central stalk takes each β subunit through each of the three conformations (Abrahams et al., 1994, Rees et al., 2012).

In this rotational catalysis mechanism (Figure 8), a given β subunit begins the catalysis cycle in its β_{DP} conformation, binding ADP and P_i; at this point the β subunit assumes the β_{TP} form that firmly binds and stabilizes the ATP molecule. Finally, the β subunit is further modified, assuming the β_E conformation which

has very low affinity for ATP, and so the newly synthesized nucleotide leaves the enzyme. Another cycle of catalysis begins when this subunit takes again the β_{DP} form and binds ADP and P_i. The conformational changes at the basis of this rotational mechanism are due to the flow of protons through the F_O portion of the F-ATP synthase. Proton translocation takes place through the interface of the a and c subunits (Allegretti et al., 2015), and drives the rotation of the the c ring and the γ subunit around the $\alpha_3\beta_3$ F_1 subcomplex. For each 360° rotation, (i.e. for a complete cycle of the β subunits through the three possible conformations), three molecules of ATP are synthesized or hydrolysed. The γ subunit rotates clockwise (viewed from the matrix side of the membrane) when the enzyme is synthesizing ATP, and in the opposite direction when it is hydrolysing ATP (Abrahams et al., 1994, Masaike et al., 2008). In the first case, the clockwise rotation of the c ring, is powered by proton translocation into the mitochondrial matrix, and it drives γ subunit rotation, which comes subsequently in contact with the three β subunits thus allowing the release of three ATP molecules. During hydrolysis of ATP, the counterclockwise rotation of the γ subunit and of the c ring, causes proton translocation into the IMS (Walker, 2013, Noji, Ueno & McMillan, 2017). However, the mechanism that converts the chemical energy of ATP into mechanical work is still unknown. The rotation is not continuous, but proceeds in distinct 120° steps; each step brings the γ subunit in contact with a different β subunit, and this contact forces the β subunit to assume the final empty conformation (Noji, Ueno & McMillan, 2017, Yasuda et al., 1998). These 120° steps where subsequently resolved into smaller substeps, each taking only a fraction of a millisecond. In the bacterial F_1 the first substep of 80° is driven by ATP binding, and the last 40° substep by release of ADP or Pi (Adachi et al., 2007, Masaike et al., 2008). In the mammalian F_1 the angle of these substeps differs, and substeps of about 65°, 25°, and 30° were seen (Bason et al., 2014, Suzuki et al., 2014).

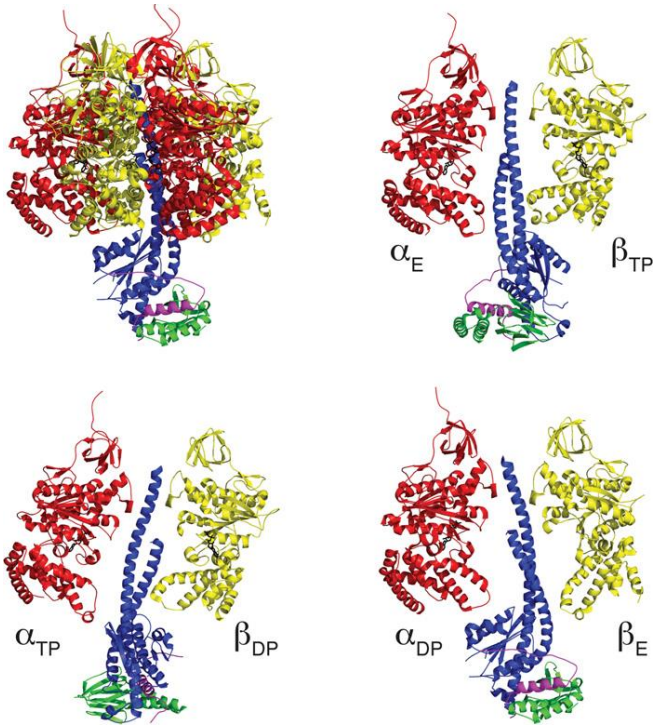

Figure 8. Bovine F-ATP synthase F1 domain structure during catalysis. The α-, β-, γ-, δ- and ε-subunits are red, yellow, blue, green and purple respectively. Top left: the complete F_1 domain with the catalytic core and the central stalk. Top right and bottom figures: representation of the three different conformations of the catalytic β subunits together with the central stalk (γ-, δ- and ε-subunits) and an α subunit, for reference. Each of the three β subunits has been obliged by the asymmetry of the γ subunit to adopt a different conformation, denoted β_{TP}, β_{DP} and β_E, with different affinities for nucleotides. During the catalytic cycle of ATP synthesis or hydrolysis, the rotation of the central stalk takes each β subunit through each of the three conformations (Walker, 2013).

1.2.2.2 F-ATP synthase organization in mitochondria

In the IMM the F-ATP synthase is organized in dimers and oligomers, while monomers are rarely found. The first evidence of this macromolecular organization of the F-ATP synthase comes from an electron microscopy analysis performed in *Paramecium multimicronucleatum*. This analysis revealed the presence of double rows of dimers, located along the highly curved ridges of the *cristae* (Allen, Schroeder & Fok, 1989). At the beginning this was thought to be peculiar of this organism, but the same organization was then reported for mitochondria from other species, including mammals (Davies et al., 2011). The only exception are bacteria in which the F-ATP synthase enzyme is only present as a monomer. These long rows of dimers (Figure 9A) were described by Cryo-EM in mitochondria from rat liver, bovine heart (Strauss et al., 2008, Davies et al.,

2011), *Polytomella* (Dudkina et al., 2010), *Yarrowia lipolytica*, *Saccharomyces cerevisiae*, *Podospora anserina,* and potato (Davies et al., 2011). The studies performed in mammals, revealed a V-shaped dimer with a fixed angle of 86° between monomers (Davies et al., 2012). In keeping with these results, BN-PAGE analysis of the mitochondrial F-ATP synthase has shown that it forms dimers and oligomers when solubilized with mild detergents (Wittig, Schagger, 2008). Of note, no F-ATP synthase dimers or oligomers were detected in the flat *cristae* regions, but they were found exclusively in the *cristae* edges (Figure 9A), where they interact with the IMM through the F_O subunits. These rows are more or less straight and follow the undulations of the *cristae* edges (Davies et al., 2011).

Dimers and oligomers are predicted to generate a high local curvature in the inner mitochondrial membrane (Strauss et al., 2008, Blum et al., 2019, Davies et al., 2012). The membrane deformation imposed by the V-like shape of the dimers, according to molecular-simulation analysis, originates an attractive driving force which allows the formation of dimer rows (Anselmi, Davies & Faraldo-Gomez, 2018). These highly folded membrane structures maximize the surface area available for oxidative phosphorylation. Calculations on the distribution of protons at the *cristae* ridges have suggested a physiological role in optimizing also ATP synthesis (Figure 9B) (Strauss et al., 2008, Davies et al., 2011).

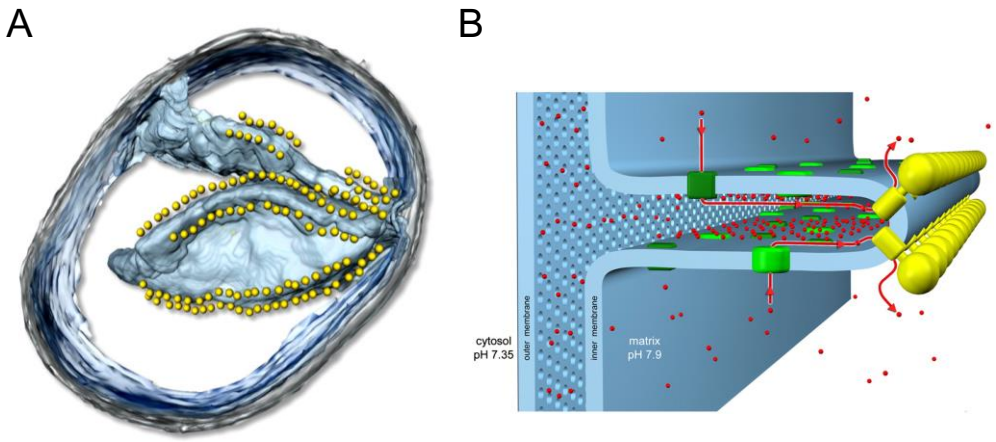

Figure 9. Rows of F-ATP synthase dimers in mitochondria and molecular organization of cristae membranes. (A) Segmented surface representation of a mitochondrion from Podospora anserina showing arrays of dimeric F-ATP synthases (yellow spheres) in cristae membranes. (B) F-ATP synthase dimer rows (yellow) at the cristae tips, and the electron transfer chain (green) predominantly at the adjacent membrane regions. Protons (red) pumped into the cristae space by the electron transport complexes flow back into the matrix through the ATP synthase rotor,

driving ATP production. This conserved arrangement generates a local proton gradient in the cristae space, optimizing mitochondrial ATP synthesis, and providing a functional role for the mitochondrial cristae. Grey, outer membrane; blue, cristae membranes; blue-transparent, inner boundary membrane; yellow ATP synthase; green, electron transport chain; red, protons. Adapted from (Davies et al., 2011).

Based on computer simulations, it was proposed that membrane curvature induced by the F-ATP synthase dimer in a simple lipid membrane, is sufficient to drive the formation of long dimer rows, which would then give rise to highly curved membrane ridges and lamellar cristae. The dimer alone can drive its own self-association and the bending of the IMM (Blum et al., 2019, Anselmi, Davies & Faraldo-Gomez, 2018). Other studies performed on bovine F-ATP synthase proposed that the transmembrane region of a monomer is sufficient to bend the lipid bilayer. This membrane deformation is a prerequisite for the self-association of F-ATP synthases into dimers and of dimers into rows (Baker et al., 2012, Jiko et al., 2015). The advantage of a membrane-driven self-assembly over a protein-mediated interaction resides in the energetic cost of remodelling, in the first case less energy is required, while in the latter case much more energy would be needed to disrupt each protein-protein interaction. Since mitochondria are highly dynamic organelles, it is essential that they can remodel their IMM quickly and without unnecessary energy consumption.

The correlation between the oligomeric organization of F-ATP synthase and mitochondrial morphology was revealed upon modulation of dimer/oligomer-specific subunits. For example, in yeast mitochondria the removal of the e, g or the first helix of subunit b in the peripheral stalk results in the formation of mitochondria where classical *cristae* are replaced by "onion-like" structures (Figure 10A-B) as observed by EM (Velours et al., 2009, Paumard et al., 2002, Carraro et al., 2018, Arnold et al., 1998). In these yeast strains, the F-ATP synthase is monomeric and is randomly distributed within the membrane, while no rows of dimers are detected at the *cristae* edges (Figure 10C-D). In human cells subunits e and g are also essential for dimer stability and their absence causes defects in mitochondrial morphology that are described as "arch-like" or longitudinal *cristae* morphology (Habersetzer et al., 2013). Similarly, subunit a has been demonstrated to be involved in F-ATP synthase dimer/oligomers

formation both in yeast (Wittig, Schagger, 2008, Guo, Bueler & Rubinstein, 2017) and in mammals (Wittig et al., 2010).

A stabilizing effect of mammalian F-ATP synthase dimers (Cabezon et al., 2000, Campanella et al., 2008) and oligomers (Gu et al., 2019) has been reported also for the inhibitory protein IF1. However, the importance of IF1 in the oligomerization process is still a matter of debate. Yeast F-ATP synthase dimer formation does not require Inh1, the homolog of IF1 (Dienhart et al., 2002); and dimerization of the bovine heart species is independent of the binding of IF1(Tomasetig et al., 2002).

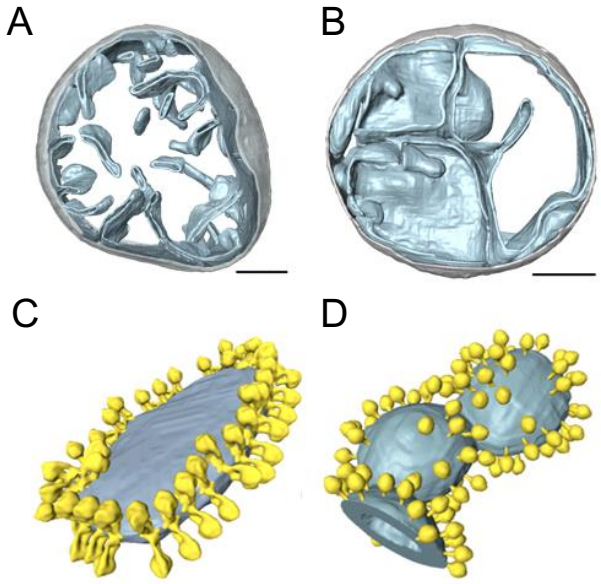

Figure 10. Mitochondrial morphology and F-ATP synthase distribution in isolated mitochondrial membranes from wild-type and yeast mutant strains. Surface-rendered volume of a mitochondrion from (A-C) wild-type and (B-D) g subunit deleted yeast strain. (A) Wild-type mitochondria have cristae with highly curved edges whereas (B) mitochondria from mutants lacking either subunit e, g, or the first helix of subunit b (su4ΔTM1) contain a number of separate inner membrane vesicles but few or no cristae. Mitochondrial morphologies of Δe, Δg, and su4ΔTM1 strains are indistinguishable. (D) In the mutants, the F-ATP synthase complexes are monomeric, and randomly distributed over flat or gently curving membrane regions. (C) By contrast F-ATP synthase from wild-type mitochondria form rows of dimers along the highly curved ridges of disk-shaped cristae vesicles. Light grey-outer membrane, sky blue-inner membrane, F-ATP synthase yellow. Scale bar, 200 nm. From (Davies et al., 2012).

1.2.2.3 F-ATP synthase regulation

As for other protein complexes, regulation of F-ATP synthase is exerted both at the expression and activity levels. The regulation of protein expression of the

mammalian enzyme occurs both at the transcriptional and post-transcriptional levels (Garcia-Bermudez, Cuezva, 2016, Nesci et al., 2017). The activity is not only modulated by the oligomeric state, but also through some biochemical events, such as reversible association with regulatory proteins, and post-translational modification (PTMs). A high number of modifications have been identified in the various subunits of F-ATP synthase, including phosphorylation, acetylation, trimethylation, nitration, s-nitrosylation and tryptophan oxidation (Kaludercic, Giorgio, 2016, Haynes et al., 2010, Vassilopoulos et al., 2014, Covian, Balaban, 2012). However, in most cases it remains unknown what are the signalling pathways responsible for these posttranslational modifications, in which tissues or biological conditions they occur, what impact they have on the biochemical activity of the target protein and how much of the target protein can be modified.

The major modulator of F-ATP synthase activity is the endogenous inhibitor protein **IF1**. This protein was first described in the 1960s in cardiac muscle of bovine heart (Pullman, Monroy, 1963), but its presence was then confirmed in yeast (Hashimoto, Negawa & Tagawa, 1981), plant (Norling et al., 1990) and *Caenorhabditis elegans* (Ichikawa, Ando & Fumino, 2006) mitochondria. When a cell is under hypoxic conditions (such as during ischemia), the electrochemical gradient across the IMM collapses and the enzyme switches its catalytic activity from ATP synthesis to ATP hydrolysis. In this condition, IF1 binds the catalytic core of the enzyme and preserves ATP from dissipation, in a process that in mammals is favored by matrix acidification (Boreikaite et al., 2019). Upon re-energization of mitochondria IF1 can dissociate from F_1 and it is released. The underlying physiological function is presumably to prevent a wasteful hydrolysis of ATP inside mitochondria.

IF1 is an α-helical protein that contains an inhibitory domain at the N-terminus, and a dimerization domain at the C-terminus. While the N-terminus is intrinsically disordered in solution and becomes folded just after binding to F_1-ATPase, the C-terminus has an α-helix secondary structure (Gledhill et al., 2007).

Dimerization is driven by the formation of an antiparallel α-helical coiled-coil structure between the C-terminal domains (residues 44-84 in the bovine sequence)

exposing the two N-terminal minimal inhibitory regions (residues 14-47) at different ends of the helical structure. Tetramer formation involves the N-terminal regions of dimers, and in this scenario the minimal inhibitory portion of the protein is masked, and the inhibitor became inactive (Cabezon et al., 2000, Cabezon et al., 2001). One amino acid has been proved to be involved in the regulation of IF1 activity and oligomeric state. Site-directed mutagenesis of H49 into a lysine generates a mutant IF1 active at all pH values, since protonation/deprotonation of this residue is not possible and tetramers cannot form (Bason et al., 2011, Schnizer et al., 1996).

In mammals IF1 is present as monomer, dimer and tetramer, even if the active form is the dimeric one. In mitochondria the oligomeric state of IF1 and its inhibitory potency are modulated by a combination of pH and cation type (Boreikaite et al., 2019). At pH values around or below neutrality (≥ 7.5), IF1 dimerizes and forms a 1:1 complex with the F_1-ATPase (Figure 11A-B). The interactions occur between the N-terminal domain of IF1 and the C-terminal domain of the α_{DP} β_{DP} subunits and the coiled coil region of γ subunit (Bason et al., 2011, Bason et al., 2014). Moreover, the formation of the inhibited complex requires the hydrolysis of two ATP molecules, i.e. two rotations of 120° of the γ subunit (Bason et al., 2011, Bason et al., 2014).

Dissociation of tetramers into dimers of IF1 is promoted also by Ca^{2+} ions, and leads to rapid inactivation of ATPase activity (Boreikaite et al., 2019).

The activity of IF1 is also regulated at the posttranslational level. Indeed, phosphorylation of S39 in human IF1by the action of PKA, prevents its binding to the F-ATP synthase and subsequently its inhibitory function (Garcia-Bermudez et al., 2015).

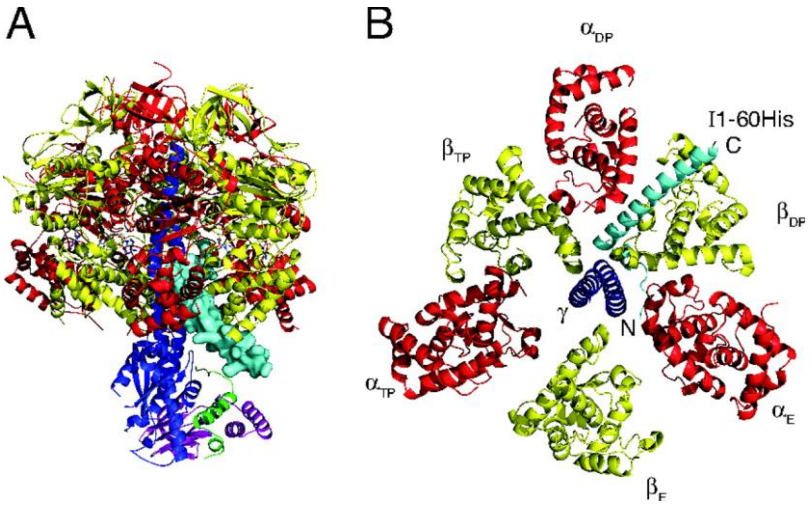

Figure 11. The structure of the bovine F1-IF1 (I1-60His) complex. (A) Overall view of the complex. The α-, β-, γ-, δ-, and ε-subunits are shown in ribbon form in red, yellow, dark blue, magenta, and green, respectively. Residues 8–50 of I1–60His are shown in light blue solid representation. (B) View upward (away from the foot of the central stalk), along the axis of the γ-subunit showing the orientation of the long α-helix of I1–60His relative to the C-terminal domains of the α- and β-subunits. From (Gledhill et al., 2007).

Besides IF1, other proteins were identified to interact with and regulate F-ATP synthase, but they are less precisely characterized.

For example, S100A1 (a Ca^{2+}-sensing protein of the EF-hand family, expressed predominantly in the heart) interacts in a Ca^{2+}-dependent manner, with the α and β subunits of the F-ATP synthase. This interaction was shown to increase F-ATP synthase activity and ATP production in cardiomyocytes (Boerries et al., 2007).

Recently it has been reported that the F-ATP synthase interacts with the **Sirtuin3 (SIRT3)** regulatory protein at the α-β-γ and OSCP subunits (Vassilopoulos et al., 2014, Yang et al., 2016). These subunits contain SIRT3-specific reversible acetyl-lysines that are evolutionary conserved. An example is K139 in the OSCP protein, the acetylation of which decreases the ATP synthetic activity of the enzyme (Vassilopoulos et al., 2014). Moreover, when matrix pH decreases, this pool of SIRT3 bound to OSCP is released, leading to rapid deacetlyation of matrix proteins and recovery of membrane potential (Yang et al., 2016). In line with these results, the genetic knockout of *Sirt3* results in decreased F-ATP synthase activity, and of mitochondrial ATP levels *in vivo* and *in vitro* (Ahn et al., 2008, Wu et al., 2013). The role of mitochondrial SIRT3 appears to be regulation of mitochondrial metabolism and function via changes in the acetylation status of proteins (including F-ATP synthase).

Also **p53**, an onco-suppressor protein, has been reported to interact with the OSCP subunit, an interaction that appears to be important for the assembly and stabilization of the mature complex (Bergeaud et al., 2013). The OSCP subunit was also found to interact with **amyloid β (Aβ) protein**. Intriguingly, OSCP loss and its interplay with Aβ causes a deregulation of the F-ATP synthase activity in Alzheimer's disease, while its overexpression ameliorates Aβ-mediated mitochondrial impairment and the resultant synaptic injury (Beck et al., 2016).

Another interactor is **Cyclophilin D (CyPD)**, a mitochondrial isoform of the family of peptidyl-prolyl *cis-trans* isomerases, which binds to the OSCP subunit and partially inhibits both ATP synthesis and hydrolysis (Giorgio et al., 2009, Giorgio et al., 2013). It is also known as a regulator of the PTP, a conserved high-conductance channel located in the IMM (Carraro et al., 2019). The identification of the interaction between CyPD and the OSCP subunit was an essential step in revealing the molecular nature of the PTP, which will be further discussed later.

1.3 The Permeability Transition Pore (PTP)

The permeability transition (PT) defines an increased permeability of the mitochondrial inner membrane to ions and solutes with molecular masses up to 1.5 KDa, leading to matrix swelling. The PT is mediated by opening of a regulated channel, the permeability transition pore (PTP).

The occurrence of swelling in isolated mitochondria, has been discovered very early (RAAFLAUB, 1953a, RAAFLAUB, 1953b). The term "permeability transition" was introduced by Haworth, Hunter and Southard. In their manuscript they concluded that Ca^{2+} addition to isolated bovine heart mitochondria, induced an "…uncoupling of oxidative phosphorylation and a nonspecific increase in the permeability of the inner membrane, resulting in entry of sucrose into the matrix space and the observed configurational transition (swelling) of mitochondria" (Hunter, Haworth & Southard, 1976). Furthermore, they characterized the basic features of the process as (i) a permeability increase selectively induced by Ca^{2+}; (ii) a regulated process inhibited by Mg^{2+}, ADP, and bovine serum albumin (BSA); and (iii) a reversible event (Hunter, Haworth, 1979a, Haworth, Hunter, 1979, Hunter, Haworth, 1979b).

Initially the PT was largely considered an *in vitro* artifact, and not a physiological pathway. Occurrence of a PT *in situ* was not generally considered possible by the scientific community, since it appeared to be in contrast with the mechanism of energy conservation defined by the chemiosmotic theory of Peter Mitchell (MITCHELL, 1961). The presence of a large channel causing depolarization and allowing solute and ion equilibration across the IMM appeared to contradict the need to maintain a proton gradient to drives the synthesis of ATP.

The occurrence and potential role of the PT in pathophysiology was consolidated by the discovery that nanomolar concentrations of cyclosporin (Cs) A can inhibit or delay the onset of pore opening (Fournier, Ducet & Crevat, 1987, Broekemeier, Pfeiffer, 1989, Crompton, Ellinger & Costi, 1988, Halestrap, Davidson, 1990). CsA binds matrix CyPD, and this binding leads to inhibition of the enzymatic activity of CyPD and to inhibition of the PT (Connern, Halestrap, 1992, Griffiths, Halestrap, 1991, Nicolli et al., 1996). These discoveries thus identified a protein regulator for the PTP (CyPD) and a drug (CsA) to test its occurrence in cells and living organisms.

Another key piece of evidence came from electrophysiology. In the 1990s an ion channel in the IMM was discovered and named mitochondrial megachannel (MMC)(Kinnally, Campo & Tedeschi, 1989, Petronilli, Szabo & Zoratti, 1989). This channel has all the features of the PTP, including activation by Ca^{2+} and thiol oxidants, inhibition by Mg^{2+}/ADP, CsA and H^{+} (Szabo, Bernardi & Zoratti, 1992, Bernardi et al., 1992). The maximal conductance state was in the range of 1-1.3 nS and the channel had an apparent diameter of about 3 nm, thus able to allow diffusion of solutes with a molecular mass up to 1.5 KDa (Massari, Frigeri & Azzone, 1972a, Szabo, Zoratti, 2014).

A third important observation was the involvement of the PT in cell death (Crompton, 1999, Duchen et al., 1993, Pastorino et al., 1993).

Over the last 20 years, the PT has been shown to be implicated in a variety of diseases. It is the major regulator of the extent of ischemia-reperfusion injury, it is implicated in many types of cancers, neurodegenerative diseases, and several forms of muscular dystrophies (reviewed in (Bernardi et al., 2015, Hurst, Hoek & Sheu, 2017).

PTP opening is not associated just to the dramatic scenario of cell death, but appears to be involved also in the control of Ca^{2+} homeostasis (Bernardi, Petronilli, 1996, Lu et al., 2016, Barsukova et al., 2011) (Figure 12). Transient openings of the pore (also called flickering) have been documented *in situ* in intact cells with sub-conductance states (Petronilli et al., 1999), and are necessary for the fast mitochondrial release of excess of Ca^{2+}. Long-lasting openings of the PTP instead are associated to mitochondrial swelling, rupture of the OMM, cytochrome *c* release and cell death (Petronilli et al., 2001, Rasola, Bernardi, 2007).

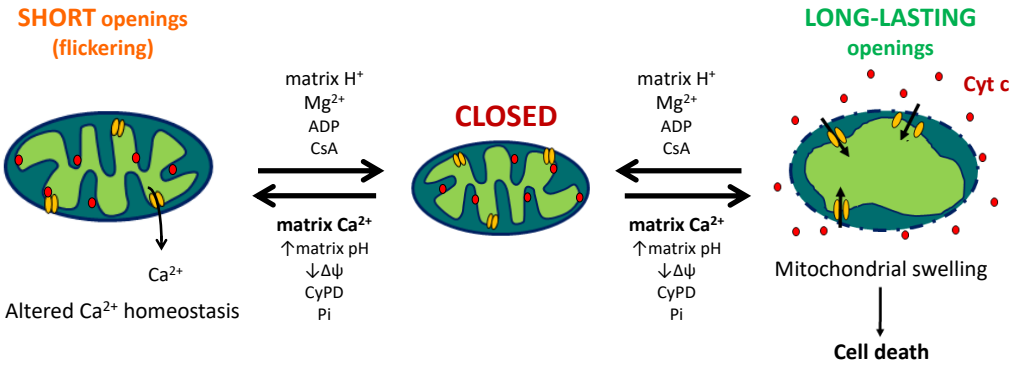

Figure 12. Permeability Transition Pore (PTP) openings, and its matrix and membrane regulators. The PTP can undergo short- (left) or long-lasting (right) openings. In the case of long-lasting openings permeability transition is associated to cytochrome *c* (Cyt *c*) release and cell death, while the transient opening allows only fast mitochondrial Ca^{2+} release. The open or closed state of the PTP is regulated by multiple effectors that can either induce PTP opening (Ca^{2+}, CyPD, Pi, and collapse of membrane potential), or its inhibition (matrix H, Mg^{2+}, adenine nucleotides, and CsA). Yellow, PTP; red, Cyt c.

1.3.1 PTP regulation

Studies performed in isolated mitochondria from mammalian tissues allowed a characterization of the properties and of the regulation of the channel. Pore opening is regulated by multiple compounds that can either sensitize or desensitize the PTP. The main compounds are discussed below and summarized in Figure 12.

As already mentioned, **Ca^{2+}** is a "permissive factor", meaning that matrix Ca^{2+} is necessary (but not always sufficient) to observe PTP opening. Although Ca^{2+} is essential (Hunter, Haworth & Southard, 1976, Giorgio et al., 2018), the threshold matrix Ca^{2+} required for PTP opening varies with the experimental conditions and organism. Importantly, all other **divalent cations** e.g. Mg^{2+}, Sr^{2+} and Mn^{2+} have a desensitizing effect, and appear to compete for the same matrix binding site of Ca^{2+} (Bernardi et al., 1992).

Among the physiological modulators of the pore, **matrix pH** plays a major role. The PTP/MMC is inhibited as matrix pH decreases below 7.0 (Szabo, Bernardi & Zoratti, 1992, Bernardi et al., 1992, Nicolli, Petronilli & Bernardi, 1993, Johans et al., 2005). The pore open-closed probability is regulated by the reversible protonation of histidine residues (Nicolli, Petronilli & Bernardi, 1993).

The PTP is also modulated by **arginine residues**, the modification of which through **glyoxal** derivatives can cause PTP sensitization or desensitization depending on the specific reagent (Eriksson, Fontaine & Bernardi, 1998, Linder et al., 2002, Johans et al., 2005). In rat liver mitochondria, PTP is inhibited by methylglyoxal (MGO) and phenylglyoxal (PGO), while it is activated by OH-PGO (Eriksson, Fontaine & Bernardi, 1998, Johans et al., 2005). As recently discovered, the effects of PGO on the PTP are species-specific with inhibition in

mouse and yeast and induction in human and Drosophila mitochondria (Guo et al., 2018).

The **membrane potential (Δψ)** is an upstream key factor for regulation of the pore, which indeed displays a voltage-dependent behaviour. Collapse of the Δψ favors pore opening, whereas a high inside-negative Δψ tends to stabilize it in the closed conformation (Bernardi, 1992), as also observed at the single channel level (Szabo, Zoratti, 2014).

Important regulators of the PTP are **CsA** and **CyPD**. CyPD modulates the PTP by decreasing the Ca^{2+} load required for opening of the pore, and this effect is prevented by CsA. In CyPD-null mice the PTP is desensitized and insensitive to CsA, but it otherwise responds to other modulators similarly to wild type mice although the Ca^{2+} sensitivity is decreased. This latter finding suggests that CyPD is a key PTP modulator but not an essential structural component (Baines et al., 2005, Basso et al., 2005).

It should also be mentioned that **matrix inorganic phosphate** (**P_i**) has complex effects on the pore. In mammals it sensitizes PTP opening through a mechanism that is not well understood but may be due, in part at least, to increased CyPD binding to the PTP. Indeed P_i becomes a PTP inhibitor in CyPD-null mouse liver mitochondria, suggesting that the inducing effects of P_i may depend on CyPD (Basso et al., 2008).

1.3.2 PTP Molecular Nature: models

The PTP is a non-selective pore through with both ionic and non-ionic substrates can flow (Hunter, Haworth & Southard, 1976). While its pathophysiological role has been extensively studied, the molecular identity of the pore remains controversial.

The multi conductance nature of the PTP suggests that it is likely to be a multi-subunit complex, and that it can olygomerize to varying degrees resulting in the observed range of conductances. Over the years, many hypotheses have been proposed concerning the molecular nature of the pore.

In the early 1990s the PTP was thought to be a supramolecular complex that resides at contact sites between the inner and the outer mitochondrial membrane

(OMM) (Figure 13A). The proteins involved in its formation were proposed to be the voltage-dependent anion channel (VDAC) and the mitochondrial benzodiazepine receptor (TSPO) in the OMM; the adenine nucleotide translocator (ANT) in the IMM, with CyPD residing on the matrix and hexokinase II (HK II) and Bcl-2 facing the cytosol. This hypothesis arose from co-purification studies, for example TSPO was shown to associate to VDAC and ANT (McEnery et al., 1992), as well as to HKII and Bcl2 (Beutner et al., 1996, Marzo et al., 1998); and from the analysis of specific PTP regulators. For example benzodiazepines (PTP inducers) are ligands of TSPO (Kinnally et al., 1993); and ADP, bongkrekate and atractylate (inhibitors or activator of the PTP, respectively) are substrate and regulators of the ANT, respectively (Haworth, Hunter, 2000). This model was also supported by electrophysiological studies; both ANT (Brustovetsky et al., 1996) and VDAC (Szabo, De Pinto & Zoratti, 1993) display a high-conductance channel activity.

However, subsequent genetic inactivation studies apparently ruled out VDAC, ANT, CyPD and TSPO as essential pore forming units. Indeed, the pore could still be detected in mouse liver mitochondria where both ANT1 and ANT2 isoforms had been eliminated (Kokoszka et al., 2004); in mitochondria of VDAC-null mice (Krauskopf et al., 2006); in cells were all VDAC isoforms had been eliminated (Baines et al., 2007); and in mitochondria lacking CyPD (Baines et al., 2005, Basso et al., 2005, Nakagawa et al., 2005, Schinzel et al., 2005) and TSPO (Sileikyte et al., 2014).

Subsequently, the phosphate carrier (P_iC) was also proposed to be a component of the PTP complex (Figure 13B). This hypothesis emerged when CyPD was found to bind the P_iC in a CsA-sensitive manner (Leung, Varanyuwatana & Halestrap, 2008), but also because P_i is an inducer of PTP opening. However, by patch-clamp experiments the P_iC revealed to be an anion-selective channel with currents of only 20-30 pS, too low to consider the P_iC a constituent of the PTP (Herick, Kramer & Luhring, 1997). Additionally, genetic knockdown of P_iC in HeLa cells (Varanyuwatana, Halestrap, 2012), or in mouse heart (Gutierrez-Aguilar et al., 2014), did not affect PTP opening and function. Genetic deletion of the P_iC in the

mouse heart desensitized the PTP, suggesting a regulatory rather than a constitutive role in PTP formation (Kwong et al., 2014).

The latest proposed model considers the F-ATP synthase enzyme as the critical component of the PTP (Figure 13 C-D). Three main observations contributed to this hypothesis. The first was that, through BN-PAGE and F-ATP synthase immunoprecipitation, CyPD was found to interact with the F-ATP synthase, resulting in a partial (about 30%) inhibition of the enzyme. Both features were relieved upon CsA addition and CyPD displacement from the enzyme (Giorgio et al., 2009). The second observation was that the binding partner of CyPD is OSCP (a subunit of the peripheral stalk of F-ATP synthase), and that this interaction could be favoured by P_i, or blocked by the benzodiazepine receptor agonist Bz-432, a compound that causes also PTP activation (Giorgio et al., 2013). Finally, gel purified F-ATP synthase generated Ca^{2+}-dependent currents after incorporation in lipid bilayers (Giorgio et al., 2013, Alavian et al., 2014, Carraro et al., 2014, von Stockum et al., 2015)

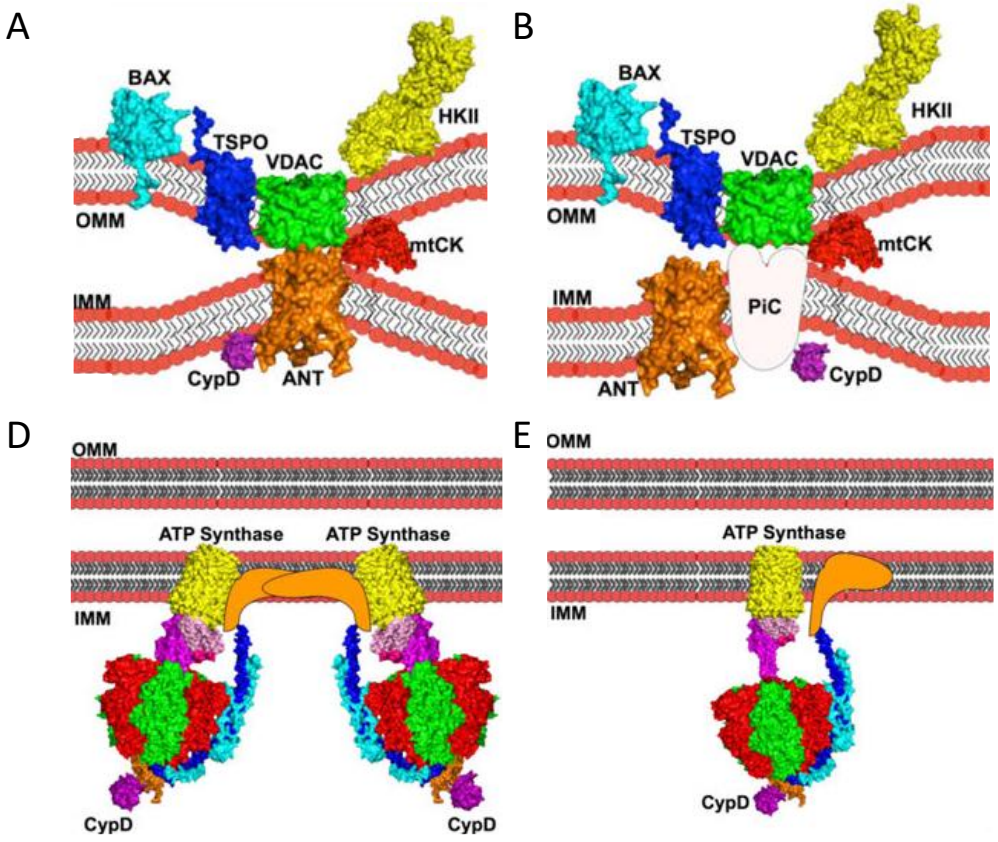

Figure 13. Representative diagrams of the proposed models of the PTP. (A) Classical model composed of BCL-2-associated-X-protein (BAX), Voltage Dependent Anion Channel (VDAC), the Perepheral Benzodiazepiene receptor (TSPO), Hexokinase II (HKII) on the Outer Mitochondrial Membrane (OMM), Mitochondrial Creatine Kinase (mtCK) in the intermembrane space, Adenine Nucleotide Transporter (ANT) in the inner mitochondrial membrane (IMM), and mitochondrial cyclophilin D (CypD) bound to ANT in the matrix. (B) Phosphate Carrier model composed of BAX, VDAC, TSPO, HKII, mtCK, ANT, and CypD, bound to the phosphate carrier (P_iC). (C) Dimers of the F-ATP synthase and (E) uncoupling of the F-ATP synthase. Adapted from (Hurst 2017).

1.3.3 Channel formation from F-ATP synthase

So far, two main sites of possible pore formation in mitochondrial F-ATP synthase have been proposed: the monomer-monomer interface (Figure 13D) and the c ring (Figure 13E). The first model was based on electrophysiological studies (Giorgio et al., 2013), and it is our current working hypothesis. Our proposal is that channel forms from dimers of F-ATP synthase after replacement of Mg^{2+} with Ca^{2+} in the catalytic site.

In the second hypothesis, the pore originates in the c ring after the uncoupling of the F_1 from the F_O complex of the F-ATP synthase. According to Alavian et al. the two domains should dissociate during PTP formation (Alavian et al., 2014).

1.3.4 Evidence that F-ATP synthase forms the PTP

Pieces of evidence that the PTP forms from F-ATP synthase have been obtained through two different approaches, i.e. reconstitution of channel activity and genetic manipulation of the enzyme (reviewed in (Carraro et al., 2019), Figure 14). Despite the fact that further experiments need to be performed in order to better elucidate the precise site and the mechanism(s) of channel formation, it is encouraging that the F-ATP synthase can accommodate the key regulators of the PTP activity (Mg^{2+}, Ca^{2+}, adenine nucleotides, CyPD).

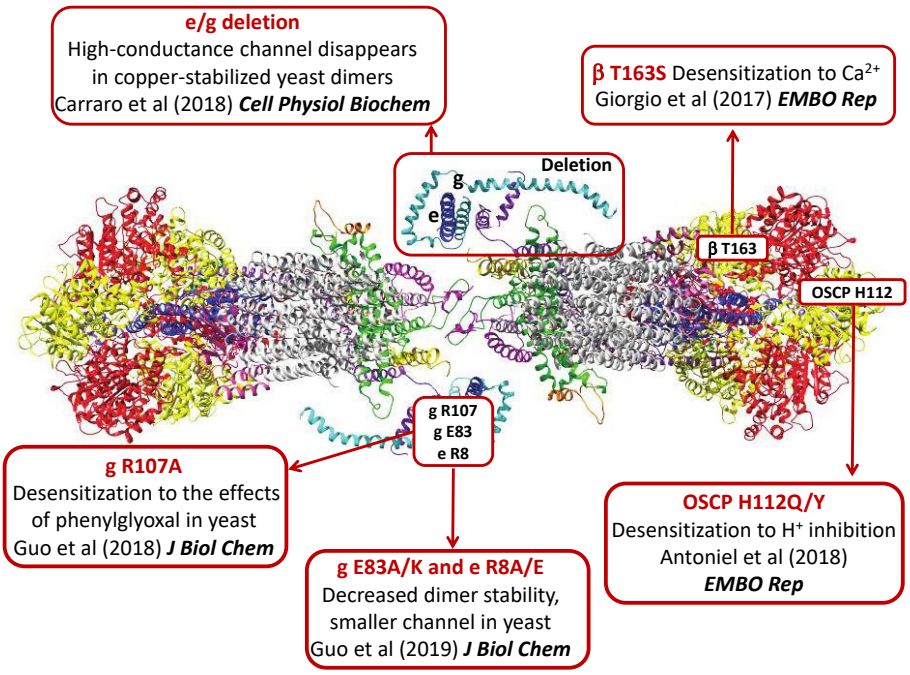

Figure 14. Map of mutations of F-ATP synthase and their effects on the permeability transition. Mutations of F-ATP synthase are mapped onto the structure of the yeast enzyme from Guo et al., 2017 and their phenotypic effects are indicated. From Carraro et al., 2019.

1.3.4.1 Reconstitution of channel activity with different F-ATP synthase preparations

In 2013, our group was the first to provide evidence that gel-purified F-ATP synthase dimers from bovine heart, inserted into lipid bilayer form a Ca^{2+}-activated channel, with a maximal conductance of 1.0-1.3 nS, and various subconductance states including a major one of 500 pS (Giorgio et al., 2013). The measured conductance closely matched the features of the MMC/PTP (Kinnally, Campo & Tedeschi, 1989, Petronilli, Szabo & Zoratti, 1989, Szabo, Bernardi & Zoratti, 1992). Channel activity was triggered by PTP inducers like Ca^{2+}, Bz-423 and phenylarsine oxide (one of the most powerful sensitizers of the pore), and fully inhibited in the presence of ADP, Mg^{2+}, and by the F-ATP synthase inhibitor AMP-PNP (a non-hydrolyzable ATP analogue). Importantly, dimers but not monomers were able to generate currents in spite to the same overall subunit composition, suggesting that the pore may form at the interface between monomers (Giorgio et al., 2013).

It could be argued that the presence of contaminants could have affected these results, and/or that the protein may have lost its native conformation after gel-elution and incorporation in the membrane, however (i) the dimer preparation was devoid of ANT and VDAC (Giorgio et al., 2013) and (ii) the same conductance was also recorded in a highly pure and active F-ATP synthase preparation from bovine hearts after incorporation into planar lipid bilayers (Urbani et al., 2019).

Using the same strategy as in Giorgio 2013, the channel-forming property of F-ATP synthase was also found in mitochondria of *Saccharomyces cerevisiae* (Carraro et al., 2014), and *Drosophila melanogaster* (von Stockum et al., 2015). The conductance recorded was 300 pS and 50 pS, respectively. Interestingly, removal of the dimerization subunits e and g, in yeast decreased the conductance of the F-ATP synthase channel about tenfold (from 300 pS to 30 pS), and conductance was further decreased by the additional ablation of the first transmembrane domain of subunit b (Carraro et al., 2018).

Jonas and co-workers provided independent evidence that the liposome-reconstituted c ring displays Ca^{2+} activated currents with peak of conductance up to 1.5-2.0 nS, resembling the PTP channel activity. They suggested that channel opening requires Ca^{2+}-mediated displacement of F_1, whereas its closure would be mediated by CsA, as well as by β subunit (Alavian et al., 2014). However, it is not known how the identified PTP modulators can interact or regulate the subunit c, or how the pore may form in the c ring lumen.
Molecular dynamics simulations addressed the feasibility of the c ring as a channel and concluded that, when correctly folded and assembled, the interior of the c ring is so hydrophobic that it prevents formation of a water-filled channel permeable to solutes (Zhou et al., 2017).

1.3.4.2 Genetic manipulation of the F-ATP synthase

Channel formation from F-ATP synthase has been confirmed in human cells where the c subunit was downregulated by siRNA. The c downregulation resulted in PTP inactivation as it attenuated Ca^{2+}-induced IMM depolarization and PTP opening (Bonora et al., 2013, Alavian et al., 2014).

Following two of the main regulators of the pore, matrix Ca^{2+} and matrix pH, in our laboratory two important point mutations were analyzed (Figure 14).
The T163 residue in the β subunit of mammalian F-ATP synthase is known to be essential for the binding of Mg/ADP to the catalytic site (Rees et al., 2012). In the proteobacterium *Rhodospirillum rubrum* the relative affinity for Ca^{2+} and Mg^{2+} in the catalytic core of the F-ATP synthase, could be modulated with a point T159S mutation in the β subunit (this position is equivalent to T163 in mammals). This amino acidic substitution leads to decreased Ca^{2+}-ATPase and increased Mg^{2+}-ATPase activities (Nathanson, Gromet-Elhanan, 2000, Du et al., 2001). Following these findings, we showed in a HeLa cell model, that partial T163S substitution (i) increases Mg^{2+}-ATPase and inhibits Ca^{2-}ATPase activity, (ii) decreases sensitivity of the PTP to Ca^{2+}, (iii) it protects against PT-dependent cell death, and (iv) lowers incidence of apoptosis in developing zebrafish embryos (Giorgio et al., 2017). Thanks to *in silico* studies, we hypothesized that Ca^{2+} binding to the catalytic site may induce a conformational change that is transmitted to the peripheral stalk through OSCP, leading to PTP opening within the membrane (Giorgio et al., 2017).

An important physiological PTP inhibitor is matrix pH, with channel block at pH 6.5. The inhibition is reversible and mediated by protonation of histine residues (Nicolli, Petronilli & Bernardi, 1993). In HEK cells, PTP inhibition by protons is mediated by the highly conserved histidyl residue (H112 in the human mature protein) in the OSCP subunit of F-ATP synthase (Figure 14). Mitochondrial PTP-dependent swelling cannot be inhibited by acidic pH in H112Q and H112Y OSCP mutants, and the corresponding measured megachannels were insensitive to acidic pH too. Importantly these mutations did not affect F-ATP synthase assembly, function, cell viability and the single channel features of the MMC (Antoniel et al., 2018).

Our laboratory performed several genetic manipulations (gene deletion or site-directed mutagenesis) of yeast F-ATP synthase.

By taking advantage of the discovery that phenyglyoxal (PGO, a modulator of the PTP) affects the PTP in a species-specific manner (Guo et al., 2018), and of the fact that the modulatory effect is mediated by conserved arginine(s) (Eriksson, Fontaine & Bernardi, 1998, Linder et al., 2002, Johans et al., 2005), the target of PGO target was identified (Figure 14). Yeast mitochondria bearing a R107A mutated g subunit were totally resistant to PTP inhibition by PGO. Notably, the mutation did not affect assembly or catalytic activity of the F-ATP synthase (Guo et al., 2018).

Yeast mutants lacking the dimer-specific subunit e and g of the F-ATP synthase (Figure 14), turned out to be resistant to Ca^{2+}-dependent PTP opening (Carraro et al., 2014). The same mutants did not undergo swelling in a sucrose-based medium, supporting the conclusions that the pore forms at the monomer interface, and that the size of the channel in these mutants is smaller (Carraro et al., 2018). Through site-directed mutagenesis, another important residue for pore formation has been identified in the e subunit (Guo et al., 2019), Figure 14). Individual R8A/R8E substitutions in the e subunit, decreased the interaction between subunit e and g and affected the stability of dimeric F-ATP synthase to digitonin. When these dimers were eluted from BN-PAGE gels and tested for Ca^{2+}-dependent PTP opening, they display currents of smaller conductance compared to wild-type ones, suggesting again that the e and g subunit, and their interaction is important for the generation of the full-conductance PTP from F-ATP synthase (Guo et al., 2019).

1.3.5 Is there more than one PTP?

The hypothesis that the PTP forms from FATP synthase has been recently questioned by Walker and co-workers (He et al., 2017a, He et al., 2017b, He et al., 2018, Carroll et al., 2019). These authors genetically ablated the genes encoding for subunit c (He et al., 2017b), OSCP and b (He et al., 2017a), and e, g, f, DAPIT and 6.8PL (Carroll et al., 2019), and studied whether PTP formation and opening still occurred using several assays (CRC, calcein loading-cobalt quenching and swelling). Since many of the properties of the PTP were preserved, they concluded that dimeric F-ATP synthase complex does not generate the PTP.

Careful analysis of their results, however, suggests that the PTP was actually affected by deletion of the above-mentioned subunits, and that its size was smaller in the mutants. Importantly, these cells displayed severe respiratory defects, and an F-ATP synthase that was not properly assembled (Bernardi, 2018).

At variance from the conclusions of Walker et al., recent electrophysiological data performed in mitoplasts from HAP1 cells lacking subunit c indicate that the high-conductance PTP is no longer present. In these cells a smaller conductance could be detected, that like the PTP could be inhibited by CsA, but unlike the PTP was also inhibited by bongkrekate (Neginskaya et al., 2019), thus suggesting that it may arise from the ANT. The observed conductance was indeed similar to that previously reported for the ANT (Brustovetsky et al., 1996, Brustovetsky et al., 2002). In keeping with the existence with a smaller pore, cells still exhibited mitochondrial CsA-sensitive Ca^{2+} release that was also sensitive to bongkrekate. In line with these results, a recent paper from the group of Molkentin showed that loss of ANT1, ANT2 and ANT4 gene desensitizes the PTP to Ca^{2+}, yet permeabilization to sucrose can still occur (Karch et al., 2019).

Thus, the hypothesis that the PTP forms from a specific, Ca^{2+}-dependent conformation of F-ATP synthase remains fully viable, even if the involvement of other proteins (as the ANT) cannot be ruled out. Taken together, these studies support the existence of two distinct pores, one formed by the ANT and one by F-ATP synthase.

2 AIM

AIM OF THE STUDY

Considering the role of the PTP in Ca^{2+} homeostasis and cell death initiation, it is important to investigate its molecular nature and modulation. According to our recent findings, the PTP may form from F-ATP synthase, at the dimer interface. The goal of my PhD project is to elucidate the function of the f subunit of F-ATP synthase in human cells, and define its roles (i) in F-ATP synthase catalysis and assembly, (ii) in maintenance of mitochondrial morphology, and (iii) in PTP modulation and/or formation. We investigated its role using two different techniques i.e. CRISPR/Cas9 and RNA interference, to generate human cells lacking or with a decrease level of the f subunit, respectively.

3 MATERIALS and METHODS

3.1 Molecular Biology

3.1.1 Vectors

To perform the knock out (KO) of the f subunit through the CRISPR/Cas9 technology, we used the plentiCRISPRv2 vector (Addgene plasmid #52961) (Figure 15A). Its main features are: ampicillin resistance gene for selection in bacteria; puromycin resistance gene for selection in mammalian cell lines; hCMV promoter for transcription of the viral genome in mammalian cells; gRNA scaffold to recognize the genomic target sequence; the CRISPR-associated endonuclease (Cas9) to induce double-strand breaks.

The plentiCRISPR-EGFP sgRNA (Addgene plasmid #51760) (Figure 15B) was used as control. It has the same main features as the plentiCRISPRv2 vector, but it contains a gRNA targeted against a GFP gene (human cells, do not have this gene in their genome).

The knock down (KD) of the f subunit through the RNA interference approach, was performed using the pLKO.1-puro vector (purchased from Sigma) (Figure 15C). Its main features are: ampicillin resistance gene for selection in bacteria; puromycin resistance gene for selection in mammalian cell lines; an hPGK promoter for transcription of the viral genome in mammalian cells; shRNA construct recognizing the target mRNA sequence.

The empty pLKO.1-puro vector (Sigma), without any shRNA sequences, was used as control. The panel of shRNAs inserted in the viral vector, targeting the human f subunit mRNA, were the following:

shRNA 1	5’ CGGGTACCAGTGAAGGACAAGAAACTCGAGTTTCTTGTCCTTCACTGGTACTTTTTG 3’
shRNA 2	5’ CGGCCGGTACTACAACAAGTACATCTCGAGATGTACTTGTTGTAGTACCGGTTTTTG 3’
shRNA 3	5’ CGGCTGGATCTTGATGCGGGACTTCTCGAGAAGTCCCGCATCAAGATCCAGTTTTTG 3’
shRNA 4	5’ CGGCGTGCTCTTTAGCTACTCCTTCTCGAGAAGGAGTAGCTAAAGAGCACGTTTTTG 3’
shRNA 5	5’ CGGCGGAGCGTTTCAAAGAGGTTACTCGAGTAACCTCTTTGAAACGCTCCGTTTTTG 3’

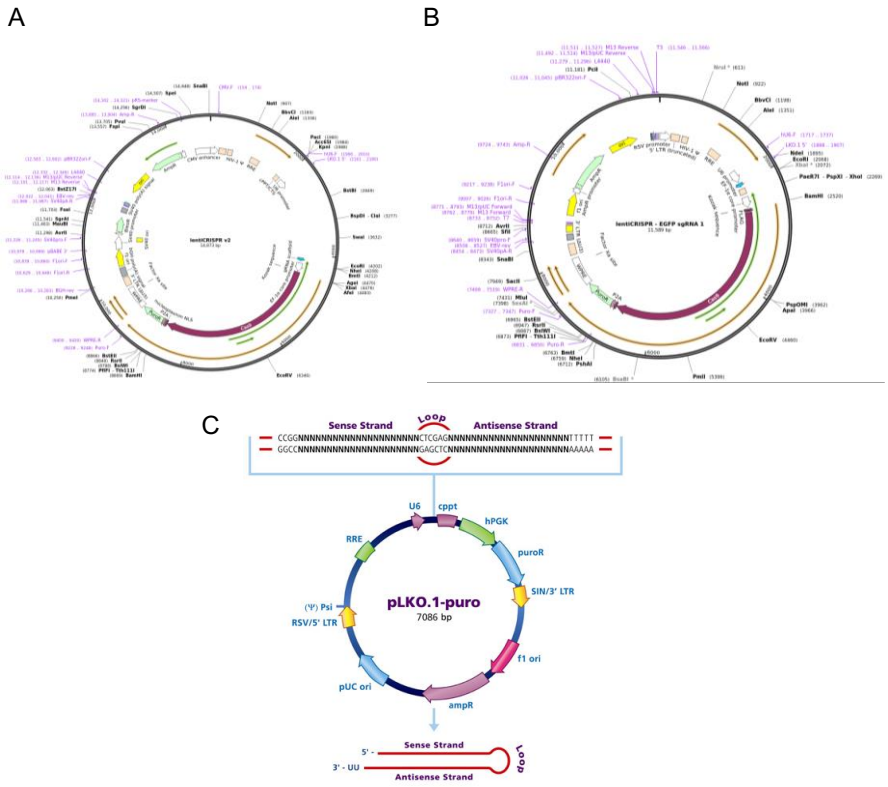

Figure 15. Detailed map of the vector used. (A) plentiCRISPRv2 vector used to obtain the full knock out of the f subunit. (B) plentiCRISPR-EGFP sgRNA vecor as control. (C) pLKO.1-puro vector used to obtain a stable knock down of the f subunit.

3.1.2 Lentiviral vector engineering

We engineered the plentiCRISPRv2 vector to clone specific gRNAs targeting the *ATP5J2* gene. For the entire procedure, we followed the lentiCRISPRv2 and lentiGuide oligo cloning protocol provided by Zhang Lab (Sanjana, Shalem & Zhang, 2014); it consists of a stepwise procedure, i.e. oligonucleotides production, lentiviral vector digestion, oligonucleotides annealing and cloning into the digested vector.

Sequences of oligonucleotide guides recognizing the human f subunit gene were generated using the CRISPR design tool (http://www.crispr.mit.edu), and were chosen according to their quality score (>80) and to the number of off target sites (no off targets in mitochondrial genes). The chosen sequences are the following:

G1	5'- CACCGATGCGGGACTTCAGTCCTAG -3'
G2	5'- GGCGTCAGTTGGTGAGTGTC -3'
G3	5'- CTCACCAACTGACGCCATTT -3'
G5	5'- CACCGGACTCCAAAATGGCGTCAGT -3'

Briefly, 5 µg of the lentiviral CRISPR vector was digested with the *BsmBI* restriction enzyme for 1,5 h at 55°C, and then purified after gel electrophoresis separation, using the Gel Extraction Kit (Quiagen). The designed complementary oligonucleotides, that have to be inserted in the viral vector, were phosphorylated and annealed as following:

- 1 µl Oligo 1 (100 µM)
- 1 µl Oligo 1 (100 µM)
- 1 µl 10X T4 Ligation Buffer (NEB)
- 6.5 µl ddH_2O
- 0.5 µl T4 PNK (polynucleotide kinase, NEB)

The reaction was placed in a thermocycler using the following parameters:

37°C	30 min
95°C	5 min and then ramp down to 25°C at 5°C/min

At this point, the annealed oligonucleotides were diluted 1:200 into sterile water, and then cloned into the CRISPR digested vector. The ligation reaction was performed as following:

- 50 ng *BsmBI* digested vector
- 1 µl diluted oligonucleotides
- 1 µl 10X T4 Ligation Buffer (NEB)
- 1 µl T4 Ligase (NEB)
- X µl ddH_2O to a total of 11 µl

The ligation reaction was incubated 1 h at room temperature and used to transform Stbl3 bacteria.

3.1.3 Bacteria Transformation

For bacteria transformation we used the heat shock method. 50 µl of Stbl3 bacteria were mixed with 2 µl of plasmid DNA and the next following incubations were performed:

Incubation on ice for 30 min
Incubation at 42°C for 45 sec
Incubation on ice for 2 min

Transformed bacteria were then grown with shaking in 250 µL of SOC medium at 37°C for 1 h. Subsequently, the bacterial culture was spread on a prewarmed LB agar plate containing the antibiotic resistance carried by the vector. Plates were incubated overnight at 37°C. The day after colonies must be analysed with colony PCR, they should contain the vector cloned with the correct paired oligonucleotides.

3.1.4 DNA purification from transformed bacteria

After we had chosen a positive colony, we cultured it overnight at 37°C in 2 mL or in 250 mL (depending on the amount of DNA required) of LB medium supplemented with ampicillin (100 µg/mL). Then the plasmid DNA was isolated using the Plasmid Mini Kit (Invitrogen) or Plasmid Maxi Kit (Invitrogen), according to the manufacturer's instructions, and was quantified using the Nanodrop (Thermo Fisher Scientific). The plasmid DNA obtained after the mini kit extraction was sequenced to verify that no mutations occurred during the cloning procedure. The plasmid DNA obtained after the maxi kit extraction instead, was used to transfect HEK cells for the viral particles production.

3.2 Biological Samples

3.2.1 Cells and cell culture

We used human embryonic Kidney (HEK) 293T cells as host for lentivirus production and HeLa cells as cellular model. Cells were grown in 75 cm^2 Falcon flasks and incubated at 37°C in a 5% CO_2 humidified incubator. Once a confluence of 70-80% was reached, cells were split and plated again on 75 cm^2 flasks. Cells were first washed with PBS, detached with tripsin at 37°C, 5% CO_2 using 0.05% Trypsin-EDTA in Phenol red (GIBCO). To stop the action of trypsin, DMEM medium was added and cells were diluted 1:10 for their maintenance.

HEK cells and CTR, sh2-sh5 f KD HeLa cells were cultured in a standard DMEM culture medium: Dulbecco's modified Eagle's medium (DMEM; Lonza, Basel, Switzerland) supplemented with fetal bovine serum (10% v/v), glutamine (4 mM), penicillin and streptomycin (Thermo Fisher Scientific, Waltham, MA, USA). In CTR, sh2-sh5 f KD HeLa cells the medium was also supplement of 0.8 µg/mL puromycin (Sigma). This was the minimum concentration of the antibiotic able to kill all the untransduced cells in a titration curve.

CTR and f KO HeLa clones were cultured in Dulbecco's modified Eagle's medium (DMEM; Lonza, Basel, Switzerland) supplemented with fetal bovine serum (10% v/v), glutamine (4 mM), penicillin, streptomycin (Thermo Fisher Scientific, Waltham, MA, USA), Non-Essential amino acids solution (Sigma), MEM vitamin solution (Sigma) and uridine (Sigma).

For the glucose deprivation assay, CTR, sh2 and sh5 f KD cells were cultured in Dulbecco's modified Eagle's medium (DMEM without glucose and pyruvate, GIBCO) and supplemented with fetal bovine serum (10% v/v), glutamine (4 mM), penicillin, streptomycin (Thermo Fisher Scientific, Waltham, MA, USA), glucose 2.5 mM, and pyruvate 5 mM.

3.2.2 Lentivirus production and cell transduction

We used HEK 293T cells as packaging cells for lentiviral particle production.

To generate lentiviruses for the CRISPR/Cas9 procedure, HEK cells were transfected with the plentiCRISPRv2-EGFP control plasmid (as negative control), or the plentiCRISPRv2+gRNA (G1-5) targeting the *ATP5J2* gene. For the RNA interference approach instead, HEK cells were transfected with the pLKO.1 empty vector (as negative control), or pLKO.1+shRNA (sh1-5) targeting the f subunit mRNA.

Cells (2 millions) were plated in 10 cm^2 tissue culture plates in the standard culture medium without antibiotics, so that they reached 70-80% of confluence. The day after, cells were transfected with a combination of the following vectors: (i) retroviral packaging plasmids, encoding *gag, pol* (10 µg, pMDL) and *rev* (5 µg, pREV), (ii) the Vesicular Stomatitis Virus G glycoprotein (VSV-G) envelop plasmid (6 µg, pMD2.G); and (iii) the retroviral plasmid (20 µg). For the latter, 4

different vectors were used: plentiCRISPRv2-EGFP, and plentiCRISPRv2+gRNA; or pLKO.1 empty vector and pLKO.1+shRNA. After 24 h the medium was removed and replaced with 8 mL of standard culture medium, and 48 h post-transfection the virus-containing supernatants were collected and filtered. This medium was then used for cell transduction.

The day before virus transduction, 20,000 HeLa cells were plated in a six-well tissue culture plate. After 24 h the culture medium was removed and replaced with 2 mL of virus-containing supernatant particles supplemented with 6 µg/mL polybrene per well. The following day, the medium containing viruses was removed and replaced with fresh, standard DMEM medium. 48 h post-transduction the infected cells were subjected to puromycin selection (0.8 µg/mL; Sigma) for 7 days in order to kill all the untransduced cells.

3.2.3 f subunit KO cell generation

Viruses containing the different guides RNA (G1-5) were used to transduce HeLa cells as previously described. After puromycin selection, and once all the untransduced cells are dead, Western Blotting analysis was performed to check the efficiency of the CRISPR/Cas9 procedure. To have a full and stable KO of the f subunit, the mixed cell population with the lowest f subunit expression level, was used for single-cell cloning. To isolate single-cell clones, serial cell dilutions were performed until a final concentration of 0.5 cells/well. The last dilution was plated in a 96-well tissue culture plate. Single colonies were visible at the microscope after few days, and after 2 weeks these clones were expanded and analysed by Western Blotting to check the absence of the f subunit.

3.2.4 f subunit KD cell generation

Stable interference of the f subunit was obtained in a similar manner. HeLa cells were transduced with the collected viruses (containing the panel of shRNAs targeting the human f subunit mRNA) as described above. After 7 days of puromycin selection, cells were analyzed by Western Blotting to check the down regulation of the f subunit protein level. Cell populations with the lowest

expression level were chosen and cultured to check the stable downregulation of the f subunit.

3.2.5 Growth curve

HeLa cells that had been grown in flasks, were detached with trypsin, counted, and then seeded at 10,000 cells per well in a 12-wells tissue culture plate with DMEM (25 mM glucose). Cells were incubated at 37°C in a 5% CO_2 humidified incubator and cultured for 96 hours. After 24-48-72 or 96 hours cells were harvested with trypsin and counted with Burker's chamber.

3.2.6 Mitochondrial isolation

HeLa cells were transferred from 75 cm^2 flasks to 150 cm^2 flasks and to 500 cm^2 dishes in order to isolate a large amount of mitochondria. When a confluence of 90% was reached also in the biggest dishes, cells were washed with PBS, detached using a scraper and then collected in a 50 mL tube. After centrifugation at 1,000 x *g* for 5 min at 4°C, the supernatant was taken off, the cell pellet was suspended in a cold buffer composed of 250 mM sucrose, 10 mM Tris-HCl, 0.1 mM EGTA-Tris, pH 7.4, and transferred to a pre-cooled glass tube. Mitochondria were isolated after cell disruption with a glass-Teflon potter as previously described (Frezza, Cipolat & Scorrano, 2007). The concentration of mitochondria in the suspension was measured using the Pierce™ BCA Protein Assay Kit, and mitochondria were then used for BN-PAGE, swelling assay or Western Blotting analysis.

3.2.7 Cells permeabilization

HeLa cells were permeabilized as described below. Cells were detached with trypsin, centrifuged at 1,000 × g for 5 min, the supernatant was removed and the cell pellet was washed twice with PBS. The cell suspension was centrifuged at the same conditions as before and the PBS supernatant was discarded. The obtained cell pellet was gently suspended in KCl-based medium (130 mM KCl, 10 mM Mops-Tris, pH 7.4, containing 1 mM EGTA-Tris and 150 µM digitonin (Merck)), and was incubated for 20 min on ice. To stop the digitonin reaction, cells were

then diluted 1:10 in KCl medium containing 10 μM EGTA-Tris and centrifuged at 1,000 × g in a refrigerated centrifuge (4°C) for 5 min. The final pellet, containing permeabilized cells, was suspended and used for Mg^{2+}-ATP hydrolysis or CRC measurements.

3.3 Mitochondrial bioenergetics

3.3.1 Measurement of Oxygen Consumption Rate (OCR) and Extracellular Acidification Rate (ECAR)

The Oxygen Consumption Rate (OCR) and Extracellular Acidification Rate (ECAR) were measured in adherent cells using the XF24 Extracellular Flux Analyzer (Agilent technologies). The instrument measures in real time the extracellular flux changes of oxygen and protons in the medium immediately above adherent cells cultured in a XF24 cell culture microplate. Each XF24-microplate was coupled to a disposable sensor cartridge, embedded with 24 pairs of probes for measuring oxygen concentration and changes in pH.

HeLa cells that had been grown in flasks, were detached, counted, and seeded in microplates at 50,000 (CTR, sh2 or sh5 f KD) or 60,000 (f KO) cells per well. The cells were seeded in order to reach a homogeneous monolayer (90% of confluence) for the next day. Cells were incubated at 37°C in a 5% CO_2 humidified incubator for 24 h. The day after, about 30 min before the experiment, the culturing medium was removed from the cells and replaced with 670 µl of Seahorse medium prewarmed at 37°C to allow temperature and pH equilibration. The Seahorse medium used was: DMEM (Sigma D5030) supplemented with 25 mM or 2.5 mM glucose, 10 mM sodium pyruvate and 2 mM glutamine. The microplates were then kept at 37°C until used for measurement.

A titration with carbonyl cyanide 4-(trifluoromethoxy) phenylhydrazone (FCCP) was performed for each different cell line to determine the optimal FCCP concentration that stimulates respiration maximally, which was found to be 0.1µM for all cell types. This step is necessary to identify the optimal FCCP concentration that maximally stimulates respiration, and to avoid the toxic effect at higher doses.

During the experiment before the sequentially addition of the chemicals to the cells, we measured the baseline respiration. The OCR after each injection was analyzed three times for 2 min and the changes in oxygen and pH were monitored.

In details, when the baseline respiration was established, 70µl of each solution containing oligomycin, FCCP, rotenone and antimycin A were sequentially added to each well to reach a final concentration of 1 µg/ml oligomycin, 0.1 µM FCCP,

1 µM rotenone and antimycin A (Figure 16). All the compounds were purchased from Merck. Oligomycin inhibits F-ATP synthase activity and the coupled proton pumping from the intermembrane space to the mitochondrial matrix. Thereby, the electron flow within the respiratory chain is strongly reduced as protons can no longer be transported to the same extent as before, and as consequence the oxygen consumption of the cells decreases (Figure 16). FCCP is a membrane permeable uncoupling agent that binds protons and carries them from the intermembrane space to the matrix. It is used to maximally stimulate oxidative phosphorylation, and indeed an increase in oxygen consumption can be visualized during the experiment. Rontenone and antimycin A inhibits complex I and complex III of the respiratory chain, respectively. Upon the addition of those chemicals only the non-mitochondrial oxygen consumption remains detectable (Figure 16).

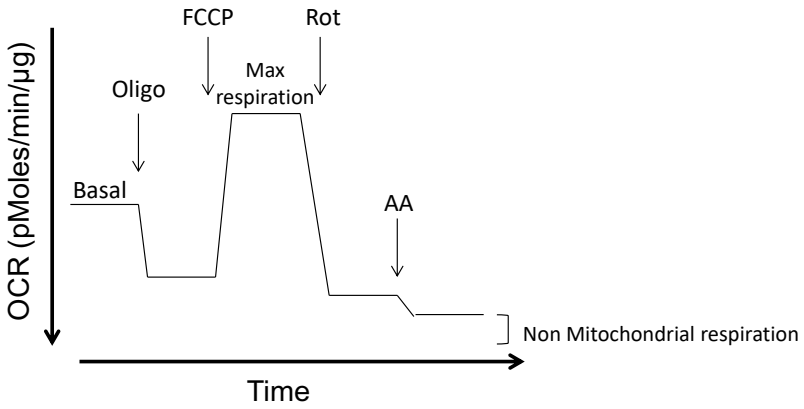

Figure 16. Schematic representation of a Seahorse experiment. Oxygen consumption rate (OCR) in plated cells following additions of Oligomycin (oligo) to inhibit the F-ATP synthase, FCCP to reach the maximal respiration, and Rotenone (Rot) and Antimycin A (AA) to inhibit complex I and complex III, respectively.

To ensure that alterations in respiration are not due to differences in the protein content, the cells of each well were collected after the measurement, and the protein content was determined using the Pierce™ BCA Protein Assay Kit.

3.3.2 Measurement of ATP hydrolysis

The maximal catalytic activity of F-ATP synthase can be assessed by measuring the rate of hydrolysis of ATP. ATPase activity was measured in permeabilized HeLa cells (obtained as described above) at the concentration of 0.4×10^6 cells/well in a final volume of 0.2 mL. For the analysis we used an ATP-regenerating system in which a constant ATP level is provided to the enzyme

(Figure 17). CTR, sh2 or sh5 f KD permeabilized cells were suspended in a buffer (50 mM KCl, 50 mM Tris-HCl, 30 mM sucrose, 4 mM $MgCl_2$, 2 mM EGTA, pH 7.4) supplemented with 4 units/ml pyruvate kinase (PK), 3 units/ml lactate dehydrogenase (LDH), 4 mM phosphoenolpyruvate (PEP), 2 mM ATP, 0.2 mM NADH, 10 µM alamethicin, and 10 µM sodium decavanadate. The oxidation of NADH was measured spectrophotometrically at 340 nm, 37°C using a Fluoroskan Ascent FL (Thermo Electron, Waltham, MA, USA) plate reader, and was used to measure the amount of ATP hydrolyzed. The hydrolysis rate was next quantified as nmol of ATP hydrolyzed per mg of protein per minute. Inhibition of Mg^{2+}-ATPase activity was obtained by adding 2 µM oligomycin to wells.

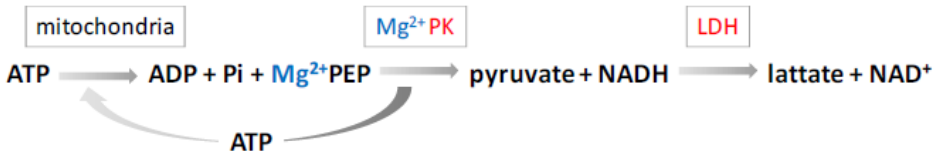

Figure 17. ATP-regenerating system. The reaction sequence is: F-ATP synthase converts ATP in ADP + P_i , the PK uses these substrates and transfer P_i from PEP to ADP, yielding one molecule of ATP and pyruvate. To prevent reaction saturation, pyruvate is rapidly metabolized by lactate dehydrogenase (LDH) that converts it into lactate at the expense of NADH. Thus, the ATP hydrolysis is directly proportional to the NADH oxidation.

3.4 Permeability transition

3.4.1 Measurement of matrix swelling

The evaluation of matrix swelling is used to assess pore opening as well as changes in its size. This can be achieved by measuring optical density changes of the mitochondrial suspension in response to various stimuli. Indeed, intact mitochondria scatter light at 540 nm, and an increase in matrix volume (due to pore opening) leads to a decrease of light scattering (Figure 18). Changes in optical density of the mitochondrial volume were monitored in a 96-well transparent plate, in a final volume of 0.2 mL. Freshly prepared mitochondria from CTR, sh2 or sh5 f KD HeLa cells were suspended at the concentration of 0.5 mg/ml in a KCl-based medium (130 mM KCl, 10 mM MOPS-Tris, 10 µM EGTA) or sucrose-based medium (0.2 M sucrose, 10 mM MOPS-Tris, 10 µM EGTA) supplemented with 5 mM succinate-Tris and 1 mM Pi-Tris. Absorbance was read for about 5 min to get the baseline value using a Multiskan EX (Thermo

Scientific) plate reader. Then, different concentration of Ca^{2+} (25-50-100 µM) were added, as indicated in Figure legends, to induce mitochondrial swelling, and the absorbance changes were followed for 30 min. Alamethicin 10 µM was added at the end of each experiment to get the maximal mitochondrial swelling (Figure 18). Fraction of swollen mitochondria is calculated as in (Petronilli et al., 1993).

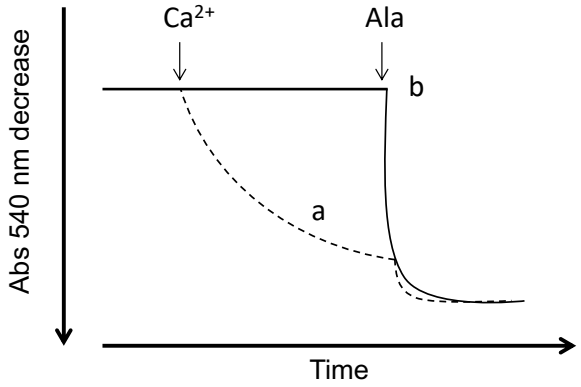

Figure 18. Schematic representation of absorbance changes as indicator of mitochondrial swelling. Addition of Ca^{2+}(PTP inducer) to isolated mitochondria leads to changes in mitochondrial volume (swelling), characterized by a decrease in Abs 540 nm (trace a), compared with a control trace without any additions (trace b). At the end of the experiment Alamethicin (Ala) is added to get the maximal mitochondrial swelling.

3.4.2 Measurement of mitochondrial Ca^{2+} retention capacity

The mitochondrial calcium retention capacity (CRC) assay was used to assess Ca^{2+} sensitivity of the permeability transition pore opening in permeabilized HeLa cells. Extra-mitochondrial Ca^{2+} was measured with Ca^{2+} Green-5N fluorescence probe using a Fluoroskan Ascent FL (Thermo Electron, Waltham, MA, USA) plate reader. Calcium Green-5N (Invitrogen) is a Ca^{2+} sensitive dye not able to cross the mitochondrial inner membrane; this probe is not fluorescent by itself, but it emits a fluorescent signal at a wavelength of 532 nm, upon Ca^{2+} binding. During the CRC measurement, every 6 min a pulse of 2.5 µM $CaCl_2$ is added to the medium of the cells, increasing the fluorescence intensity. As the plasma membrane is permeabilized, Ca^{2+} is taken up by mitochondria leading to a decrease in fluorescence until the next Ca^{2+} pulse is added (Figure 19a). Thereby, traces consisting of peaks are generated, these traces represent sequential Ca^{2+} additions followed by mitochondrial Ca^{2+} uptake (Figure 19b). When the cells are exposed to a Ca^{2+} concentration equal to the threshold for PTP opening,

mitochondria undergo permeability transition, the PTP opens and the fluorescent signal increases (Figure 19c). Briefly, CTR, sh2 or sh5 cells were permeabilized and were resuspended at the concentration of $10^6 \times mL^{-1}$ in a KCl- based medium (130 mM KCl, 10 mM MOPS-Tris, 10 µM EGTA) or sucrose- based medium (0.2 M sucrose, 10 mM MOPS-Tris, 10 µM EGTA) supplemented with 5 mM succinate-Tris, 1 mM Pi-Tris and 0.5 µM Ca^{2+} Green-5N, pH 7.4, to a final volume of 0.2 mL. At the end of the measurement the experiment was stopped, and the cells were collected in a clean 1.5 mL tube to quantify the amount of protein using the Pierce™ BCA Protein Assay Kit.

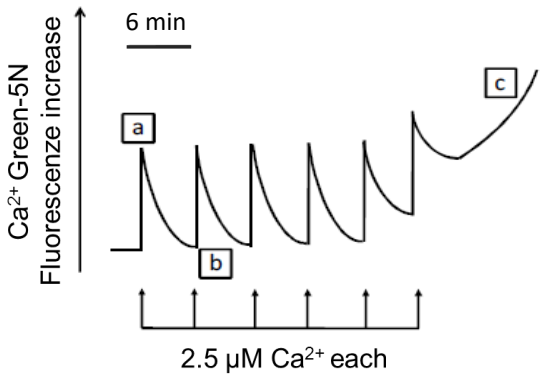

Figure 19. Ca^{2+} Retention Capacity (CRC) assay. Extra-mitochondrial Ca^{2+} was measured with the Calcium Green-5N fluorescent probe. (a) Ca^{2+} pulses addition leads to a sudden increase in fluorescence values because of the Ca^{2+} binding with the dye. (b) Energized mitochondria take up available cations, resulting in a decrease of the signal. (c) Once a certain matrix Ca^{2+} threshold is reached, the PTP opens leading to cations release and to a quick increase in fluorescence.

3.5 Preparation of cell lysates

Cells were plated in a 10 cm^2 tissue culture dish, once confluency was reached, they were washed with 1X PBS, detached with tripsin, resuspended in DMEM in 1:10 dilution and transferred to a 15 mL Falcon. They were centrifuged at 1,000 x g for 5 min. The resulting supernatant was discarded, and the pellet was resuspended in a small volume of lysis buffer (150 mM NaCl, 20 mM Tris, 5 mM EDTA-Tris, pH 7.4 with the addition of 1% (v/v) Triton X-100, 10% (v/v) glycerol) supplemented with protease inhibitor cocktail (PIC, Sigma-Aldrich; 1:100). To lyse cells and solubilize proteins cells were kept on ice for 30 min, and then the solution was cleared by centrifugation at 18,000 × g for 20 min, 4°C. The

protein concentration of the collected supernatant was measured using Pierce™ BCA Protein Assay Kit.

3.6 Sodium Dodecyl Sulfate-Polyacrilamide Gel Electrophoresis (SDS-PAGE) and Western Blotting

SDS-PAGE and Western Blotting were used to analyse subunit composition of the F-ATP synthase enzyme and OXPHOS complexes content. 50 µg of proteins from whole cell lysates, or 30 µg of mitochondrial proteins we denatured with 1X Laemmli buffer (500 mM Tris-HCl, 50% v/v glycerol, 10% w/v SDS, 25% v/v β-mercaptoethanol and 0.2% w/v bromophenol blue, pH 6.8) at 90°C for 5 min. Samples were separated by a polyacrylamide gradient gel (NuPAGE™, 12% Bis-Tris, Invitrogen) at 20 mA constant current until the dye front reached the bottom of the gel. The separated proteins were transferred electrophoretically onto nitrocellulose membranes (Bio-Rad) using the XCell II Blot Module (Invitrogen). The transfer was performed at 400 mA for 1 h using the NuPAGE® Transfer Buffer supplemented with 20% methanol. Before proceeding, the membrane was stained with Red Ponceau dye (Merck) to check transfer efficiency. The membrane was saturated for 1 h at room temperature with 5% (w/v) non-fat dry milk in PBS buffer supplemented with 0,1% Tween-20 (T-PBS), as blocking solution, and then incubated overnight with the following primary antibodies: anti-OXPHOS complexes (1:1000, Abcam, OXPHOS Human WB Antibody Cocktail in T-PBS); anti-β, -α, -OSCP, -b, -f, -e, -g subunits and IF1 (1:1000, Abcam in T-PBS); anti-γ subunit (1:1000, Genetex in T-PBS); prohibitin (1:1000, NeoMarkers); and citrate synthase (1:1000 Abcam in T-PBS).

The day after, membranes were then rinsed three times with T-PBS to remove unbound reagents, and incubated for 1.5 h with the secondary antibody (anti-mouse, -rabbit and -goat 1:5000) prepared in the blocking solution. The membrane was washed again three times in T-PBS buffer plus 0.1% Tween 20 and developed using the UVITEC (Eppendorf) according to the manufacturer's protocol.

3.7 Electrophysiology

Patch Clamp analysis, was used to study the electrophysiological behavior of the mitochondrial channel, by measuring its activity across the IMM. Patch clamp experiments were performed as follows. Mitochondria from CTR or f KO HeLa cells were diluted (1:100) in an hypotonic solution of 30 mM Tris–HCl (pH 7.3), and left on ice for 10 min to obtain mitoplasts (i.e. mitochondria without the outer membrane). The suspension was then inserted in the patch clamp chamber and washed with the recording medium. Patch clamp was performed as previously described (Szabo et al., 2005) using a solution of 150 mM KCl, 0.3 mM $CaCl_2$, 10 mM Hepes pH 7.3 both in the pipette and in the bath. Additional $CaCl_2$ was possibly dissolved in the bath during experiments. Data were acquired and analyzed with the PClamp8.0 program set as described in (De Marchi et al., 2006). Inducers and inhibitors were added during the experiment.

G_{max} is the average of the maximal current conductance recorded in symmetrical 150 mM KCl solutions in the successful trials. Given the presence of multiple conductance sub-states, G_{mean} is calculated as the average of the mean conductance measured during channel activity (zero-current values were omitted) of each trial. The Q parameter represents the average of the total charge passing through the channel in a time rage of 4 seconds, centred at the maximal conductance point for each recorded experiment.

3.8 Nonyl Acridine Orange (NAO) staining

NAO staining has been used to measure the mitochondrial content in cells. The binding of the dye to mitochondria is reported to be independent of the membrane potential, and it binds specifically cardiolipin, a phospholipid located exclusively in bacterial and mitochondrial membranes where it is intimately associated with the enzyme complexes of the respiratory chain.

CTR, sh2 and sh5 f subunit KD cells, that had been grown in flasks, were detached, counted, and then were seeded at 50,000 cells per well in a 24-wells tissue culture plate with standard DMEM medium. Cells were incubated at 37°C in a 5% CO_2 humidified incubator, and cultured for 24 hours. The day after, The

NAO dye (200 nM, Sigma) was added to the culture medium, and cells were stained for 30 min at 37°C in a 5% CO_2 humidified incubator. Cells were detached with trypsin, centrifuged at 1,000 x g for 5 min, and suspended in 1X PBS. Mitochondrial mass was assessed by flow cytometry using the FACS Canto II flow cytometer (Becton Dickingson).

3.9 Transmission Electron Microscopy

To analyze the mitochondrial morphology we used the Transmission Electron Microscopy (TEM). Briefly, HeLa cells that had been grown in flasks, were detached, counted, and then were seeded at 30,000 (CTR, sh2 or sh5 f KD) or 40,000 (f KO) cells per well in a 24-well tissue culture plate. Cells were incubated at 37°C in a 5% CO_2 humidified incubator and cultured for 24 h in order to reach 70-80% of confluence. The day after, the growth medium was discarded; cells were washed with phosphate-buffered saline (PBS), fixed with 2.5% (v/v) glutaraldehyde in 0.1 M sodium cacodylate buffer, pH 7.4 at 4°C overnight, and incubated with a solution of 1% (v/v) of tannic acid for 1h. The samples were postfixed with 1% (v/v) osmium tetroxide in 0.1 M sodium cacodylate buffer for 1 hour, 4°C. After three washes in water, samples were dehydrated in a graded ethanol series and embedded in an epoxy resin (Sigma-Aldrich). Ultrathin sections (60-70 nm) were obtained with an Ultrotome V (LKB) ultramicrotome, counterstained with uranyl acetate and lead citrate and viewed with a Tecnai G2 (FEI) transmission electron microscope operating at 100 kV. Images were captured with a Veleta (Olympus Soft Imaging System) digital camera.

3.10 Sequence analysis and homology prediction of the human f subunit 3D structure

The 3D structure of dimeric Fo from *Saccharomyces cerevisiae* (PDBid: 6B2Z) was visualized with Chimera (Pettersen 2004). The 3D structure of the human f subunit was predicted with SWISS model (Bienert et al., 2017), selecting 6B2Z:chain f as template. Networks of interacting residues were calculated with RING 2.0 (Piovesan, Minervini & Tosatto, 2016). The sequences of the f subunit from *Saccharomyces cerevisiae*, *Yarrowia lipolytica*, *Bos Taurus* and *Homo*

sapiens were retrieved from Uniprot, aligned with T-coffee (Notredame, Higgins & Heringa, 2000), and visualized with Jalview (Waterhouse et al., 2009).

4 RESULTS AND DISCUSSION

4.1 Inspection and sequence analysis of the f subunit

According to the structural data presented in the introduction, the f subunit has an important role in dimer stabilization in *Yarrowia lipolytica* (Hahn et al., 2016), *Saccharomyces cerevisiae* (Guo, Bueler & Rubinstein, 2017), and as recently reported also in mammals (Gu et al., 2019).

To better understand the position and the interactions of the f subunit, we performed some bioinformatic analysis in collaboration with Prof. Silvio C.E. Tosatto and Dr. Giovanni Minervini from our Department, and we focused on the dimeric F_O domains from *Saccharomyces cerevisiae* (Guo, Bueler & Rubinstein, 2017) and on the tetrameric F_O domains from *Sus scrofa domesticus* (Gu et al., 2019). The analyses performed on *Saccharomyces cerevisiae* showed that some residues in the C-terminus of the f subunit form a number of hydrophobic interactions with the two a subunits, each belonging to a monomeric F_O (indicated as a or a', Figure 20A, right panel). The high number of contacts present in this specific region also suggests that the f subunit may play a role in stabilizing the a-a' dimer within the membrane, thus contributing to F-ATP synthase dimer stability in yeast. The analyses performed on the mammalian tetrameric structure of the F-ATP synthase (Figure 20B) showed that also in mammals subunit f contacts many different subunits of the F_O domain (g, e, a and DAPIT subunits) and also some of the peripheral stalk (b, d subunits). The quality of the Cryo-EM structure in this region however was not sufficient to highlight the specific residues that are involved in these interactions (for almost all the amino acids the side chains are missing), so in the zoomed area we present just the chains of the aforementioned subunits that are at a distance of interaction, but we cannot say exactly how they are interacting.

The **human** f subunit has not been resolved yet, and therefore we analyzed which of the structural characteristics of the yeast subunit are preserved in humans. Interestingly, the yeast hydrophobic residues F75, I80, F82 are functionally conserved in the human sequence (Figure 20A, B). The structural role of the yeast Y89 pointing to the a subunit of the other monomer (a' in Figure 20A) might be replaced by Y82 in humans. In yeast, there is also an electrostatic interaction, which bridges residues E87 of the f subunit with R19 of the a subunit of the same monomer (Fig. 20A). Taking into consideration the hydrophobic environment of

the F_O sector, we suspect that this f:E87- a:R19 electrostatic interaction is relevant in arranging the f subunit in the direction of the a subunit in the inner membrane. In the human sequence the same region is enriched in hydrophilic amino acids, which may form multiple hydrogen bonds with the a subunit, replacing the role of the yeast E87, which is substituted by S81 (Figure 20C). Downstream the aforementioned part of the f subunit, there is the hydrophilic C-terminal end, this domain is highly conserved among species, indeed homology prediction of the 3D structure of the human f subunit suggests that its conformation is similar to the yeast and porcine one (Figure 20D).

Our bioinformatics study shows that in the region 64-83 the human f subunit forms a long α-helix characterized by several hydrophobic residues that well fit in a membrane environment.

In conclusion, sequence analysis and homology prediction indicates that the human f subunit shares the C-terminal 3D organization with its yeast homologue, as well as key interactions with the a subunits at the monomer-monomer interface. These interactions with the a subunit are also well described in the published structures of the F-ATP synthase (Guo, Bueler & Rubinstein, 2017, Hahn et al., 2016, Srivastava et al., 2018), and were recently confirmed in the mammalian Cryo-EM structure of the F-ATP synthase (Gu et al., 2019).

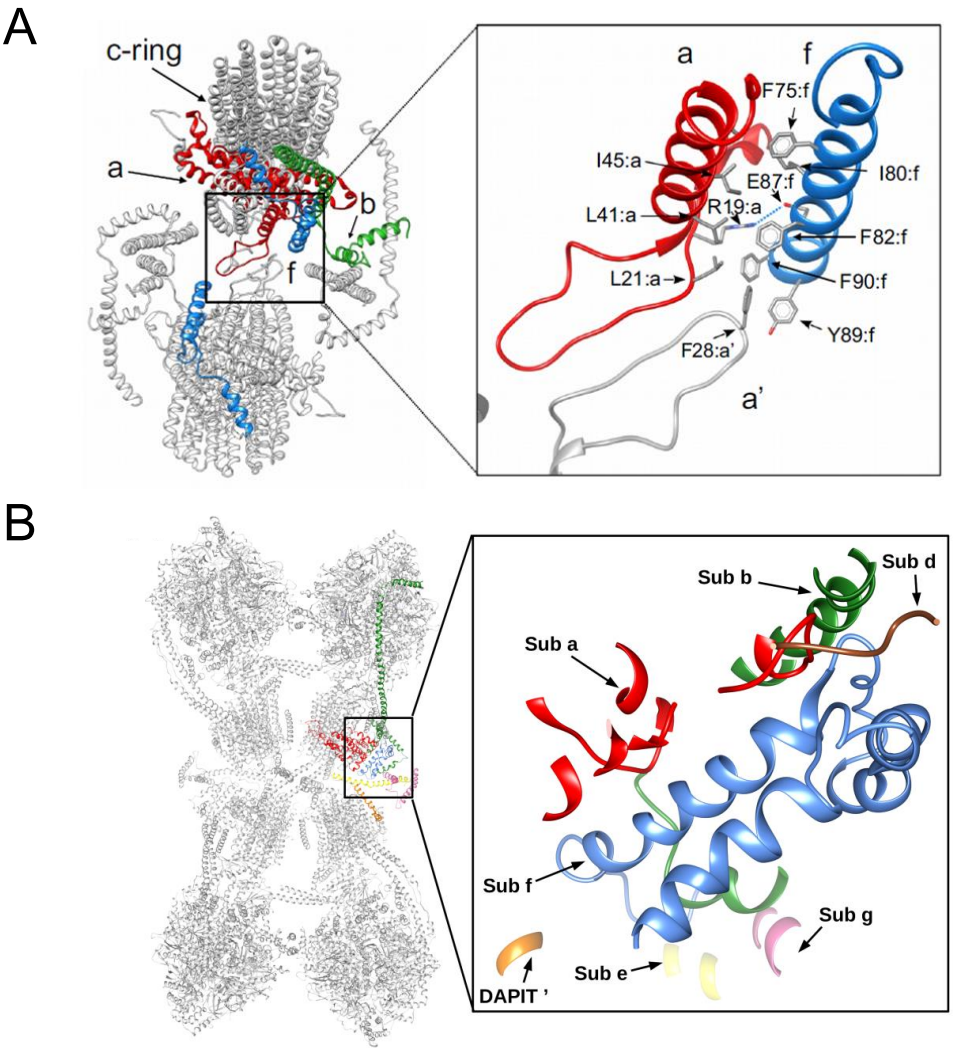
A
c-ring
a
b
f
a
f
F75:f
I45:a
E87:f
I80:f
L41:a
R19:a
F82:f
L21:a
F90:f
Y89:f
F28:a'
a'
B
Sub b
Sub d
Sub a
Sub f
Sub g
Sub e
DAPIT '
C
Homo sapiens
Bos taurus
Saccharomyces cerevisiae
Yarrowia lipolytica
Helix of interaction with subunit a
D
Pro25
Pro41
S. cerevisiae
Leu92
H. sapiens
Pro8
His94

Figure 20. Overview of the Fo-Fo dimer of F-ATP synthase and f subunit sequence/3D structure analysis. Overview of the subunits in the Fo sector according to the latest **(**A) Cryo-EM yeast structure (Guo, Bueler & Rubinstein, 2017) or (B) Cryo-EM mammalian structure (Gu et al., 2019). The 3D structure of the f subunit is presented in blue, while subunits a, b, g, e and DAPIT are presented in red, green, purple, yellow and orange respectively. Right (zoomed area), yeast or mammalian residues of the subunit f forming interactions with the other subunits of the F_O domain. (C) Sequence alignment of the f subunit from Homo sapiens, Bos taurus, Saccharomyces cerevisiae and Yarrowia lipolytica. Predicted α-helixes are highlighted (α1-4), including α3 which is responsible for the interactions with a subunit in the Cryo-EM structure (PDBid: 6B2Z). Residue numbers refer to the human sequence. (D) Homology 3D model of the human f subunit (right) superimposed to the corresponding subunit from Saccharomyces cerevisiae (left). Bottom, a structure-based sequence alignment. Blue and orange dots indicate sequences from yeast or human, respectively. Red boxes include regions that are structurally related in the two species, with grey labels highlighting regions with residue conservation.

4.2 Characterization of f subunit role(s) in human cells

In order to elucidate the function of the human f subunit in enzyme assembly and catalysis, mitochondrial morphology and PTP modulation we used two different approaches. The (i) CRISPR/Cas9, and the (ii) RNA interference technique for a stable knock out or knock down of the f subunit protein, respectively. Both strategies were performed in a cell model that heavily relies on glycolysis for ATP synthesis, i.e human cervical carcinoma HeLa cells.

4.2.1 f KO cells

To obtain genetic ablation of the f subunit in HeLa cells we used the CRISPR/Cas9 genome engineering tool (Doudna, Charpentier, 2014). With this technique, it is possible to precisely disrupt the h*ATP5J2* gene open reading frame (ORF) using the plentiCRISPRv2 vector (see Materials and Methods). We designed and tested four gRNAs (see Materials and Methods) targeting different regions of the f subunit ORF in order to find the most potent one. The best combination of gRNAs was the G_1+G_5, but the western blot analysis clearly showed the presence of a mixed population of cells (Figure 21A upper panel): there is just a decrease of the f subunit protein level and not its full ablation. To get an homogenous population of full KO cells, we performed single cell cloning through several cell dilutions, and we selected single-cell clones. Among them as expected we identified some wild type clones, with the band of the f subunit at the right molecular weight (15kDa), and some mutated ones where we could not detect the protein, confirming the disruption of the human gene (Figure 21A lower panel). These f KO cells were then used to assess their biochemical phenotype and understand the f importance in human cells.

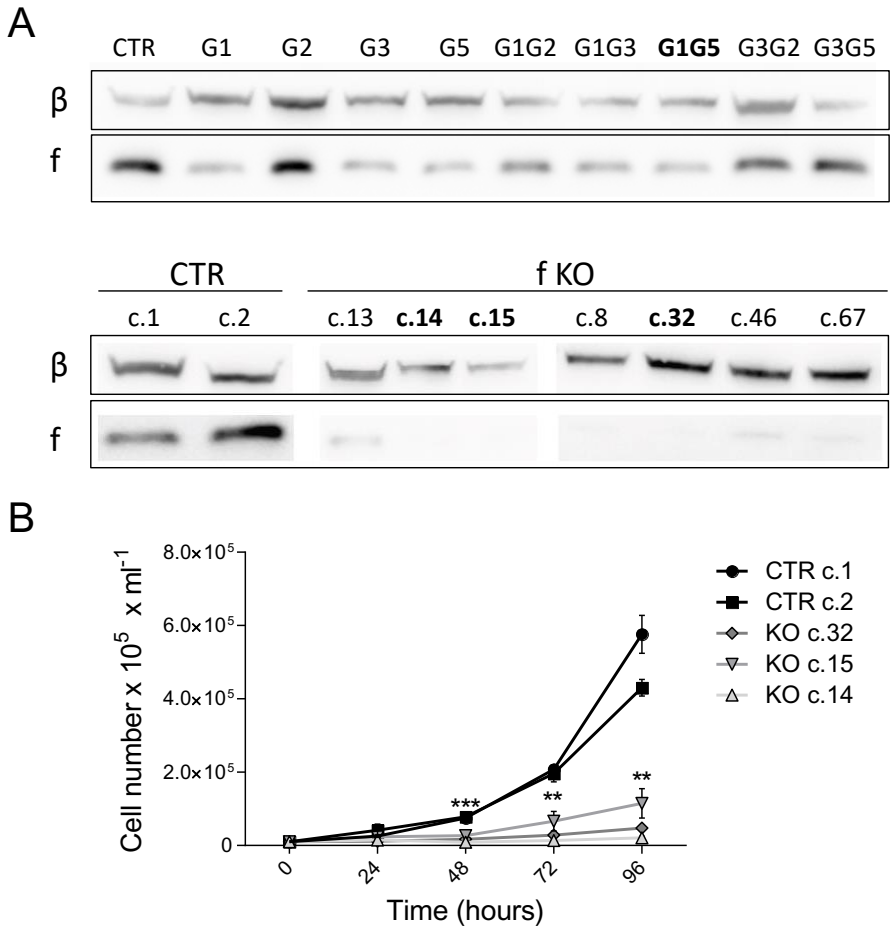

Figure 21. The subunit f knock out through the CRISPR/Cas9 technology affects HeLa cell growth. (A) Upper panel, Western Blotting of the F-ATP synthase β and f subunits in lysates of control (CTR) or f subunit knocked out (f KO) HeLa cells, generated by viral infections with scramble (CTR), or different oligonucleotide guides (G1, G2, G3, G5) for CRISPR/Cas9 genome editing. Lower panel, clones were obtained by cell cloning and puromycin selection of the mixed cell population, gained from the G1 and G5 combination. (B) Growth curves of CTR (c.1 and c.2) and f KO (c.14, c.15 and c.32) HeLa clones. Cells are detached and counted every 24 hrs. Data are mean of 3 independent experiments ± SEM (**P<0.01; ***P=0.00015 among CTR c.1 and f KO c.15).

4.2.1.1 Effects of f subunit KO on cell growth, mitochondrial respiration, glycolytic rate and enzyme assembly

KO of f subunit slowed down the rate of cell growth compared to CTR cells (Figure 21B). The three f KO clones (14, 15, 32) showed the same decrease of cell growth, and this behaviour became statistically significant after 48 hours of culture. After 72-96 hours, the growth of KO clones levelled off possibly because of high mortality or senescence. To facilitate cell growth and survival of these f KO cells, we replaced the high glucose DMEM medium, with a new medium

enriched in amino acids, vitamins and uridine. We took advantage of the medium used for culture of ρ° cells, which do not have functional mitochondria because they lack mitochondrial DNA, and they rely entirely on glycolysis for ATP synthesis.

The metabolism of these f-null cells was measured monitoring both ATP synthase activity and glycolysis. Hereinafter, for all the experiments, just CTR clone 1 and f KO clone 15 were used.

We assessed oxygen consumption rate (OCR) and extracellular acidification rate (ECAR) with the sensitive Seahorse technology. Basal respiration largely reflects mitochondrial oxygen consumption linked to ATP synthesis, as shown by its inhibition with oligomycin (Oligo). Oligomycin is used to inhibit the F-ATP synthase activity by suppressing the flux of protons from the IMS to the mitochondrial matrix, through the channels formed at the c-a subunit interface in the F_O domain. Addition of the protonophore FCCP, after oligomycin, allows to determine the maximal respiratory rate; the subsequent addition of rotenone, (selective inhibitor of respiratory complex I) and antimycin A (inhibitor of complex III), allows to define the residual non mitochondrial respiration. As the impact of FCCP may be variable depending on the cell line and on the cell monolayer, the minimal amount of FCCP necessary to maximally stimulate oxygen consumption was determined for each experiment, using an FCCP titration curve.

We observed a drastic decrease in basal and maximal (FCCP-stimulated) respiration in f subunit KO cells. (Figure 22A-B). This result was also associated to an increased glycolysis in f subunit KO cells, measured in situ at basal condition monitoring the ECAR (Figure 22D-E). In line with this ECAR result, we observed that f subunit depletion led to rapid acidification of cellular media, indicating a shift in metabolism to a more glycolytic state. Furthermore, KO of the f subunit abolished the oligomycin-sensitive respiration, calculated subtracting from the basal respiration the one obtained after oligomycin addition (Figure 22C). The same oligomycin insensitivity was observed in yeast mutant strains lacking the f subunit (Spannagel et al., 1997).

Interestingly, in the f KO cells an FCCP-stimulation was seen, suggesting that

probably the respiratory defects rely on the activity and correct assembly of the F-ATP synthase enzyme and not on the activity of the respiratory chain complexes.

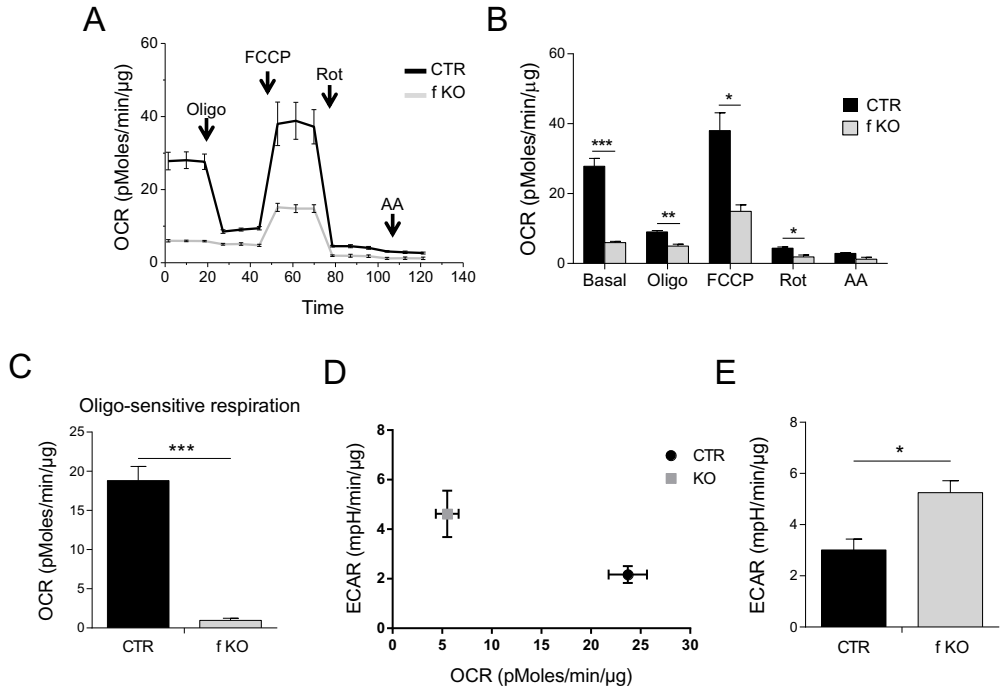

Figure 22: The subunit f knock out through CRISPR/Cas9 technology affects HeLa bioenergetics. (A) Oxygen consumption rate (OCR) of control clone 1 (CTR) and f-null clone 15 (f KO) HeLa cells in situ, seeded at the concentration of 50000 and 60000 cell/well, respectively. A representative experiment is shown ± SD. OCR is measured before (basal) or after treatment with oligomycin (Oligo); carbonyl cyanide p-(trifluoromethoxy) phenylhydrazone (FCCP); rotenone (Rot) and antimycin A (AA). The quantification of the protein level in each well at the end of the measurements confirmed a comparable cellular content in CTR and f KO wells. (B) Mean OCR of 3 independent experiments ± SEM (*P<0.05, **P=0.0038, ***P=0.00063). (C) Mean oligomycin-sensitive respiration of 3 independent experiments ± SEM (***P=0.0062), measured subtracting at the basal respiration the one obtained after oligomycin addition. (D) Representative plot distribution of extracellular acidification rate (ECAR) and OCR in CTR clone (black square) and f-null clone (grey square) during basal respiration ± SD. (E) Mean ECAR during basal respiration of 3 independent experiments ± SEM (*P=0.024)

To further clarify the biochemical results obtained in the f KO cells, we performed a Western Blotting analysis assessing the abundance (i) of the OXPHOS complexes, and (ii) of the other subunits of the F-ATP synthase enzyme. We found that the content of the respiratory chain complexes (CI-CII-CIV-CIV), was significantly reduced compared to prohibitin (Figure 23A). For this analysis, we assessed the expression levels of a panel of subunits (one for each complex) important for the full assembly or functioning of the specific

complex. This result was in line with the respiratory profile observed in the f KO cells, indicating a metabolic shift toward glycolysis. Nevertheless, the few OXPHOS complexes still present in the IMM are enzymatically active since mitochondrial respiration can be further stimulated using the uncoupler. Moreover, KO of f subunit caused a decreased amount of other subunits of the F-ATP synthase, like the e-g-b-subunits, and of subunits a and c, known targets of oligomycin (Figure 23B). This latter feature matches the oligomycin-insensitive respiration that was seen in the f KO cells; indeed the targets of the drug are not present anymore, and this is a possible explanation for the respiratory profile. Given the lower levels of subunits a and c subunit in the f subunit KO cells, the rate of proton translocation by F-ATP synthase slows down. A similar phenotype was observed for a G8969>A mutation of subunit a in a patient with nephropathy. Yeast with an equivalent mutation failed to grow on non-fermentable carbon sources due to the lack of F_O-mediated proton translocation (Skoczen et al., 2018, Wen et al., 2016).

As already mentioned, the f subunit localizes at the dimer interface but also contributes to formation of the peripheral stalk (Guo, Bueler & Rubinstein, 2017, Srivastava et al., 2018) where it is highly connected with virtually all subunits of the F_O sector (e,g,b) as also demonstrated with cross linking experiments (Stephens, Nagley & Devenish, 2003, Lee et al., 2015). The drastic phenotype seen in subunit f KO cells is probably due to lack of proper enzyme assembly and to decreased overall stability of the enzyme. Thus, taken together, the f subunit is essential for F-ATP synthase assembly and function.

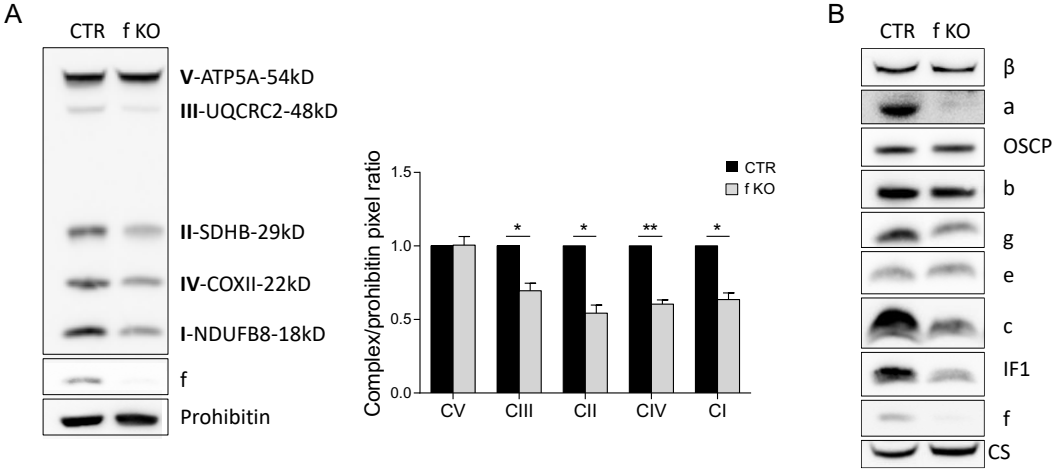

Figure 23. Knocking out of the subunit f decreases the level of OXPHOS complexes and of F-ATP synthase subunits. (A) Western Blotting for the indicated OXPHOS complex subunits, f subunit of F-ATP synthase and prohibitin (loading control) is assayed on clone 1 (CTR) and clone 15 (f KO) mitochondria. Right panel, quantification of 3 independent experiments is expressed in Complex/prohibitin pixel ratio (% of control) ± SEM. P values are 0.027 for CIII, 0.014 for CII, 0.005 for CIV, 0.015 for CI). (B) Western Blotting of control or f KO cell lysates recognizing the subunits of the F_1 and F_O sectors of F-ATP synthase and citrate synthase as loading control.

The phenotype we observed perfectly matches what described in yeast (Spannagel et al., 1997) and human HAP1 cells (He et al., 2018). In yeast the lack of the f protein was lethal, the disrupted strain was unable to grow on 2% lactate or glycerol medium, and was associated to a decreased abundance of other F_O subunits; in human f-null HAP1 cells a decrease in mitochondrial respiration as well as in the content of subunits a and A6L was seen. Also in our model the ablation of the f subunit had a significant effect on F-ATP synthase assembly and caused decreased F-ATP synthase activity, which may explain the effect on respiration. These alterations in enzyme assembly may also have a direct impact on *cristae* membrane structure (see below).

4.2.1.2 Effects of f subunit KO on PTP channel activity

The electrophysiological features of the PTP were analysed by Dr. Andrea Carrer by patch clamp analysis of mitoplasts (i.e. mitochondria devoid of the outer membrane). In 9 successful trials with mitoplasts deriving from 8 different preparations of CTR mitochondria we observed single channel activity displaying multi-conductance substates (indicated as O1, O2) (Figure 24A). As expected, the maximal conductance recorded was about 1070 ± 86 pS (O2, Figure 24A), in the range of the one already described for the MMC in mitoplast (Szabo, Bernardi & Zoratti, 1992, Szabo, De Pinto & Zoratti, 1993) and in reconstituted F-ATP synthase (Urbani et al., 2019, Giorgio et al., 2013). Numerous subconductance states (O1, Figure 24A) were recorded at 300-800 pS, and this is the typical behaviour of the MMC (Giorgio et al., 2013, Urbani et al., 2019). The high-conductance channel of control mitochondria was inhibited by 1 mM Gd^{3+}, a general inhibitor of cation channels able to block the MMC/PTP (Carraro et al., 2018).

In f KO cells a striking difference was observed. The f-null mitoplasts exhibited

PTP currents only in 5 out of 12 trials, and the channel activity reached the maximal conductance of 1000 pS just in 1 out of the 5 successful trials. This high conductance opening was in a flickering behaviour, it rapidly switched to other long-lasting sub-states. The lower sub-states, were the only currents measurable in the remaining 4 successful trials out of 12 experiments, with a conductance of about 550 pS (O1, Figure 24B). Summarizing, the average maximal and mean conductance activity were significantly lower compared to CTR mitoplasts, as evident from the current traces, the corresponding amplitude histograms (on the right of the current traces) and their quantification (Figure 24C-D). Moreover, also the Q parameter, an index representing the maximal charge passing through the open channel (see Methods section for detailed information), was significantly reduced in the f null clone (Figure 24E).

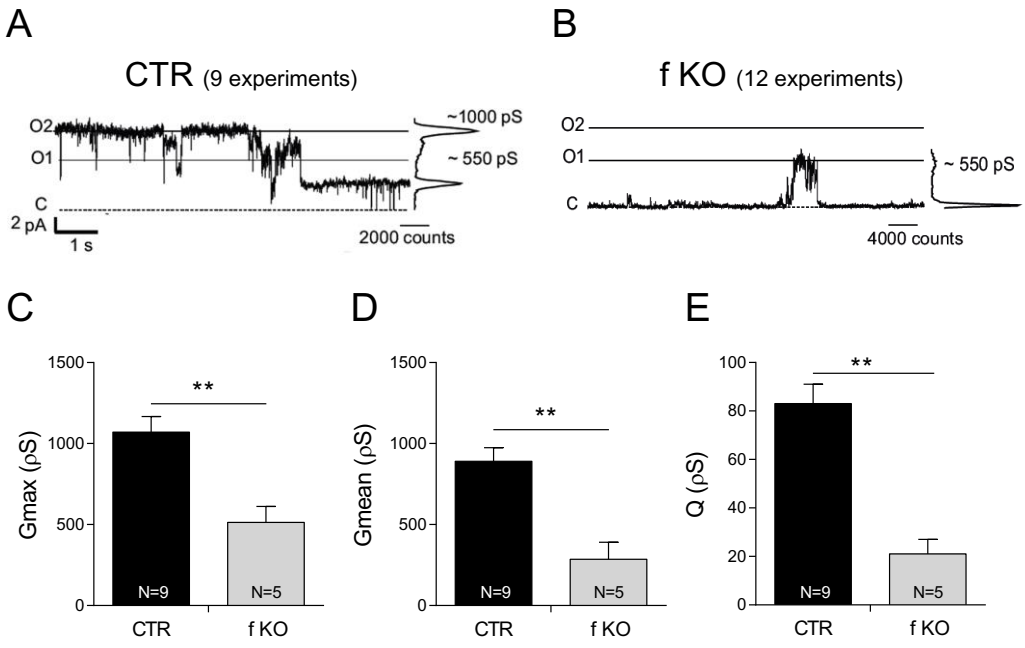

Figure 24. Subunit f affects single channel features of the MCC in mitoplasts. (A-B) PTP (MMC) representative current traces are recorded at $V_{(pipette)}$ +20 mV from mitoplasts derived from control (CTR clone 1) or f subunit knocked out (f KO clone 15) HeLa clones. Channel currents (left) and corresponding amplitude histograms (right) are recorded in 9 CTR and 5 f KO preparations. Note that both in CTR and f KO traces different conductance states can be detected in the amplitude histograms as Gaussian peaks. C, closed; O2, average conductance level of maximal long-lasting opening for CTR; O1, average conductance level of long-lasting opening for f KO. (C) Histograms represent the average maximal conductance obtained in CTR and f KO clones (error bars represent SEM, **P=0.01). (D) Histograms represent the average mean conductance obtained in CTR and f KO clones. Values corresponding to closed state were omitted from the calculation (error bars represent SEM, **P=0.01). (E) Histograms represent the average of the total charge passing through the channel in a time rage of 4 seconds centred at the

maximal conductance point of recorded current (error bars represent SEM, ***P=0.001).

These electrophysiological results suggest an involvement of the f subunit in channel formation within the F-ATP synthase enzyme, even if the participation of other F_O subunits (that are down regulated) is extremely likely. We have already found that the e-g subunits are important in the formation of the full conductance MMC in yeast. Yeast strains lacking subunits e, g and the first transmembrane domain of subunit b, indeed displayed decreased channel activity, which was about tenfold smaller than that of the wild type (Guo et al., 2019, Carraro et al., 2018). Patch-clamp of mitoplasts from c-null HAP1 cells (Neginskaya et al., 2019) has also revealed the absence of high-conductance channels, while smaller conductances were still observed, including one of 300 pS. This latter conductance is inhibited by bongkrekic acid (inhibitor of the ANT) and similar to the one reported for the ANT (Brustovetsky et al., 1996), suggesting that the residual conductance is probably due to Ca^{2+}-dependent channel formation by the ANT.

4.2.2 f subunit KD cells

For a better clarification of f subunit function(s) in HeLa cells we tried to obtain a less severe phenotype by modulating f subunit expression levels. We tested five different short hairpin RNAs (shRNAs, see Materials and Methods), four of which (sh1, sh2, sh4, sh5) were able to stably down regulate the f subunit (Figure 25A). We studied two populations of cells with a reduction of the f subunit protein level to 30% (sh2) or 70% (sh5) (Figure 25A low panel).

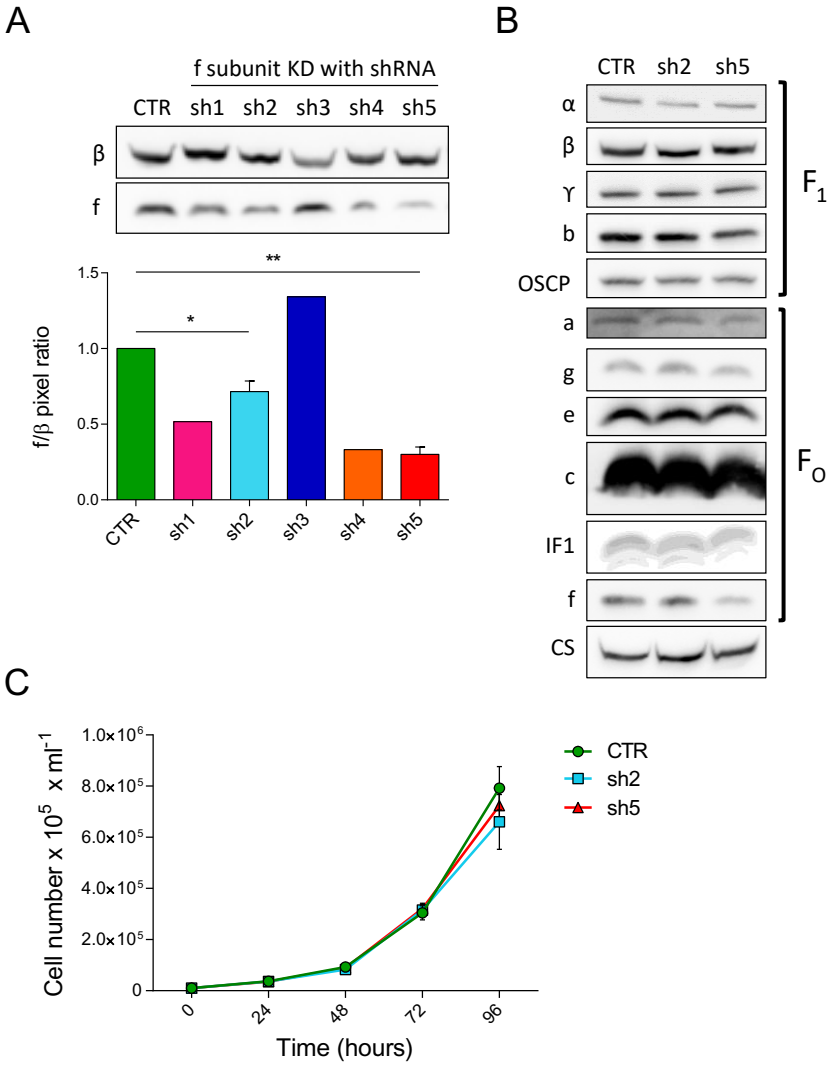

Figure 25. The subunit f knock down through the shRNA interference does not alter F-ATP synthase subunit composition or HeLa growing rate. (A) Western Blotting of f and β subunits in control (CTR) or f knock down (KD) HeLa cells (upper) and their band pixel ratio, ± SEM (5 experiments) (below). Sh1-5 represent different oligonucleotides used for shRNA interference, an empty vector is used for control (*P=0.016; **P=0.001). (B) Western blotting of CTR and f KD (sh2; sh5) cell lysates recognizing the subunits of the F_1 and F_O sectors of F-ATP synthase and citrate synthase as loading control. (C) Growth curves of CTR and f KD (sh2 and sh5) HeLa cells. Cells are detached and counted every 24 hrs. Data are mean of 3 independent experiments ± SEM.

4.2.2.1 Effects of f subunit KD on F-ATP synthase catalysis and assembly

Importantly, the KD of f subunit did not slow down the rate of cell growth (Figure 25C), and the main difference was in the f subunit abundance as assessed by western blotting of whole cell lysates, which showed that level of other F-ATP synthase subunits was not altered (Figure 25B). Basal, oligomycin-sensitive and

maximal respiration were not affected by the decreased levels of subunit f, in either the sh2 or sh5 cell line (Figure 26A-B). This is an indication that respiratory function and mitochondrial ATP production are unaffected by subunit f down-regulation, consistent with its location in a region far from the catalytic core of the enzyme, and with the early definition of subunits, e, f and g as "accessory" or "supernumerary" (Collinson et al., 1994). In line with the OCR measurement, no effects in the OXPHOS complexes content were observed (Figure 26C).

Considering the interactions between the f subunit and the a subunit in the F_O sector, we also tested if the down regulation of the f subunit might have affected the maximal ATPase activity of the F-ATP synthase. Permeabilized cells were suspended in a buffer (see materials and methods), and the oligomycin-sensitive ATP hydrolysis rate was determined in the presence of an ATP-regenerating system.

As for ATP synthesis, no significant changes in the maximal ATP hydrolysis were detected in the sh2 and sh5 cell lines (Figure 26D), in keeping with the unaltered IF1 level (Figure 25C). It is noteworthy that sh2 and sh5 cells maintained a very high sensitivity to oligomycin, with inhibition of about 98% (Figure 26D). Importantly, these cells lines did not undergo changes of mitochondrial content as measured with staining with Nonyl Acridine Orange (NAO) (Figure 26E), a dye that specifically binds the cardiolipin molecules, and as also suggested by the normal levels of OXPHOS complexes.

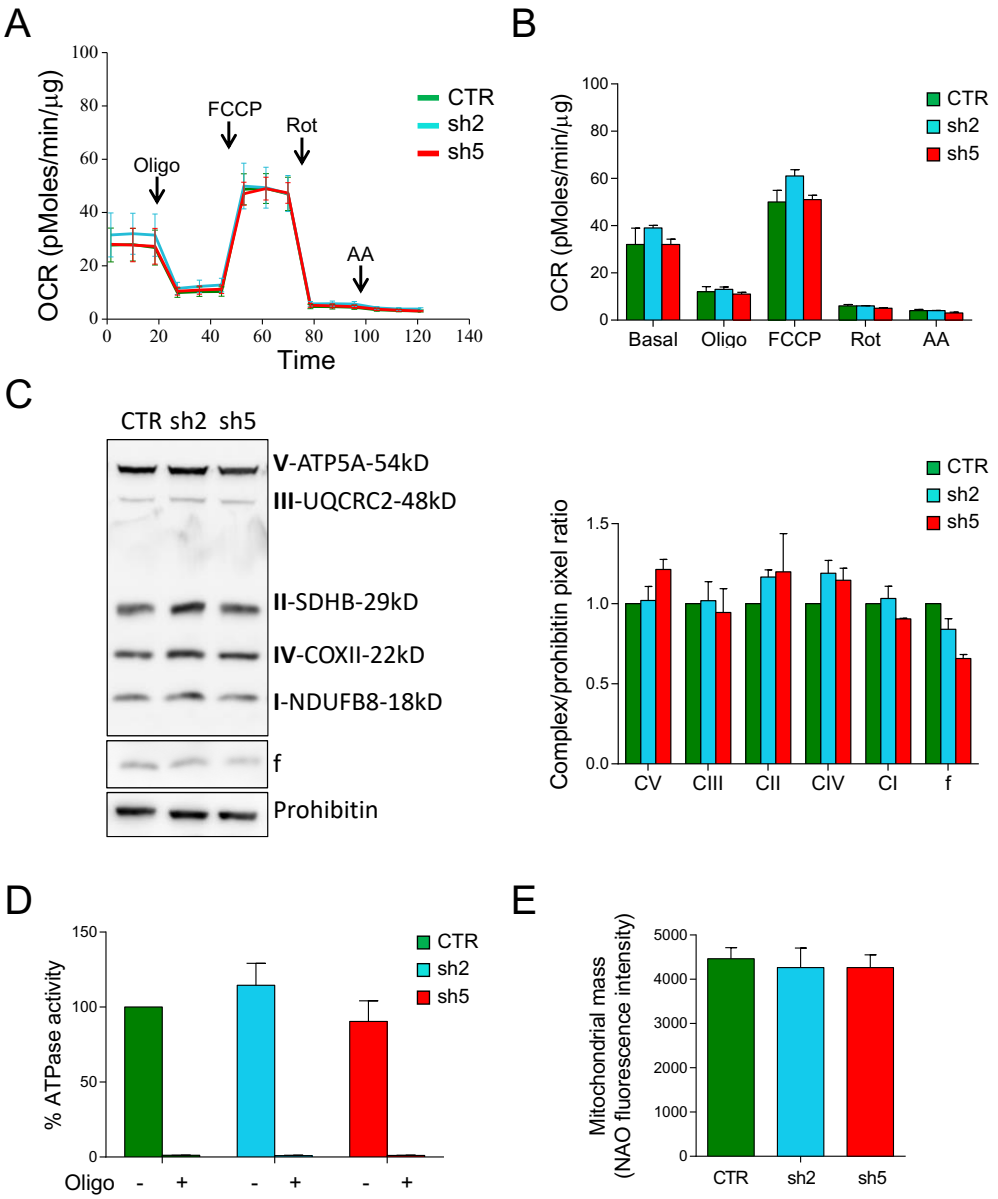

Figure 26. The subunit f knock down through shRNA interference does not alter mitochondrial respiration, ATP synthesis/hydrolysis, or OXPHOS levels in HeLa cells. (A-B) Oxygen consumption rate (OCR) of control (CTR) and f subunit KD (sh2; sh5) HeLa cells. OCR is measured before (basal) or after treatment with oligomycin (Oligo); carbonyl cyanide p-(trifluoromethoxy) phenylhydrazone (FCCP); rotenone (Rot) and antimycin A (AA). Left panel, representative OCR measurements of adherent cells in situ, seeded at the concentration of 50000 cell/well. Right, quantification of 3 independent experiments ± SEM is shown. (C) Western blotting for OXPHOS complex subunits, F-ATP synthase and prohibitin (loading control) in CTR and f KD (sh2; sh5) mitochondria. Right panel, mean pixel ratio of complex band quantification on prohibitin in 3 independent experiments ± SEM. (D) Maximal oligomycin-inhibited (2µM oligomycin) ATPase activity is shown as % of control. ATP hydrolysis is determined spectrophotometrically at 340 nm in permeabilized CTR or f KD (sh2; sh5) HeLa cells ($2x10^6$ cells per 1 ml of ATP-regenerating system), 37°C, in the presence of 10 µM alamethicin and 10 µM decavanadate. Values are mean of 6 or 3 experiments run in triplicates ± SEM, in the absence (-) or presence (+) of oligomycin, respectively. E) Nonyl Acridine Orange (NAO, 200µM) staining quantification ((fluorescence arbitrary units) in CTR, and sh2, sh5 f KD cells is shown.

Collectively, this set of findings suggests that the KD of subunit f does not alter the functional activity of the F-ATP synthase; indeed both ATP synthesis and ATP hydrolysis were similar to CTR cells.

This biochemical phenotype was different from what we observed in f subunit KO cells, and from what is reported for HeLa cells depleted of e or g subunit (Habersetzer et al., 2013). In this latter cell model mitochondrial respiration was decreased, and matched by an increase of lactate concentration in the medium (Habersetzer et al., 2013).

4.2.2.2 Structural role of the f subunit in mitochondria

Given the number of interactions occurring in the enzyme structure between the f subunit and the a-a' dimers (as revealed by our bioinformatic analysis in Figure 20A), and since the a subunit in the CryoEM yeast structure of Gu 2017 is described to hold together yeast dimers (Guo, Bueler & Rubinstein, 2017), we investigated the possibility that f subunit might be relevant in the stabilization of the two F_O-monomers and as consequence if it is involved in *cristae* biogenesis. Dimerization of F-ATP synthase and *cristae* morphology are indeed two related events (Davies et al., 2012, Davies et al., 2011, Blum et al., 2019).

We assessed mitochondrial architecture and *cristae* shape trough Transmission Electron Microscopy (TEM) on adherent HeLa cells. TEM is a powerful technique to study ultrastructure in health and disease, and it provides critical information about mitochondrial content and *cristae* density, organization and morphology.

Mitochondria from wild type cells displayed a canonical elongated or curved morphology with numerous transverse *cristae*, and with a well-defined inner membrane (Figure 27A). In sh2 and sh5 f KD cells we observed a mixed population of mitochondria (Figure 27A). Some had normal *cristae*, while the majority of mitochondria rather displayed an "arch-like" or "longitudinal" *cristae* morphology (Figure 27A) and smaller, spherical mitochondria were also seen.

Counting the number of normal and abnormal mitochondria (on the basis of *cristae* morphology) per image, we observed that the number of abnormal mitochondria was about 70% of the total in the sh5 f KD cell line (Figure 27C).

Cristae junctions (CJ, tubular structures that connect a mitochondrial *crista* to the mitochondrial inner boundary membrane) were decreased to 35% and 50% in sh2 and sh5 cells, respectively (Figure 27D).

Interestingly, the full ablation of the f subunit in HeLa clones also caused abnormal *cristae* morphology (Figure 27B), and a decrease in the number of CJ up to 70% (Figure 27E). While in f KD cells a small population of functional mitochondria was preserved (around 30%, Figure 27C), in these f KO cells all mitochondria had abnormal *cristae* ultrastructure. Thus, this is probably the explanation of why the KD model was less severe.

The different mitochondrial organization in f subunit KD or KO cells is similar to what is described for yeast strains lacking e-g subunits (Paumard et al., 2002, Carraro et al., 2018, Giraud et al., 2002, Arselin et al., 2004), and for HeLa cells with reduced levels of the same subunits (Habersetzer et al., 2013). In these cases, the absence of e and g subunits prevents F-ATP synthase dimerization, or causes dimer instability, and since F-ATP synthase dimers are known to be crucial for mitochondrial morphology (Davies et al., 2012), the direct consequence is abnormal cristae morphology. Thus, the mitochondrial morphology alterations seen in f KO or KD HeLa cells may be due to F-ATP synthase dimers instability, as also described in He et al, 2018 (He et al., 2018).

At the level of the *cristae* junction other protein complexes have been recently shown to be involved in shaping mitochondrial morphology (Rabl et al., 2009, Eydt et al., 2017, Rampelt et al., 2017). These complexes, known as "mitochondrial contact site and *cristae* organization system" (MICOS), stabilize the highly curved membrane structure and establish an inner membrane architecture by anchoring the inner to the outer mitochondrial membrane (Rampelt et al., 2017). A connection between MICOS and the F-ATP synthase via the MICOS core component Mic10 and the e subunit of the F-ATP synthase have been found (Eydt et al., 2017). This physical interaction seems to be important in regulating F-ATP synthase oligomeric state, and CJ formation.

A possible explanation for the decreased number of CJ per mitochondrion observed in the f KD or KO cells (Figure 27D, E), is that other subunits involved in F-ATP synthase dimer stability, like the g and the f subunits, might be involved in the interaction of the enzyme with these MICOS protein complexes, and so in

the formation of the *cristae* junctions.

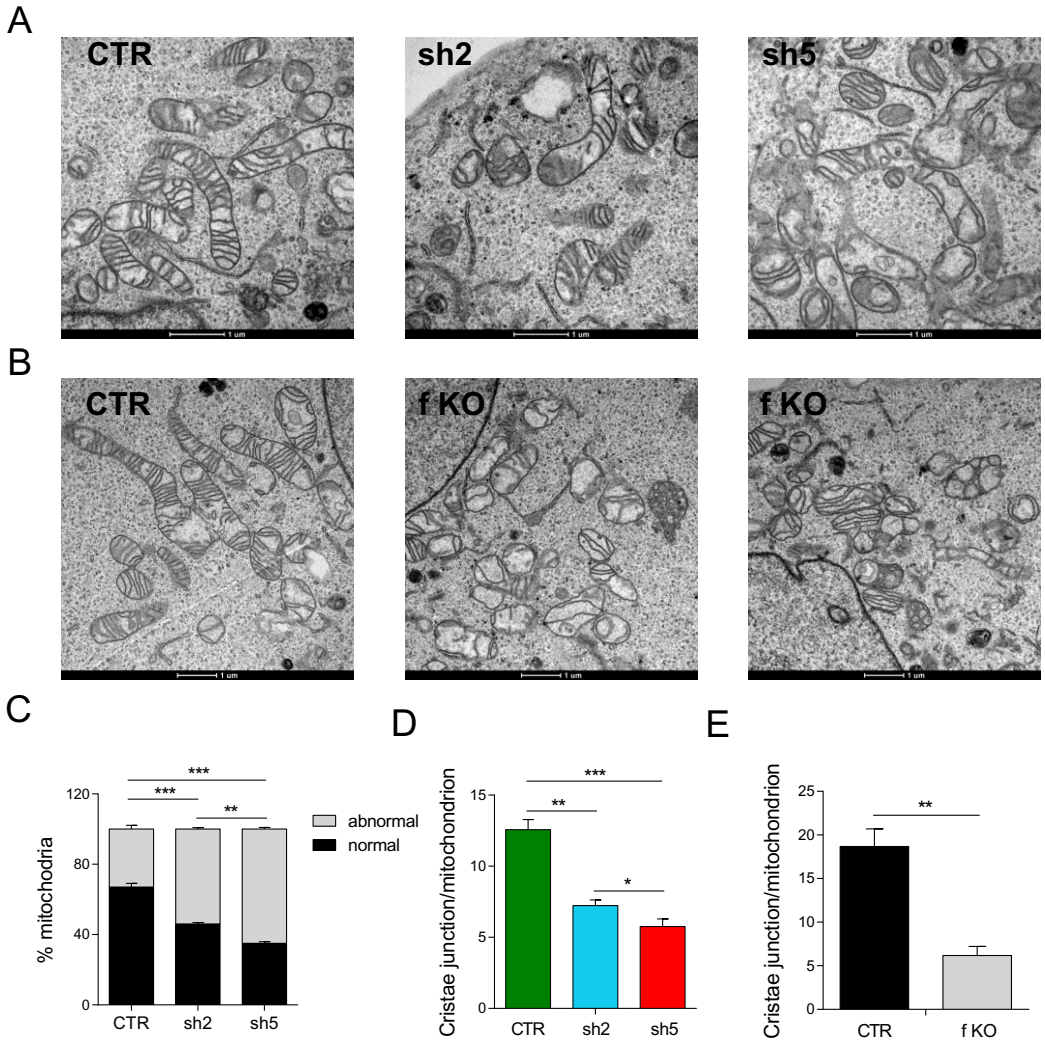

Figure 27. The subunit f knock down or knockout in HeLa cells alters mitochondrial cristae morphology. (A) Representative transmission electron microscopy images of CTR, sh2 and sh5 f subunit KD fixed HeLa cells. Scale bar 1 µm. (B) Representative transmission electron microscopy images of CTR (clone 1) and f-null (clone 15) fixed HeLa clones. Scale bar 1 µm. (C) Histogram representing the mean number of normal and abnormal mitochondria ± SEM (3 independent experiments are analysed, 5 images each experiment per condition, **P=0.001; ***P=0.0008 for sh2; ***P=0.0002 for sh5). (D) Histogram representing the mean number of cristae junctions per mitochondrion ± SEM in CTR and f KD cells (the images analysed are the same as in panel C, *P=0.0043; **P=0.0029; ***P=0.0009). (E) Histogram representing the mean number of cristae junctions per mitochondrion ± SEM in CTR and f KO cells (3 independent experiments are analysed, 5 images each experiment per cell type, **P=0.0053). Scale bar 1 µm.

4.2.2.3 Mitochondrial respiration under stress conditions

The results presented so far suggest that the f subunit is important for dimer-oligomer stabilization, and that the KD or KO of this subunit alters mitochondrial *cristae* morphology. However, looking at the TEM images there is also an

inconsistency. Given the differences in *cristae* morphology it is surprising that mitochondrial respiration is completely unaffected in f subunit KD cells. To further explore the bioenergetics of these cells we therefore shifted from a DMEM medium containing 25 mM glucose to a DMEM medium containing 2.5 mM glucose and pyruvate for 24 hours. Under low glucose condition, both basal and maximal respiration in the sh5 f subunit KD cell line were significantly lower than in wild type cells (Figure 28A,B). In CTR cells the OCR values (pmoles/min/µg) in low-glucose condition increased compared to high-glucose ones (from 32 ± 3.17 to 56 ± 6.95 in basal condition, in high and low glucose respectively, Figure 26B and Figure 28B); while in the sh5 f subunit KD cells the OCR (28 ± 5.56 and 32 ± 2.3 for high and low glucose respectively, Figure 26B and Figure 28B) could not be stimulated further. The sh2 cells, which are characterized by a smaller decrease in the f protein content (Figure 26A), in low-glucose condition displayed an intermediate phenotype: the basal OCR value was 39 ± 1.11 (Figure 28B). This OCR value is higher compared to the sh5 cells, but lower compared to wild type cells.

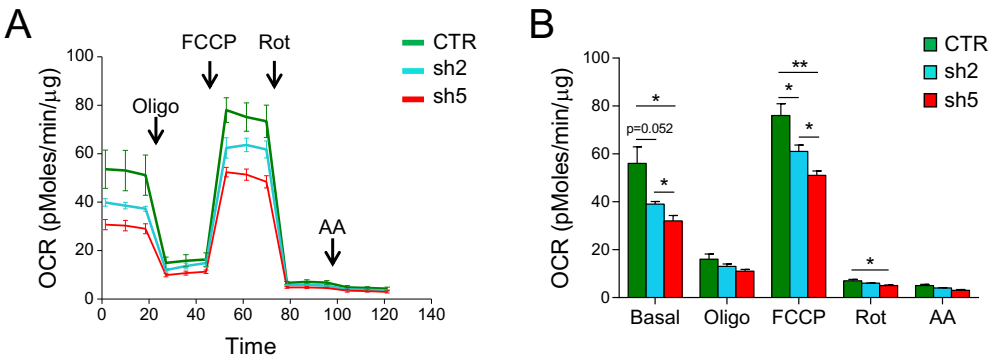

Figure 28: Mitochondrial respiration in subunit f knock down cells grown in glucose depletion. Oxygen consumption rate (OCR) of control (CTR) and f subunit KD (sh2; sh5) HeLa cells after 24 hours of culture in a 2.5 mM glucose containing DMEM medium. OCR is measured before (basal) or after treatment with oligomycin (Oligo); carbonyl cyanide p-(trifluoromethoxy) phenylhydrazone (FCCP); rotenone (Rot) and antimycin A (AA). (A) Representative OCR measurement of adherent cells in situ, seeded at the concentration of 50000 cell/well. The quantification of the protein level in each well at the end of the measurements confirmed a comparable cellular content in CTR and f KD wells. (B) Mean OCR of 4 independent experiments ± SEM (*P<0.05, **P=0.0034).

An explanation for these differences could be the altered mitochondrial

morphology (Figure 27), and as consequence a decrease in the supercomplexes content, since the total mitochondrial mass, as already mentioned, was unchanged in the three different cell lines (Figure 26E). It is indeed reported, that *cristae* morphology determines assembly, stability and function of RCSs, and hence optimal mitochondrial respiratory function (Cogliati et al., 2013, Cogliati, Enriquez & Scorrano, 2016); and that in mammalian cells, the endoplasmic reticulum stress and the glucose deprivation, stimulates mitochondrial bioenergetics, and formation of RCSs through the proteinkinase R-like ER kinase (PERK) (Balsa et al., 2019).

4.2.2.4 (Patho) Physiological role (PTP modulation) of the f subunit

We next tested whether the f subunit affects PTP formation and/or regulation.

4.2.2.4.1 Effects of f subunit KD on pore formation

A PTP-dependent swelling assay was used to analyze the effect of subunit f downregulation on PTP modulation. To test whether pore size was affected, we studied mitochondrial swelling in KCl- or sucrose-based media (Figure 29A). Medium solutes diffuse through the open channel according to their size, allowing mitochondria to swell (Massari, Frigeri & Azzone, 1972b). The exclusion size of the PTP (about 1.5 kDa, which corresponds to a diameter of about 3 nm) allows diffusion of both sucrose and KCl, while pores of smaller size may exclude sucrose but not KCl.

Swelling and PTP opening were measured as the decrease of absorbance at 540 nm after addition of different concentrations of Ca^{2+}. After Ca^{2+}-dependent pore opening we observed that in a KCl-based medium the fraction of swollen mitochondria was comparable between wild type and subunit f KD cells (Figure 29B-D), indicating that decreased level of f subunit did not prevent PTP opening. In sucrose-based medium fast swelling only took place in wild type mitochondria, while it was minimal in the sh5 and intermediate in sh2 cells, respectively (Figure 29C-E), matching the f subunit expression level. The decreased fraction of swollen mitochondria (Figure 29E) and of the rate of swelling (Figure 29F)

observed in the sh5 f KD mitochondria in sucrose-based medium, suggests that knock down of the f subunit decreases PTP size. Indeed, calibration with alamethicin, a pore-forming agent, is yielded comparable swelling in all cells, indicating that the permeability differences are not due to the altered mitochondrial morphology.

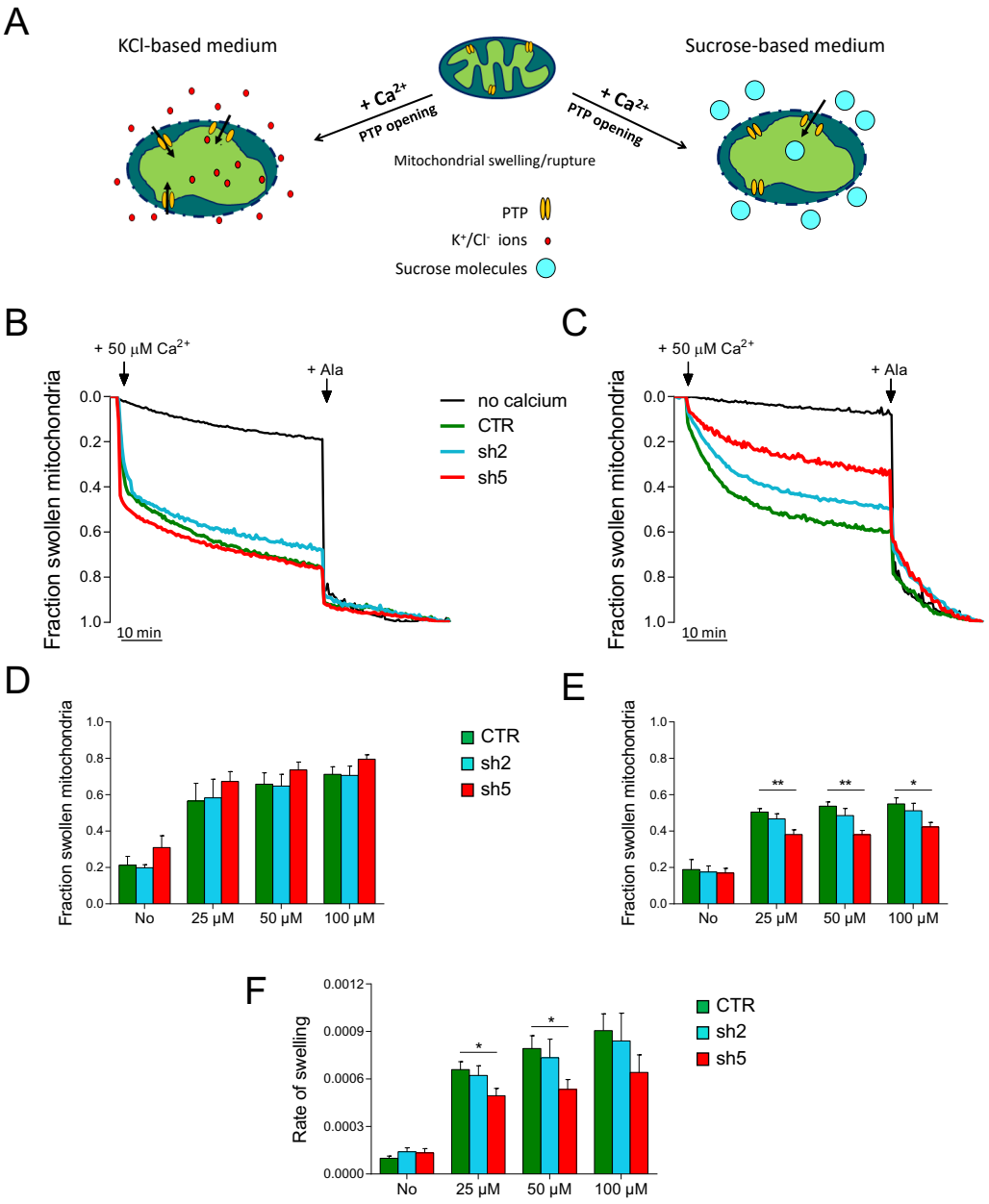

Figure 29. The subunit f knock down affects the size of the permeability transition pore in HeLa cells. (A) Schematic representation of the events leading to PTP opening and mitochondrial swelling in KCl- or sucrose-based medium. Ca^{2+} promotes PTP opening which is rapidly followed by mitochondrial swelling in a KCl-based medium, because K^+/Cl^- ions (of small size) can permeate through small and large pores. In sucrose based-medium, swelling is observed upon PTP opening

only in the presence of large channels allowing sucrose molecules to permeate. PTPs are in yellow, K^+/Cl^- ions are in red, sucrose molecules are in light blue. (B,C.) Mitochondria isolated from CTR, sh2 and sh5 f subunit KD HeLa cells are assayed in a KCl- (B) or a sucrose- (C) based medium. Swelling is measured as decrease of absorbance at 540 nm. Where indicated 50 µM Ca^{2+} and 1 µM alamethicin (Ala) are added. Traces are representative of 4 or 5 independent experiments in KCl- or a sucrose-based medium, respectively. (D,E.) The fraction of swollen mitochondria after PTP opening is calculated and normalized to the maximal swelling induced by alamethicin (referred as 1). Histograms refer to the mean ± SEM of swollen mitochondria 15 minutes after the Ca^{2+} additions (0-100 µM) in KCl- and sucrose-based media (4 or 5 independent experiments each Ca^{2+} concentration per condition, ** indicates P values of 0.0047 or 0.0015 for sh5 at 25 µM or 50 µM, respectively, *P=0.015 for sh5 at 100 µM). (F) The rate of swelling is calculated drawing the tangent of the curve after each Ca^{2+} addition. Histograms refer to the mean ± SEM of mitochondria in a sucrose-based media. (5 independent experiments, *P=0.042 for sh5 at 25 µM, *P=0.035 for sh5 at 50 µM).

This observation nicely matches the results obtained in the patch-clamp experiments (Figure 24). Together, these data provide evidence that subunit f may be involved in PTP formation in a human cell. The occurrence of smaller channel openings in the absence of f subunit suggests that additional subunits are involved in channel formation, such as the e and g subunits as already described in yeast (Guo et al., 2019, Carraro et al., 2014, Carraro et al., 2018).

4.2.2.4.2 Effects of f subunit KD on the Ca^{2+} sensitivity of the PTP

The ability of cells to undergo PT was next evaluated with the sensitive calcium retention capacity (CRC) assay. The CRC is the amount of Ca^{2+} that can be taken up by energized mitochondria before onset of the PTP, which is marked by a rapid Ca^{2+} release due to PTP-dependent depolarization. Importantly, this assay does not provide information on the size of the PTP, but our aim was to test if the downregulation of the f subunit affects also the PTP sensitivity to Ca^{2+}, as seen in yeast (Carraro et al., 2018).

Digitonin-permeabilized cells were suspended in a KCl- or sucrose-based assay buffers supplemented with Calcium Green-5N, a probe that increases its fluorescence emission upon Ca^{2+} binding. Cells were subjected to a train of Ca^{2+} pulses of 2.5 µM Ca^{2+} each. PTP opening is marked by a sudden Ca^{2+} release in the extra-mitochondrial space causing an increase in fluorescence. The CRC assay showed that the Ca^{2+} sensitivity of the channel was slightly, but significantly decreased in sh5 cells. This decreased sensitivity supports the idea that the pore may form at the monomer-monomer interface, upon Ca^{2+}-mediated

conformational changes that are transmitted to the F_O, through the peripheral stalk (Giorgio et al., 2017, Giorgio et al., 2018). The f position at the base of the peripheral stalk might be important for the transmission of the signal to the membrane, so that its absence could delay PTP opening upon Ca^{2+} binding to the catalytic core of the F-ATP synthase.

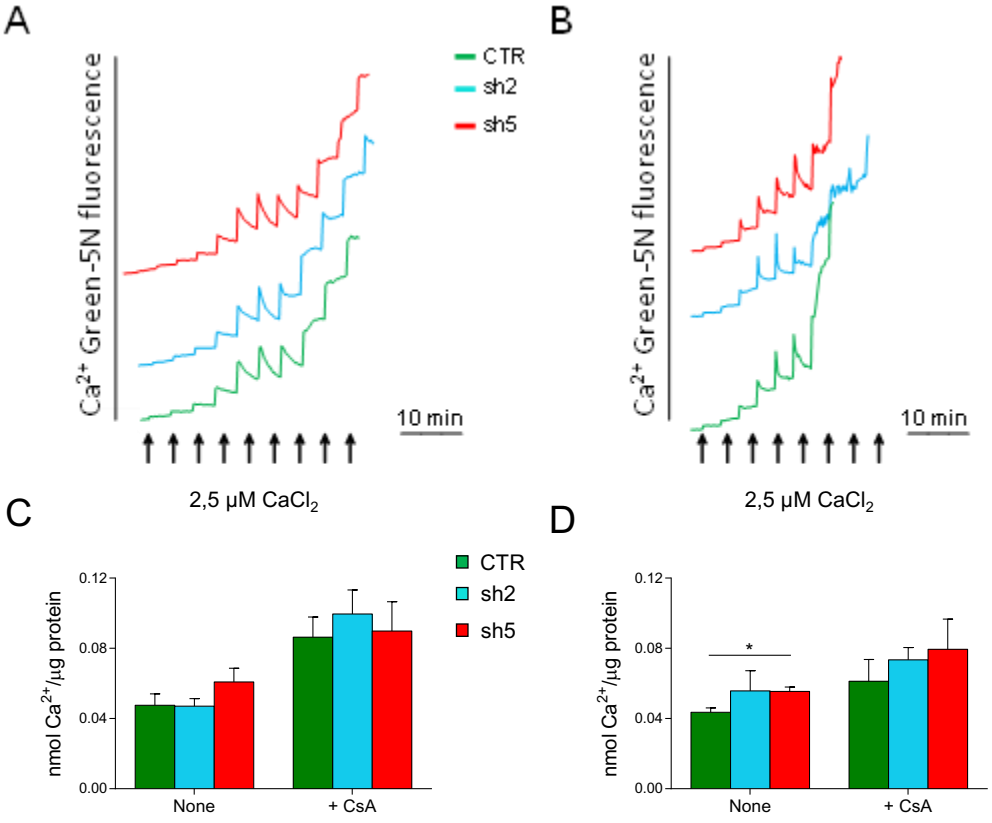

Figure 30. The subunit f knock down affects Ca^{2+} sensitivity of the permeability transition pore in HeLa cells. Ca2+ retention capacity (CRC) was assessed in permeabilized CTR, sh2 and sh5 HeLa cells in a KCl- (A-C) or a sucrose- (B-D) based medium, supplemented with 5 mM succinate, 1 mM phosphate and with the membrane-impermeable Ca^{2+} sensor, Ca^{2+} Green-5N. Ca^{2+} Green-5N fluorescence was monitored following the repeated addition of Ca^{2+} pulses. A return of Ca^{2+} Green-5N fluorescence to baseline reflects Ca^{2+} mitochondrial uptake, while a sudden increase in fluorescence is indicative of PTP opening. One experiment representative of 3 is shown in A and B panels. (C-D) Histograms represent nmols of Ca^{2+} per µg of protein retained by CTR (green bars), sh2 (light blue bars) and sh5 (red bars) under basal conditions (none) or in the presence of 1.6 µM cyclosporin A (CsA). Data represent the mean ± SEM of 3 independent experiments run in triplicate each condition, *P=0.029.

5 CONCLUSIONS

CONCLUSIONS

The results presented in this Thesis document the critical role of subunit f of F-ATP synthase in the modulation of the PTP. These data strongly indicate that the PTP and the F-ATP synthase are the same entity, and suggest that the dimer interface of the enzyme could be the site of Ca^{2+}-dependent channel formation. The current results support previous data demonstrating the importance of subunits e and g, which concur with subunit f in dimer stabilization.

We showed that subunit f downregulation, in keeping with its location at the dimer interface and far from the catalytic core of the enzyme, does not alter either the functional activity of the F-ATP synthase or its subunit stoichiometry, but does affects proper *cristae* formation and mitochondrial morphology.

The f subunit contributes to determine the size of the PTP, and its removal desensitizes PTP opening as shown by both electrophysiological studies on f-null cells and swelling experiments. These data do not exclude the role of additional subunits in PTP formation, but rather suggest that "accessory" subunits (like e, f and g) may have evolved to confer this novel channel function to F-ATP synthase of eukaryotes.

6 BIBLIOGRAPHY

BIBLIOGRAPHY

Abrahams, J.P., Leslie, A.G., Lutter, R. & Walker, J.E. 1994, "Structure at 2.8 A resolution of F1-ATPase from bovine heart mitochondria", *Nature,* vol. 370, no. 6491, pp. 621-628.

Acin-Perez, R., Bayona-Bafaluy, M.P., Fernandez-Silva, P., Moreno-Loshuertos, R., Perez-Martos, A., Bruno, C., Moraes, C.T. & Enriquez, J.A. 2004, "Respiratory complex III is required to maintain complex I in mammalian mitochondria", *Molecular cell,* vol. 13, no. 6, pp. 805-815.

Acin-Perez, R., Fernandez-Silva, P., Peleato, M.L., Perez-Martos, A. & Enriquez, J.A. 2008, "Respiratory active mitochondrial supercomplexes", *Molecular cell,* vol. 32, no. 4, pp. 529-539.

Adachi, K., Oiwa, K., Nishizaka, T., Furuike, S., Noji, H., Itoh, H., Yoshida, M. & Kinosita, K.,Jr 2007, "Coupling of rotation and catalysis in F(1)-ATPase revealed by single-molecule imaging and manipulation", *Cell,* vol. 130, no. 2, pp. 309-321.

Ahn, B.H., Kim, H.S., Song, S., Lee, I.H., Liu, J., Vassilopoulos, A., Deng, C.X. & Finkel, T. 2008, "A role for the mitochondrial deacetylase Sirt3 in regulating energy homeostasis", *Proceedings of the National Academy of Sciences of the United States of America,* vol. 105, no. 38, pp. 14447-14452.

Alavian, K.N., Beutner, G., Lazrove, E., Sacchetti, S., Park, H.A., Licznerski, P., Li, H., Nabili, P., Hockensmith, K., Graham, M., Porter, G.A.,Jr & Jonas, E.A. 2014, "An uncoupling channel within the c-subunit ring of the F1FO ATP synthase is the mitochondrial permeability transition pore", *Proceedings of the National Academy of Sciences of the United States of America,* vol. 111, no. 29, pp. 10580-10585.

Allegretti, M., Klusch, N., Mills, D.J., Vonck, J., Kuhlbrandt, W. & Davies, K.M. 2015, "Horizontal membrane-intrinsic alpha-helices in the stator a-subunit of an F-type ATP synthase", *Nature,* vol. 521, no. 7551, pp. 237-240.

Allen, R.D., Schroeder, C.C. & Fok, A.K. 1989, "An investigation of mitochondrial inner membranes by rapid-freeze deep-etch techniques", *The Journal of cell biology,* vol. 108, no. 6, pp. 2233-2240.

Amorim, A., Fernandes, T. & Taveira, N. 2019, "Mitochondrial DNA in human identification: a review", *PeerJ,* vol. 7, pp. e7314.

Anderson, S., Bankier, A.T., Barrell, B.G., de Bruijn, M.H., Coulson, A.R., Drouin, J., Eperon, I.C., Nierlich, D.P., Roe, B.A., Sanger, F., Schreier, P.H., Smith, A.J., Staden, R. & Young, I.G. 1981, "Sequence and organization of the human mitochondrial genome", *Nature,* vol. 290, no. 5806, pp. 457-465.

Anselmi, C., Davies, K.M. & Faraldo-Gomez, J.D. 2018, "Mitochondrial ATP synthase dimers spontaneously associate due to a long-range membrane-induced force", *The Journal of general physiology,* vol. 150, no. 5, pp. 763-770.

Antoniel, M., Jones, K., Antonucci, S., Spolaore, B., Fogolari, F., Petronilli, V., Giorgio, V., Carraro, M., Di Lisa, F., Forte, M., Szabo, I., Lippe, G. & Bernardi, P. 2018, "The unique histidine in OSCP subunit of F-ATP synthase mediates inhibition of the permeability transition pore by acidic pH", *EMBO reports,* vol. 19, no. 2, pp. 257-268.

Arnold, I., Pfeiffer, K., Neupert, W., Stuart, R.A. & Schagger, H. 1998, "Yeast mitochondrial F1F0-ATP synthase exists as a dimer: identification of three dimer-specific subunits", *The EMBO journal,* vol. 17, no. 24, pp. 7170-7178.

Arselin, G., Vaillier, J., Salin, B., Schaeffer, J., Giraud, M.F., Dautant, A., Brethes, D. & Velours, J. 2004, "The modulation in subunits e and g amounts of yeast ATP synthase modifies mitochondrial cristae morphology", *The Journal of biological chemistry,* vol. 279, no. 39, pp. 40392-40399.

Baines, C.P., Kaiser, R.A., Purcell, N.H., Blair, N.S., Osinska, H., Hambleton, M.A., Brunskill, E.W., Sayen, M.R., Gottlieb, R.A., Dorn, G.W., Robbins, J. & Molkentin, J.D. 2005, "Loss of cyclophilin D reveals a critical role for mitochondrial permeability transition in cell death", *Nature,* vol. 434, no. 7033, pp. 658-662.

Baines, C.P., Kaiser, R.A., Sheiko, T., Craigen, W.J. & Molkentin, J.D. 2007, "Voltage-dependent anion channels are dispensable for mitochondrial-dependent cell death", *Nature cell biology,* vol. 9, no. 5, pp. 550-555.

Baker, L.A., Watt, I.N., Runswick, M.J., Walker, J.E. & Rubinstein, J.L. 2012, "Arrangement of subunits in intact mammalian mitochondrial ATP synthase determined by cryo-EM", *Proceedings of the National Academy of Sciences of the United States of America,* vol. 109, no. 29, pp. 11675-11680.

Balaban, R.S., Nemoto, S. & Finkel, T. 2005, "Mitochondria, oxidants, and aging", *Cell,* vol. 120, no. 4, pp. 483-495.

Balsa, E., Soustek, M.S., Thomas, A., Cogliati, S., Garcia-Poyatos, C., Martin-Garcia, E., Jedrychowski, M., Gygi, S.P., Enriquez, J.A. & Puigserver, P. 2019, "ER and Nutrient Stress Promote Assembly of Respiratory Chain Supercomplexes through the PERK-eIF2alpha Axis", *Molecular cell,* vol. 74, no. 5, pp. 877-890.e6.

Barrell, B.G., Bankier, A.T. & Drouin, J. 1979, "A different genetic code in human mitochondria", *Nature,* vol. 282, no. 5735, pp. 189-194.

Barsukova, A., Komarov, A., Hajnoczky, G., Bernardi, P., Bourdette, D. & Forte, M. 2011, "Activation of the mitochondrial permeability transition pore

modulates Ca2+ responses to physiological stimuli in adult neurons", *The European journal of neuroscience,* vol. 33, no. 5, pp. 831-842.

Bason, J.V., Montgomery, M.G., Leslie, A.G. & Walker, J.E. 2014, "Pathway of binding of the intrinsically disordered mitochondrial inhibitor protein to F1-ATPase", *Proceedings of the National Academy of Sciences of the United States of America,* vol. 111, no. 31, pp. 11305-11310.

Bason, J.V., Runswick, M.J., Fearnley, I.M. & Walker, J.E. 2011, "Binding of the inhibitor protein IF(1) to bovine F(1)-ATPase", *Journal of Molecular Biology,* vol. 406, no. 3, pp. 443-453.

Basso, E., Fante, L., Fowlkes, J., Petronilli, V., Forte, M.A. & Bernardi, P. 2005, "Properties of the permeability transition pore in mitochondria devoid of Cyclophilin D", *The Journal of biological chemistry,* vol. 280, no. 19, pp. 18558-18561.

Basso, E., Petronilli, V., Forte, M.A. & Bernardi, P. 2008, "Phosphate is essential for inhibition of the mitochondrial permeability transition pore by cyclosporin A and by cyclophilin D ablation", *The Journal of biological chemistry,* vol. 283, no. 39, pp. 26307-26311.

Beck, S.J., Guo, L., Phensy, A., Tian, J., Wang, L., Tandon, N., Gauba, E., Lu, L., Pascual, J.M., Kroener, S. & Du, H. 2016, "Deregulation of mitochondrial F1FO-ATP synthase via OSCP in Alzheimer's disease", *Nature communications,* vol. 7, pp. 11483.

Belogrudov, G.I., Tomich, J.M. & Hatefi, Y. 1996, "Membrane topography and near-neighbor relationships of the mitochondrial ATP synthase subunits e, f, and g", *The Journal of biological chemistry,* vol. 271, no. 34, pp. 20340-20345.

Bergeaud, M., Mathieu, L., Guillaume, A., Moll, U.M., Mignotte, B., Le Floch, N., Vayssiere, J.L. & Rincheval, V. 2013, "Mitochondrial p53 mediates a transcription-independent regulation of cell respiration and interacts with the mitochondrial F(1)F0-ATP synthase", *Cell cycle (Georgetown, Tex.),* vol. 12, no. 17, pp. 2781-2793.

Bernardi, P. 2018, "Why F-ATP Synthase Remains a Strong Candidate as the Mitochondrial Permeability Transition Pore", *Frontiers in physiology,* vol. 9, pp. 1543.

Bernardi, P. 1992, "Modulation of the mitochondrial cyclosporin A-sensitive permeability transition pore by the proton electrochemical gradient. Evidence that the pore can be opened by membrane depolarization", *The Journal of biological chemistry,* vol. 267, no. 13, pp. 8834-8839.

Bernardi, P. & Petronilli, V. 1996, "The permeability transition pore as a mitochondrial calcium release channel: a critical appraisal", *Journal of Bioenergetics and Biomembranes,* vol. 28, no. 2, pp. 131-138.

Bernardi, P., Rasola, A., Forte, M. & Lippe, G. 2015, "The Mitochondrial Permeability Transition Pore: Channel Formation by F-ATP Synthase, Integration in Signal Transduction, and Role in Pathophysiology", *Physiological Reviews,* vol. 95, no. 4, pp. 1111-1155.

Bernardi, P., Vassanelli, S., Veronese, P., Colonna, R., Szabo, I. & Zoratti, M. 1992, "Modulation of the mitochondrial permeability transition pore. Effect of protons and divalent cations", *The Journal of biological chemistry,* vol. 267, no. 5, pp. 2934-2939.

Beutner, G., Ruck, A., Riede, B., Welte, W. & Brdiczka, D. 1996, "Complexes between kinases, mitochondrial porin and adenylate translocator in rat brain resemble the permeability transition pore", *FEBS letters,* vol. 396, no. 2-3, pp. 189-195.

Bienert, S., Waterhouse, A., de Beer, T.A., Tauriello, G., Studer, G., Bordoli, L. & Schwede, T. 2017, "The SWISS-MODEL Repository-new features and functionality", *Nucleic acids research,* vol. 45, no. D1, pp. D313-D319.

Blum, T.B., Hahn, A., Meier, T., Davies, K.M. & Kuhlbrandt, W. 2019, "Dimers of mitochondrial ATP synthase induce membrane curvature and self-assemble into rows", *Proceedings of the National Academy of Sciences of the United States of America,* .

Boerries, M., Most, P., Gledhill, J.R., Walker, J.E., Katus, H.A., Koch, W.J., Aebi, U. & Schoenenberger, C.A. 2007, "Ca2+ -dependent interaction of S100A1 with F1-ATPase leads to an increased ATP content in cardiomyocytes", *Molecular and cellular biology,* vol. 27, no. 12, pp. 4365-4373.

Bonora, M., Bononi, A., De Marchi, E., Giorgi, C., Lebiedzinska, M., Marchi, S., Patergnani, S., Rimessi, A., Suski, J.M., Wojtala, A., Wieckowski, M.R., Kroemer, G., Galluzzi, L. & Pinton, P. 2013, "Role of the c subunit of the FO ATP synthase in mitochondrial permeability transition", *Cell cycle (Georgetown, Tex.),* vol. 12, no. 4, pp. 674-683.

Boreikaite, V., Wicky, B.I.M., Watt, I.N., Clarke, J. & Walker, J.E. 2019, "Extrinsic conditions influence the self-association and structure of IF1, the regulatory protein of mitochondrial ATP synthase", *Proceedings of the National Academy of Sciences of the United States of America,* vol. 116, no. 21, pp. 10354-10359.

Bowler, M.W., Montgomery, M.G., Leslie, A.G. & Walker, J.E. 2007, "Ground state structure of F1-ATPase from bovine heart mitochondria at 1.9 A

resolution", *The Journal of biological chemistry,* vol. 282, no. 19, pp. 14238-14242.

Boyer, P.D. 1993, "The binding change mechanism for ATP synthase--some probabilities and possibilities", *Biochimica et biophysica acta,* vol. 1140, no. 3, pp. 215-250.

Broekemeier, K.M. & Pfeiffer, D.R. 1989, "Cyclosporin A-sensitive and insensitive mechanisms produce the permeability transition in mitochondria", *Biochemical and biophysical research communications,* vol. 163, no. 1, pp. 561-566.

Brustovetsky, N., Becker, A., Klingenberg, M. & Bamberg, E. 1996, "Electrical currents associated with nucleotide transport by the reconstituted mitochondrial ADP/ATP carrier", *Proceedings of the National Academy of Sciences of the United States of America,* vol. 93, no. 2, pp. 664-668.

Brustovetsky, N., Tropschug, M., Heimpel, S., Heidkamper, D. & Klingenberg, M. 2002, "A large Ca2+-dependent channel formed by recombinant ADP/ATP carrier from Neurospora crassa resembles the mitochondrial permeability transition pore", *Biochemistry,* vol. 41, no. 39, pp. 11804-11811.

Cabezon, E., Arechaga, I., Jonathan, P., Butler, G. & Walker, J.E. 2000, "Dimerization of bovine F1-ATPase by binding the inhibitor protein, IF1", *The Journal of biological chemistry,* vol. 275, no. 37, pp. 28353-28355.

Cabezon, E., Runswick, M.J., Leslie, A.G. & Walker, J.E. 2001, "The structure of bovine IF(1), the regulatory subunit of mitochondrial F-ATPase", *The EMBO journal,* vol. 20, no. 24, pp. 6990-6996.

Calvo, S.E., Clauser, K.R. & Mootha, V.K. 2016, "MitoCarta2.0: an updated inventory of mammalian mitochondrial proteins", *Nucleic acids research,* vol. 44, no. D1, pp. D1251-7.

Campanella, M., Casswell, E., Chong, S., Farah, Z., Wieckowski, M.R., Abramov, A.Y., Tinker, A. & Duchen, M.R. 2008, "Regulation of mitochondrial structure and function by the F1Fo-ATPase inhibitor protein, IF1", *Cell metabolism,* vol. 8, no. 1, pp. 13-25.

Carraro, M., Checchetto, V., Sartori, G., Kucharczyk, R., di Rago, J.P., Minervini, G., Franchin, C., Arrigoni, G., Giorgio, V., Petronilli, V., Tosatto, S.C.E., Lippe, G., Szabo, I. & Bernardi, P. 2018, "High-Conductance Channel Formation in Yeast Mitochondria is Mediated by F-ATP Synthase e and g Subunits", *Cellular physiology and biochemistry : international journal of experimental cellular physiology, biochemistry, and pharmacology,* vol. 50, no. 5, pp. 1840-1855.

Carraro, M., Checchetto, V., Szabo, I. & Bernardi, P. 2019, "F-ATP synthase and the permeability transition pore: fewer doubts, more certainties", *FEBS letters,* vol. 593, no. 13, pp. 1542-1553.

Carraro, M., Giorgio, V., Sileikyte, J., Sartori, G., Forte, M., Lippe, G., Zoratti, M., Szabo, I. & Bernardi, P. 2014, "Channel formation by yeast F-ATP synthase and the role of dimerization in the mitochondrial permeability transition", *The Journal of biological chemistry,* vol. 289, no. 23, pp. 15980-15985.

Carroll, J., He, J., Ding, S., Fearnley, I.M. & Walker, J.E. 2019, "Persistence of the permeability transition pore in human mitochondria devoid of an assembled ATP synthase", *Proceedings of the National Academy of Sciences of the United States of America,* vol. 116, no. 26, pp. 12816-12821.

Chan, D.C. 2006, "Mitochondria: dynamic organelles in disease, aging, and development", *Cell,* vol. 125, no. 7, pp. 1241-1252.

Chandra, D. & Singh, K.K. 2011, "Genetic insights into OXPHOS defect and its role in cancer", *Biochimica et biophysica acta,* vol. 1807, no. 6, pp. 620-625.

Chen, R., Runswick, M.J., Carroll, J., Fearnley, I.M. & Walker, J.E. 2007, "Association of two proteolipids of unknown function with ATP synthase from bovine heart mitochondria", *FEBS letters,* vol. 581, no. 17, pp. 3145-3148.

Cingolani, G. & Duncan, T.M. 2011, "Structure of the ATP synthase catalytic complex (F(1)) from Escherichia coli in an autoinhibited conformation", *Nature structural & molecular biology,* vol. 18, no. 6, pp. 701-707.

Cogliati, S., Enriquez, J.A. & Scorrano, L. 2016, "Mitochondrial Cristae: Where Beauty Meets Functionality", *Trends in biochemical sciences,* vol. 41, no. 3, pp. 261-273.

Cogliati, S., Frezza, C., Soriano, M.E., Varanita, T., Quintana-Cabrera, R., Corrado, M., Cipolat, S., Costa, V., Casarin, A., Gomes, L.C., Perales-Clemente, E., Salviati, L., Fernandez-Silva, P., Enriquez, J.A. & Scorrano, L. 2013, "Mitochondrial cristae shape determines respiratory chain supercomplexes assembly and respiratory efficiency", *Cell,* vol. 155, no. 1, pp. 160-171.

Collinson, I.R., van Raaij, M.J., Runswick, M.J., Fearnley, I.M., Skehel, J.M., Orriss, G.L., Miroux, B. & Walker, J.E. 1994, "ATP synthase from bovine heart mitochondria. In vitro assembly of a stalk complex in the presence of F1-ATPase and in its absence", *Journal of Molecular Biology,* vol. 242, no. 4, pp. 408-421.

Connern, C.P. & Halestrap, A.P. 1992, "Purification and N-terminal sequencing of peptidyl-prolyl cis-trans-isomerase from rat liver mitochondrial matrix

reveals the existence of a distinct mitochondrial cyclophilin", *The Biochemical journal,* vol. 284 (Pt 2), no. Pt 2, pp. 381-385.

Covian, R. & Balaban, R.S. 2012, "Cardiac mitochondrial matrix and respiratory complex protein phosphorylation", *American journal of physiology.Heart and circulatory physiology,* vol. 303, no. 8, pp. H940-66.

Crompton, M. 1999, "The mitochondrial permeability transition pore and its role in cell death", *The Biochemical journal,* vol. 341 (Pt 2), no. Pt 2, pp. 233-249.

Crompton, M., Ellinger, H. & Costi, A. 1988, "Inhibition by cyclosporin A of a Ca2+-dependent pore in heart mitochondria activated by inorganic phosphate and oxidative stress", *The Biochemical journal,* vol. 255, no. 1, pp. 357-360.

Davies, K.M., Anselmi, C., Wittig, I., Faraldo-Gomez, J.D. & Kuhlbrandt, W. 2012, "Structure of the yeast F1Fo-ATP synthase dimer and its role in shaping the mitochondrial cristae", *Proceedings of the National Academy of Sciences of the United States of America,* vol. 109, no. 34, pp. 13602-13607.

Davies, K.M., Strauss, M., Daum, B., Kief, J.H., Osiewacz, H.D., Rycovska, A., Zickermann, V. & Kuhlbrandt, W. 2011, "Macromolecular organization of ATP synthase and complex I in whole mitochondria", *Proceedings of the National Academy of Sciences of the United States of America,* vol. 108, no. 34, pp. 14121-14126.

De Col, V., Petrussa, E., Casolo, V., Braidot, E., Lippe, G., Filippi, A., Peresson, C., Patui, S., Bertolini, A., Giorgio, V., Checchetto, V., Vianello, A., Bernardi, P. & Zancani, M. 2018, "Properties of the Permeability Transition of Pea Stem Mitochondria", *Frontiers in physiology,* vol. 9, pp. 1626.

De Marchi, U., Basso, E., Szabo, I. & Zoratti, M. 2006, "Electrophysiological characterization of the Cyclophilin D-deleted mitochondrial permeability transition pore", *Molecular membrane biology,* vol. 23, no. 6, pp. 521-530.

Dienhart, M., Pfeiffer, K., Schagger, H. & Stuart, R.A. 2002, "Formation of the yeast F1F0-ATP synthase dimeric complex does not require the ATPase inhibitor protein, Inh1", *The Journal of biological chemistry,* vol. 277, no. 42, pp. 39289-39295.

DiMauro, S. 2004, "Mitochondrial diseases", *Biochimica et biophysica acta,* vol. 1658, no. 1-2, pp. 80-88.

Doudna, J.A. & Charpentier, E. 2014, "Genome editing. The new frontier of genome engineering with CRISPR-Cas9", *Science (New York, N.Y.),* vol. 346, no. 6213, pp. 1258096.

Du, Z., Tucker, W.C., Richter, M.L. & Gromet-Elhanan, Z. 2001, "Assembled F1-(alpha beta) and Hybrid F1-alpha 3beta 3gamma -ATPases from

Rhodospirillum rubrum alpha, wild type or mutant beta, and chloroplast gamma subunits. Demonstration of Mg2+versus Ca2+-induced differences in catalytic site structure and function", *The Journal of biological chemistry,* vol. 276, no. 15, pp. 11517-11523.

Duchen, M.R., McGuinness, O., Brown, L.A. & Crompton, M. 1993, "On the involvement of a cyclosporin A sensitive mitochondrial pore in myocardial reperfusion injury", *Cardiovascular research,* vol. 27, no. 10, pp. 1790-1794.

Dudkina, N.V., Oostergetel, G.T., Lewejohann, D., Braun, H.P. & Boekema, E.J. 2010, "Row-like organization of ATP synthase in intact mitochondria determined by cryo-electron tomography", *Biochimica et biophysica acta,* vol. 1797, no. 2, pp. 272-277.

Eriksson, O., Fontaine, E. & Bernardi, P. 1998, "Chemical modification of arginines by 2,3-butanedione and phenylglyoxal causes closure of the mitochondrial permeability transition pore", *The Journal of biological chemistry,* vol. 273, no. 20, pp. 12669-12674.

Eydt, K., Davies, K.M., Behrendt, C., Wittig, I. & Reichert, A.S. 2017, "Cristae architecture is determined by an interplay of the MICOS complex and the F1FO ATP synthase via Mic27 and Mic10", *Microbial cell (Graz, Austria),* vol. 4, no. 8, pp. 259-272.

Fournier, N., Ducet, G. & Crevat, A. 1987, "Action of cyclosporine on mitochondrial calcium fluxes", *Journal of Bioenergetics and Biomembranes,* vol. 19, no. 3, pp. 297-303.

Frasch, W.D. 2000, "The participation of metals in the mechanism of the F(1)-ATPase", *Biochimica et biophysica acta,* vol. 1458, no. 2-3, pp. 310-325.

Frezza, C., Cipolat, S. & Scorrano, L. 2007, "Organelle isolation: functional mitochondria from mouse liver, muscle and cultured fibroblasts", *Nature protocols,* vol. 2, no. 2, pp. 287-295.

Garcia-Bermudez, J. & Cuezva, J.M. 2016, "The ATPase Inhibitory Factor 1 (IF1): A master regulator of energy metabolism and of cell survival", *Biochimica et biophysica acta,* vol. 1857, no. 8, pp. 1167-1182.

Garcia-Bermudez, J., Sanchez-Arago, M., Soldevilla, B., Del Arco, A., Nuevo-Tapioles, C. & Cuezva, J.M. 2015, "PKA Phosphorylates the ATPase Inhibitory Factor 1 and Inactivates Its Capacity to Bind and Inhibit the Mitochondrial H(+)-ATP Synthase", *Cell reports,* vol. 12, no. 12, pp. 2143-2155.

Garesse, R. & Vallejo, C.G. 2001, "Animal mitochondrial biogenesis and function: a regulatory cross-talk between two genomes", *Gene,* vol. 263, no. 1-2, pp. 1-16.

Gibbons, C., Montgomery, M.G., Leslie, A.G. & Walker, J.E. 2000, "The structure of the central stalk in bovine F(1)-ATPase at 2.4 A resolution", *Nature structural biology,* vol. 7, no. 11, pp. 1055-1061.

Giorgio, V., Bisetto, E., Soriano, M.E., Dabbeni-Sala, F., Basso, E., Petronilli, V., Forte, M.A., Bernardi, P. & Lippe, G. 2009, "Cyclophilin D modulates mitochondrial F0F1-ATP synthase by interacting with the lateral stalk of the complex", *The Journal of biological chemistry,* vol. 284, no. 49, pp. 33982-33988.

Giorgio, V., Burchell, V., Schiavone, M., Bassot, C., Minervini, G., Petronilli, V., Argenton, F., Forte, M., Tosatto, S., Lippe, G. & Bernardi, P. 2017, "Ca(2+) binding to F-ATP synthase beta subunit triggers the mitochondrial permeability transition", *EMBO reports,* vol. 18, no. 7, pp. 1065-1076.

Giorgio, V., Guo, L., Bassot, C., Petronilli, V. & Bernardi, P. 2018, "Calcium and regulation of the mitochondrial permeability transition", *Cell calcium,* vol. 70, pp. 56-63.

Giorgio, V., von Stockum, S., Antoniel, M., Fabbro, A., Fogolari, F., Forte, M., Glick, G.D., Petronilli, V., Zoratti, M., Szabo, I., Lippe, G. & Bernardi, P. 2013, "Dimers of mitochondrial ATP synthase form the permeability transition pore", *Proceedings of the National Academy of Sciences of the United States of America,* vol. 110, no. 15, pp. 5887-5892.

Giraud, M.F., Paumard, P., Soubannier, V., Vaillier, J., Arselin, G., Salin, B., Schaeffer, J., Brethes, D., di Rago, J.P. & Velours, J. 2002, "Is there a relationship between the supramolecular organization of the mitochondrial ATP synthase and the formation of cristae?", *Biochimica et biophysica acta,* vol. 1555, no. 1-3, pp. 174-180.

Gledhill, J.R., Montgomery, M.G., Leslie, A.G. & Walker, J.E. 2007, "Mechanism of inhibition of bovine F1-ATPase by resveratrol and related polyphenols", *Proceedings of the National Academy of Sciences of the United States of America,* vol. 104, no. 34, pp. 13632-13637.

Gray, M.W. 2012, "Mitochondrial evolution", *Cold Spring Harbor perspectives in biology,* vol. 4, no. 9, pp. a011403.

Greggio, C., Jha, P., Kulkarni, S.S., Lagarrigue, S., Broskey, N.T., Boutant, M., Wang, X., Conde Alonso, S., Ofori, E., Auwerx, J., Canto, C. & Amati, F. 2017, "Enhanced Respiratory Chain Supercomplex Formation in Response to Exercise in Human Skeletal Muscle", *Cell metabolism,* vol. 25, no. 2, pp. 301-311.

Griffiths, E.J. & Halestrap, A.P. 1991, "Further evidence that cyclosporin A protects mitochondria from calcium overload by inhibiting a matrix peptidyl-prolyl cis-trans isomerase. Implications for the immunosuppressive and toxic

effects of cyclosporin", *The Biochemical journal,* vol. 274 (Pt 2), no. Pt 2, pp. 611-614.

Gu, J., Zhang, L., Zong, S., Guo, R., Liu, T., Yi, J., Wang, P., Zhuo, W. & Yang, M. 2019, "Cryo-EM structure of the mammalian ATP synthase tetramer bound with inhibitory protein IF1", *Science (New York, N.Y.),* vol. 364, no. 6445, pp. 1068-1075.

Guo, H., Bueler, S.A. & Rubinstein, J.L. 2017, "Atomic model for the dimeric FO region of mitochondrial ATP synthase", *Science (New York, N.Y.),* vol. 358, no. 6365, pp. 936-940.

Guo, H., Suzuki, T. & Rubinstein, J.L. 2019, "Structure of a bacterial ATP synthase", *eLife,* vol. 8, pp. 10.7554/eLife.43128.

Guo, L., Carraro, M., Carrer, A., Minervini, G., Urbani, A., Masgras, I., Tosatto, S.C.E., Szabo, I., Bernardi, P. & Lippe, G. 2019, "Arg-8 of yeast subunit e contributes to the stability of F-ATP synthase dimers and to the generation of the full-conductance mitochondrial megachannel", *The Journal of biological chemistry,* vol. 294, no. 28, pp. 10987-10997.

Guo, L., Carraro, M., Sartori, G., Minervini, G., Eriksson, O., Petronilli, V. & Bernardi, P. 2018, "Arginine 107 of yeast ATP synthase subunit g mediates sensitivity of the mitochondrial permeability transition to phenylglyoxal", *The Journal of biological chemistry,* vol. 293, no. 38, pp. 14632-14645.

Gutierrez-Aguilar, M., Douglas, D.L., Gibson, A.K., Domeier, T.L., Molkentin, J.D. & Baines, C.P. 2014, "Genetic manipulation of the cardiac mitochondrial phosphate carrier does not affect permeability transition", *Journal of Molecular and Cellular Cardiology,* vol. 72, pp. 316-325.

Habersetzer, J., Larrieu, I., Priault, M., Salin, B., Rossignol, R., Brethes, D. & Paumard, P. 2013, "Human F1F0 ATP synthase, mitochondrial ultrastructure and OXPHOS impairment: a (super-)complex matter?", *PloS one,* vol. 8, no. 10, pp. e75429.

Hackenbrock, C.R., Chazotte, B. & Gupte, S.S. 1986, "The random collision model and a critical assessment of diffusion and collision in mitochondrial electron transport", *Journal of Bioenergetics and Biomembranes,* vol. 18, no. 5, pp. 331-368.

Hahn, A., Parey, K., Bublitz, M., Mills, D.J., Zickermann, V., Vonck, J., Kuhlbrandt, W. & Meier, T. 2016, "Structure of a Complete ATP Synthase Dimer Reveals the Molecular Basis of Inner Mitochondrial Membrane Morphology", *Molecular cell,* vol. 63, no. 3, pp. 445-456.

Hahn, A., Vonck, J., Mills, D.J., Meier, T. & Kuhlbrandt, W. 2018, "Structure, mechanism, and regulation of the chloroplast ATP synthase", *Science (New York, N.Y.),* vol. 360, no. 6389, pp. 10.1126/science.aat4318.

Halestrap, A.P. & Davidson, A.M. 1990, "Inhibition of Ca2(+)-induced large-amplitude swelling of liver and heart mitochondria by cyclosporin is probably caused by the inhibitor binding to mitochondrial-matrix peptidyl-prolyl cis-trans isomerase and preventing it interacting with the adenine nucleotide translocase", *The Biochemical journal,* vol. 268, no. 1, pp. 153-160.

Hara, K.Y., Kato-Yamada, Y., Kikuchi, Y., Hisabori, T. & Yoshida, M. 2001, "The role of the betaDELSEED motif of F1-ATPase: propagation of the inhibitory effect of the epsilon subunit", *The Journal of biological chemistry,* vol. 276, no. 26, pp. 23969-23973.

Hashimoto, T., Negawa, Y. & Tagawa, K. 1981, "Binding of intrinsic ATPase inhibitor to mitochondrial ATPase--stoichiometry of binding of nucleotides, inhibitor, and enzyme", *Journal of Biochemistry,* vol. 90, no. 4, pp. 1151-1157.

Hauptmann, S., Scherping, I., Drose, S., Brandt, U., Schulz, K.L., Jendrach, M., Leuner, K., Eckert, A. & Muller, W.E. 2009, "Mitochondrial dysfunction: an early event in Alzheimer pathology accumulates with age in AD transgenic mice", *Neurobiology of aging,* vol. 30, no. 10, pp. 1574-1586.

Haworth, R.A. & Hunter, D.R. 2000, "Control of the mitochondrial permeability transition pore by high-affinity ADP binding at the ADP/ATP translocase in permeabilized mitochondria", *Journal of Bioenergetics and Biomembranes,* vol. 32, no. 1, pp. 91-96.

Haworth, R.A. & Hunter, D.R. 1979, "The Ca2+-induced membrane transition in mitochondria. II. Nature of the Ca2+ trigger site", *Archives of Biochemistry and Biophysics,* vol. 195, no. 2, pp. 460-467.

Haynes, V., Traaseth, N.J., Elfering, S., Fujisawa, Y. & Giulivi, C. 2010, "Nitration of specific tyrosines in FoF1 ATP synthase and activity loss in aging", *American journal of physiology.Endocrinology and metabolism,* vol. 298, no. 5, pp. E978-87.

He, J., Carroll, J., Ding, S., Fearnley, I.M. & Walker, J.E. 2017a, "Permeability transition in human mitochondria persists in the absence of peripheral stalk subunits of ATP synthase", *Proceedings of the National Academy of Sciences of the United States of America,* vol. 114, no. 34, pp. 9086-9091.

He, J., Ford, H.C., Carroll, J., Ding, S., Fearnley, I.M. & Walker, J.E. 2017b, "Persistence of the mitochondrial permeability transition in the absence of subunit c of human ATP synthase", *Proceedings of the National Academy of Sciences of the United States of America,* vol. 114, no. 13, pp. 3409-3414.

He, J., Ford, H.C., Carroll, J., Douglas, C., Gonzales, E., Ding, S., Fearnley, I.M. & Walker, J.E. 2018, "Assembly of the membrane domain of ATP synthase

in human mitochondria", *Proceedings of the National Academy of Sciences of the United States of America,* vol. 115, no. 12, pp. 2988-2993.

Herick, K., Kramer, R. & Luhring, H. 1997, "Patch clamp investigation into the phosphate carrier from Saccharomyces cerevisiae mitochondria", *Biochimica et biophysica acta,* vol. 1321, no. 3, pp. 207-220.

Hunter, D.R. & Haworth, R.A. 1979a, "The Ca2+-induced membrane transition in mitochondria. I. The protective mechanisms", *Archives of Biochemistry and Biophysics,* vol. 195, no. 2, pp. 453-459.

Hunter, D.R. & Haworth, R.A. 1979b, "The Ca2+-induced membrane transition in mitochondria. III. Transitional Ca2+ release", *Archives of Biochemistry and Biophysics,* vol. 195, no. 2, pp. 468-477.

Hunter, D.R., Haworth, R.A. & Southard, J.H. 1976, "Relationship between configuration, function, and permeability in calcium-treated mitochondria", *The Journal of biological chemistry,* vol. 251, no. 16, pp. 5069-5077.

Hurst, S., Hoek, J. & Sheu, S.S. 2017, "Mitochondrial Ca(2+) and regulation of the permeability transition pore", *Journal of Bioenergetics and Biomembranes,* vol. 49, no. 1, pp. 27-47.

Ichikawa, N., Ando, C. & Fumino, M. 2006, "Caenorhabditis elegans MAI-1 protein, which is similar to mitochondrial ATPase inhibitor (IF1), can inhibit yeast F0F1-ATPase but cannot be transported to yeast mitochondria", *Journal of Bioenergetics and Biomembranes,* vol. 38, no. 2, pp. 93-99.

Jiko, C., Davies, K.M., Shinzawa-Itoh, K., Tani, K., Maeda, S., Mills, D.J., Tsukihara, T., Fujiyoshi, Y., Kuhlbrandt, W. & Gerle, C. 2015, "Bovine F1Fo ATP synthase monomers bend the lipid bilayer in 2D membrane crystals", *eLife,* vol. 4, pp. e06119.

Johans, M., Milanesi, E., Franck, M., Johans, C., Liobikas, J., Panagiotaki, M., Greci, L., Principato, G., Kinnunen, P.K., Bernardi, P., Costantini, P. & Eriksson, O. 2005, "Modification of permeability transition pore arginine(s) by phenylglyoxal derivatives in isolated mitochondria and mammalian cells. Structure-function relationship of arginine ligands", *The Journal of biological chemistry,* vol. 280, no. 13, pp. 12130-12136.

Kabaleeswaran, V., Puri, N., Walker, J.E., Leslie, A.G. & Mueller, D.M. 2006, "Novel features of the rotary catalytic mechanism revealed in the structure of yeast F1 ATPase", *The EMBO journal,* vol. 25, no. 22, pp. 5433-5442.

Kaludercic, N. & Giorgio, V. 2016, "The Dual Function of Reactive Oxygen/Nitrogen Species in Bioenergetics and Cell Death: The Role of ATP Synthase", *Oxidative medicine and cellular longevity,* vol. 2016, pp. 3869610.

Karch, J., Bround, M.J., Khalil, H., Sargent, M.A., Latchman, N., Terada, N., Peixoto, P.M. & Molkentin, J.D. 2019, "Inhibition of mitochondrial permeability transition by deletion of the ANT family and CypD", *Science advances,* vol. 5, no. 8, pp. eaaw4597.

Kinnally, K.W., Campo, M.L. & Tedeschi, H. 1989, "Mitochondrial channel activity studied by patch-clamping mitoplasts", *Journal of Bioenergetics and Biomembranes,* vol. 21, no. 4, pp. 497-506.

Kinnally, K.W., Zorov, D.B., Antonenko, Y.N., Snyder, S.H., McEnery, M.W. & Tedeschi, H. 1993, "Mitochondrial benzodiazepine receptor linked to inner membrane ion channels by nanomolar actions of ligands", *Proceedings of the National Academy of Sciences of the United States of America,* vol. 90, no. 4, pp. 1374-1378.

Kokoszka, J.E., Waymire, K.G., Levy, S.E., Sligh, J.E., Cai, J., Jones, D.P., MacGregor, G.R. & Wallace, D.C. 2004, "The ADP/ATP translocator is not essential for the mitochondrial permeability transition pore", *Nature,* vol. 427, no. 6973, pp. 461-465.

Krauskopf, A., Eriksson, O., Craigen, W.J., Forte, M.A. & Bernardi, P. 2006, "Properties of the permeability transition in VDAC1(-/-) mitochondria", *Biochimica et biophysica acta,* vol. 1757, no. 5-6, pp. 590-595.

Kuhlbrandt, W. 2015, "Structure and function of mitochondrial membrane protein complexes", *BMC biology,* vol. 13, pp. 89-015-0201-x.

Kwong, J.Q., Davis, J., Baines, C.P., Sargent, M.A., Karch, J., Wang, X., Huang, T. & Molkentin, J.D. 2014, "Genetic deletion of the mitochondrial phosphate carrier desensitizes the mitochondrial permeability transition pore and causes cardiomyopathy", *Cell death and differentiation,* vol. 21, no. 8, pp. 1209-1217.

Lee, J., Ding, S., Walpole, T.B., Holding, A.N., Montgomery, M.G., Fearnley, I.M. & Walker, J.E. 2015, "Organization of Subunits in the Membrane Domain of the Bovine F-ATPase Revealed by Covalent Cross-linking", *The Journal of biological chemistry,* vol. 290, no. 21, pp. 13308-13320.

Lehmann, K. & Schmidt, U. 2003, "Group II introns: structure and catalytic versatility of large natural ribozymes", *Critical reviews in biochemistry and molecular biology,* vol. 38, no. 3, pp. 249-303.

Letts, J.A., Fiedorczuk, K. & Sazanov, L.A. 2016, "The architecture of respiratory supercomplexes", *Nature,* vol. 537, no. 7622, pp. 644-648.

Letts, J.A. & Sazanov, L.A. 2017, "Clarifying the supercomplex: the higher-order organization of the mitochondrial electron transport chain", *Nature structural & molecular biology,* vol. 24, no. 10, pp. 800-808.

Leung, A.W., Varanyuwatana, P. & Halestrap, A.P. 2008, "The mitochondrial phosphate carrier interacts with cyclophilin D and may play a key role in the permeability transition", *The Journal of biological chemistry,* vol. 283, no. 39, pp. 26312-26323.

Lightowlers, R.N., Chinnery, P.F., Turnbull, D.M. & Howell, N. 1997, "Mammalian mitochondrial genetics: heredity, heteroplasmy and disease", *Trends in genetics : TIG,* vol. 13, no. 11, pp. 450-455.

Linder, M.D., Morkunaite-Haimi, S., Kinnunen, P.K., Bernardi, P. & Eriksson, O. 2002, "Ligand-selective modulation of the permeability transition pore by arginine modification. Opposing effects of p-hydroxyphenylglyoxal and phenylglyoxal", *The Journal of biological chemistry,* vol. 277, no. 2, pp. 937-942.

Lippe, G., Coluccino, G., Zancani, M., Baratta, W. & Crusiz, P. 2019, "Mitochondrial F-ATP Synthase and Its Transition into an Energy-Dissipating Molecular Machine", *Oxidative medicine and cellular longevity,* vol. 2019, pp. 8743257.

Lobo-Jarne, T. & Ugalde, C. 2018, "Respiratory chain supercomplexes: Structures, function and biogenesis", *Seminars in cell & developmental biology,* vol. 76, pp. 179-190.

Lu, X., Kwong, J.Q., Molkentin, J.D. & Bers, D.M. 2016, "Individual Cardiac Mitochondria Undergo Rare Transient Permeability Transition Pore Openings", *Circulation research,* vol. 118, no. 5, pp. 834-841.

Luban, C., Beutel, M., Stahl, U. & Schmidt, U. 2005, "Systematic screening of nuclear encoded proteins involved in the splicing metabolism of group II introns in yeast mitochondria", *Gene,* vol. 354, pp. 72-79.

Maranzana, E., Barbero, G., Falasca, A.I., Lenaz, G. & Genova, M.L. 2013, "Mitochondrial respiratory supercomplex association limits production of reactive oxygen species from complex I", *Antioxidants & redox signaling,* vol. 19, no. 13, pp. 1469-1480.

Marzo, I., Brenner, C., Zamzami, N., Susin, S.A., Beutner, G., Brdiczka, D., Remy, R., Xie, Z.H., Reed, J.C. & Kroemer, G. 1998, "The permeability transition pore complex: a target for apoptosis regulation by caspases and bcl-2-related proteins", *The Journal of experimental medicine,* vol. 187, no. 8, pp. 1261-1271.

Masaike, T., Koyama-Horibe, F., Oiwa, K., Yoshida, M. & Nishizaka, T. 2008, "Cooperative three-step motions in catalytic subunits of F(1)-ATPase correlate with 80 degrees and 40 degrees substep rotations", *Nature structural & molecular biology,* vol. 15, no. 12, pp. 1326-1333.

Massari, S., Frigeri, L. & Azzone, G.F. 1972a, "A quantitative correlation between the kinetics of solutes and water translocation in Liver Mitochondria", *The Journal of membrane biology,* vol. 9, no. 1, pp. 71-82.

Massari, S., Frigeri, L. & Azzone, G.F. 1972b, "A quantitative correlation between the kinetics of solutes and water translocation in Liver Mitochondria", *The Journal of membrane biology,* vol. 9, no. 1, pp. 71-82.

McBride, H.M., Neuspiel, M. & Wasiak, S. 2006, "Mitochondria: more than just a powerhouse", *Current biology : CB,* vol. 16, no. 14, pp. R551-60.

McEnery, M.W., Snowman, A.M., Trifiletti, R.R. & Snyder, S.H. 1992, "Isolation of the mitochondrial benzodiazepine receptor: association with the voltage-dependent anion channel and the adenine nucleotide carrier", *Proceedings of the National Academy of Sciences of the United States of America,* vol. 89, no. 8, pp. 3170-3174.

McKenzie, M., Lazarou, M., Thorburn, D.R. & Ryan, M.T. 2006, "Mitochondrial respiratory chain supercomplexes are destabilized in Barth Syndrome patients", *Journal of Molecular Biology,* vol. 361, no. 3, pp. 462-469.

Menz, R.I., Walker, J.E. & Leslie, A.G. 2001, "Structure of bovine mitochondrial F(1)-ATPase with nucleotide bound to all three catalytic sites: implications for the mechanism of rotary catalysis", *Cell,* vol. 106, no. 3, pp. 331-341.

Milenkovic, D., Blaza, J.N., Larsson, N.G. & Hirst, J. 2017, "The Enigma of the Respiratory Chain Supercomplex", *Cell metabolism,* vol. 25, no. 4, pp. 765-776.

Milenkovic, D., Muller, J., Stojanovski, D., Pfanner, N. & Chacinska, A. 2007, "Diverse mechanisms and machineries for import of mitochondrial proteins", *Biological chemistry,* vol. 388, no. 9, pp. 891-897.

Mitchell, P. 1979, "Keilin's respiratory chain concept and its chemiosmotic consequences", *Science (New York, N.Y.),* vol. 206, no. 4423, pp. 1148-1159.

MITCHELL, P. 1961, "Coupling of phosphorylation to electron and hydrogen transfer by a chemi-osmotic type of mechanism", *Nature,* vol. 191, pp. 144-148.

Nakagawa, T., Shimizu, S., Watanabe, T., Yamaguchi, O., Otsu, K., Yamagata, H., Inohara, H., Kubo, T. & Tsujimoto, Y. 2005, "Cyclophilin D-dependent mitochondrial permeability transition regulates some necrotic but not apoptotic cell death", *Nature,* vol. 434, no. 7033, pp. 652-658.

Nathanson, L. & Gromet-Elhanan, Z. 2000, "Mutations in the beta-subunit Thr(159) and Glu(184) of the Rhodospirillum rubrum F(0)F(1) ATP synthase reveal differences in ligands for the coupled Mg(2+)- and decoupled Ca(2+)-

dependent F(0)F(1) activities", *The Journal of biological chemistry,* vol. 275, no. 2, pp. 901-905.

Neginskaya, M.A., Solesio, M.E., Berezhnaya, E.V., Amodeo, G.F., Mnatsakanyan, N., Jonas, E.A. & Pavlov, E.V. 2019, "ATP Synthase C-Subunit-Deficient Mitochondria Have a Small Cyclosporine A-Sensitive Channel, but Lack the Permeability Transition Pore", *Cell reports,* vol. 26, no. 1, pp. 11-17.e2.

Nesci, S., Trombetti, F., Algieri, C. & Pagliarani, A. 2019, "A Therapeutic Role for the F1FO-ATP Synthase", *SLAS discovery : advancing life sciences R & D,* vol. 24, no. 9, pp. 893-903.

Nesci, S., Trombetti, F., Ventrella, V. & Pagliarani, A. 2017, "Post-translational modifications of the mitochondrial F1FO-ATPase", *Biochimica et biophysica acta.General subjects,* vol. 1861, no. 11 Pt A, pp. 2902-2912.

Nicolli, A., Basso, E., Petronilli, V., Wenger, R.M. & Bernardi, P. 1996, "Interactions of cyclophilin with the mitochondrial inner membrane and regulation of the permeability transition pore, and cyclosporin A-sensitive channel", *The Journal of biological chemistry,* vol. 271, no. 4, pp. 2185-2192.

Nicolli, A., Petronilli, V. & Bernardi, P. 1993, "Modulation of the mitochondrial cyclosporin A-sensitive permeability transition pore by matrix pH. Evidence that the pore open-closed probability is regulated by reversible histidine protonation", *Biochemistry,* vol. 32, no. 16, pp. 4461-4465.

Noji, H., Ueno, H. & McMillan, D.G.G. 2017, "Catalytic robustness and torque generation of the F1-ATPase", *Biophysical reviews,* vol. 9, no. 2, pp. 103-118.

Norling, B., Tourikas, C., Hamasur, B. & Glaser, E. 1990, "Evidence for an endogenous ATPase inhibitor protein in plant mitochondria. Purification and characterization", *European journal of biochemistry,* vol. 188, no. 2, pp. 247-252.

Nosek, J. & Tomaska, L. 2003, "Mitochondrial genome diversity: evolution of the molecular architecture and replication strategy", *Current genetics,* vol. 44, no. 2, pp. 73-84.

Notredame, C., Higgins, D.G. & Heringa, J. 2000, "T-Coffee: A novel method for fast and accurate multiple sequence alignment", *Journal of Molecular Biology,* vol. 302, no. 1, pp. 205-217.

Nunnari, J. & Suomalainen, A. 2012, "Mitochondria: in sickness and in health", *Cell,* vol. 148, no. 6, pp. 1145-1159.

O'Brien, T.W. 2003, "Properties of human mitochondrial ribosomes", *IUBMB life,* vol. 55, no. 9, pp. 505-513.

Orriss, G.L., Leslie, A.G., Braig, K. & Walker, J.E. 1998, "Bovine F1-ATPase covalently inhibited with 4-chloro-7-nitrobenzofurazan: the structure provides further support for a rotary catalytic mechanism", *Structure (London, England : 1993),* vol. 6, no. 7, pp. 831-837.

Papageorgiou, S., Melandri, A.B. & Solaini, G. 1998, "Relevance of divalent cations to ATP-driven proton pumping in beef heart mitochondrial F0F1-ATPase", *Journal of Bioenergetics and Biomembranes,* vol. 30, no. 6, pp. 533-541.

Pastorino, J.G., Snyder, J.W., Serroni, A., Hoek, J.B. & Farber, J.L. 1993, "Cyclosporin and carnitine prevent the anoxic death of cultured hepatocytes by inhibiting the mitochondrial permeability transition", *The Journal of biological chemistry,* vol. 268, no. 19, pp. 13791-13798.

Paumard, P., Vaillier, J., Coulary, B., Schaeffer, J., Soubannier, V., Mueller, D.M., Brethes, D., di Rago, J.P. & Velours, J. 2002, "The ATP synthase is involved in generating mitochondrial cristae morphology", *The EMBO journal,* vol. 21, no. 3, pp. 221-230.

Pernas, L. & Scorrano, L. 2016, "Mito-Morphosis: Mitochondrial Fusion, Fission, and Cristae Remodeling as Key Mediators of Cellular Function", *Annual Review of Physiology,* vol. 78, pp. 505-531.

Petronilli, V., Cola, C., Massari, S., Colonna, R. & Bernardi, P. 1993, "Physiological effectors modify voltage sensing by the cyclosporin A-sensitive permeability transition pore of mitochondria", *The Journal of biological chemistry,* vol. 268, no. 29, pp. 21939-21945.

Petronilli, V., Miotto, G., Canton, M., Brini, M., Colonna, R., Bernardi, P. & Di Lisa, F. 1999, "Transient and long-lasting openings of the mitochondrial permeability transition pore can be monitored directly in intact cells by changes in mitochondrial calcein fluorescence", *Biophysical journal,* vol. 76, no. 2, pp. 725-734.

Petronilli, V., Penzo, D., Scorrano, L., Bernardi, P. & Di Lisa, F. 2001, "The mitochondrial permeability transition, release of cytochrome c and cell death. Correlation with the duration of pore openings in situ", *The Journal of biological chemistry,* vol. 276, no. 15, pp. 12030-12034.

Petronilli, V., Szabo, I. & Zoratti, M. 1989, "The inner mitochondrial membrane contains ion-conducting channels similar to those found in bacteria", *FEBS letters,* vol. 259, no. 1, pp. 137-143.

Piovesan, D., Minervini, G. & Tosatto, S.C. 2016, "The RING 2.0 web server for high quality residue interaction networks", *Nucleic acids research,* vol. 44, no. W1, pp. W367-74.

Pogoryelov, D., Yildiz, O., Faraldo-Gomez, J.D. & Meier, T. 2009, "High-resolution structure of the rotor ring of a proton-dependent ATP synthase", *Nature structural & molecular biology,* vol. 16, no. 10, pp. 1068-1073.

PULLMAN, M.E. & MONROY, G.C. 1963, "A Naturally Occurring Inhibitor of Mitochondrial Adenosine Triphosphatase", *The Journal of biological chemistry,* vol. 238, pp. 3762-3769.

RAAFLAUB, J. 1953a, "Mechanism of adenosinetriphosphate as cofactor of isolated mitochondria", *Helvetica physiologica et pharmacologica acta,* vol. 11, no. 2, pp. 157-165.

RAAFLAUB, J. 1953b, "Swelling of isolated mitochondria of the liver and their susceptibility to physicochemical influences", *Helvetica physiologica et pharmacologica acta,* vol. 11, no. 2, pp. 142-156.

Rabl, R., Soubannier, V., Scholz, R., Vogel, F., Mendl, N., Vasiljev-Neumeyer, A., Korner, C., Jagasia, R., Keil, T., Baumeister, W., Cyrklaff, M., Neupert, W. & Reichert, A.S. 2009, "Formation of cristae and crista junctions in mitochondria depends on antagonism between Fcj1 and Su e/g", *The Journal of cell biology,* vol. 185, no. 6, pp. 1047-1063.

Rampelt, H., Zerbes, R.M., van der Laan, M. & Pfanner, N. 2017, "Role of the mitochondrial contact site and cristae organizing system in membrane architecture and dynamics", *Biochimica et biophysica acta.Molecular cell research,* vol. 1864, no. 4, pp. 737-746.

Rasola, A. & Bernardi, P. 2007, "The mitochondrial permeability transition pore and its involvement in cell death and in disease pathogenesis", *Apoptosis : An International Journal on Programmed Cell Death,* vol. 12, no. 5, pp. 815-833.

Rees, D.M., Montgomery, M.G., Leslie, A.G. & Walker, J.E. 2012, "Structural evidence of a new catalytic intermediate in the pathway of ATP hydrolysis by F1-ATPase from bovine heart mitochondria", *Proceedings of the National Academy of Sciences of the United States of America,* vol. 109, no. 28, pp. 11139-11143.

Roudeau, S., Spannagel, C., Vaillier, J., Arselin, G., Graves, P.V. & Velours, J. 1999, "Subunit f of the yeast mitochondrial ATP synthase: topological and functional studies", *Journal of Bioenergetics and Biomembranes,* vol. 31, no. 2, pp. 85-94.

Sagan, L. 1967, "On the origin of mitosing cells", *Journal of theoretical biology,* vol. 14, no. 3, pp. 255-274.

Sanjana, N.E., Shalem, O. & Zhang, F. 2014, "Improved vectors and genome-wide libraries for CRISPR screening", *Nature methods,* vol. 11, no. 8, pp. 783-784.

Schagger, H., de Coo, R., Bauer, M.F., Hofmann, S., Godinot, C. & Brandt, U. 2004, "Significance of respirasomes for the assembly/stability of human respiratory chain complex I", *The Journal of biological chemistry,* vol. 279, no. 35, pp. 36349-36353.

Schagger, H. & Pfeiffer, K. 2000, "Supercomplexes in the respiratory chains of yeast and mammalian mitochondria", *The EMBO journal,* vol. 19, no. 8, pp. 1777-1783.

Schinzel, A.C., Takeuchi, O., Huang, Z., Fisher, J.K., Zhou, Z., Rubens, J., Hetz, C., Danial, N.N., Moskowitz, M.A. & Korsmeyer, S.J. 2005, "Cyclophilin D is a component of mitochondrial permeability transition and mediates neuronal cell death after focal cerebral ischemia", *Proceedings of the National Academy of Sciences of the United States of America,* vol. 102, no. 34, pp. 12005-12010.

Schnizer, R., Van Heeke, G., Amaturo, D. & Schuster, S.M. 1996, "Histidine-49 is necessary for the pH-dependent transition between active and inactive states of the bovine F1-ATPase inhibitor protein", *Biochimica et biophysica acta,* vol. 1292, no. 2, pp. 241-248.

Scott, I. & Youle, R.J. 2010, "Mitochondrial fission and fusion", *Essays in biochemistry,* vol. 47, pp. 85-98.

Sileikyte, J., Blachly-Dyson, E., Sewell, R., Carpi, A., Menabo, R., Di Lisa, F., Ricchelli, F., Bernardi, P. & Forte, M. 2014, "Regulation of the mitochondrial permeability transition pore by the outer membrane does not involve the peripheral benzodiazepine receptor (Translocator Protein of 18 kDa (TSPO))", *The Journal of biological chemistry,* vol. 289, no. 20, pp. 13769-13781.

Skoczen, N., Dautant, A., Binko, K., Godard, F., Bouhier, M., Su, X., Lasserre, J.P., Giraud, M.F., Tribouillard-Tanvier, D., Chen, H., di Rago, J.P. & Kucharczyk, R. 2018, "Molecular basis of diseases caused by the mtDNA mutation m.8969G>A in the subunit a of ATP synthase", *Biochimica et biophysica acta.Bioenergetics,* vol. 1859, no. 8, pp. 602-611.

Spannagel, C., Vaillier, J., Arselin, G., Graves, P.V. & Velours, J. 1997, "The subunit f of mitochondrial yeast ATP synthase--characterization of the protein and disruption of the structural gene ATP17", *European journal of biochemistry,* vol. 247, no. 3, pp. 1111-1117.

Spinelli, J.B. & Haigis, M.C. 2018, "The multifaceted contributions of mitochondria to cellular metabolism", *Nature cell biology,* vol. 20, no. 7, pp. 745-754.

Srivastava, A.P., Luo, M., Zhou, W., Symersky, J., Bai, D., Chambers, M.G., Faraldo-Gomez, J.D., Liao, M. & Mueller, D.M. 2018, "High-resolution cryo-EM analysis of the yeast ATP synthase in a lipid membrane", *Science (New York, N.Y.),* vol. 360, no. 6389, pp. 10.1126/science.aas9699. Epub 2018 Apr 12.

Stephens, A.N., Nagley, P. & Devenish, R.J. 2003, "Each yeast mitochondrial F1F0-ATP synthase complex contains a single copy of subunit 8", *Biochimica et biophysica acta,* vol. 1607, no. 2-3, pp. 181-189.

Stock, D., Leslie, A.G. & Walker, J.E. 1999, "Molecular architecture of the rotary motor in ATP synthase", *Science (New York, N.Y.),* vol. 286, no. 5445, pp. 1700-1705.

Strauss, M., Hofhaus, G., Schroder, R.R. & Kuhlbrandt, W. 2008, "Dimer ribbons of ATP synthase shape the inner mitochondrial membrane", *The EMBO journal,* vol. 27, no. 7, pp. 1154-1160.

Suzuki, T., Tanaka, K., Wakabayashi, C., Saita, E. & Yoshida, M. 2014, "Chemomechanical coupling of human mitochondrial F1-ATPase motor", *Nature chemical biology,* vol. 10, no. 11, pp. 930-936.

Symersky, J., Pagadala, V., Osowski, D., Krah, A., Meier, T., Faraldo-Gomez, J.D. & Mueller, D.M. 2012, "Structure of the c(10) ring of the yeast mitochondrial ATP synthase in the open conformation", *Nature structural & molecular biology,* vol. 19, no. 5, pp. 485-91, S1.

Szabo, I., Bernardi, P. & Zoratti, M. 1992, "Modulation of the mitochondrial megachannel by divalent cations and protons", *The Journal of biological chemistry,* vol. 267, no. 5, pp. 2940-2946.

Szabo, I., Bock, J., Jekle, A., Soddemann, M., Adams, C., Lang, F., Zoratti, M. & Gulbins, E. 2005, "A novel potassium channel in lymphocyte mitochondria", *The Journal of biological chemistry,* vol. 280, no. 13, pp. 12790-12798.

Szabo, I., De Pinto, V. & Zoratti, M. 1993, "The mitochondrial permeability transition pore may comprise VDAC molecules. II. The electrophysiological properties of VDAC are compatible with those of the mitochondrial megachannel", *FEBS letters,* vol. 330, no. 2, pp. 206-210.

Szabo, I. & Zoratti, M. 2014, "Mitochondrial channels: ion fluxes and more", *Physiological Reviews,* vol. 94, no. 2, pp. 519-608.

Szendroedi, J., Phielix, E. & Roden, M. 2011, "The role of mitochondria in insulin resistance and type 2 diabetes mellitus", *Nature reviews.Endocrinology,* vol. 8, no. 2, pp. 92-103.

Tait, S.W. & Green, D.R. 2012, "Mitochondria and cell signalling", *Journal of cell science,* vol. 125, no. Pt 4, pp. 807-815.

Tetaud, E., Godard, F., Giraud, M.F., Ackerman, S.H. & di Rago, J.P. 2014, "The depletion of F(1) subunit epsilon in yeast leads to an uncoupled respiratory phenotype that is rescued by mutations in the proton-translocating subunits of F(0)", *Molecular biology of the cell,* vol. 25, no. 6, pp. 791-799.

Tomasetig, L., Di Pancrazio, F., Harris, D.A., Mavelli, I. & Lippe, G. 2002, "Dimerization of F0F1ATP synthase from bovine heart is independent from the binding of the inhibitor protein IF1", *Biochimica et biophysica acta,* vol. 1556, no. 2-3, pp. 133-141.

Urbani, A., Giorgio, V., Carrer, A., Franchin, C., Arrigoni, C., Jiko, C., Abe, K., Maeda, S., Shinzawa-Itoh, K., Bogers, J.F.M., McMillan, D.G.G., Gerle, C. & Szabò, I., & Bernardi, P., 2019, "The molecular identity of the mitochondrial megachannel (MMC)/permeability transition pore (PTP), a key effector of cell death, remains controversial. By combining highly purified, fully active bovine F-ATP synthase with preformed liposomes we show that Ca2+ dissipates the H+ gradient generated by ATP hydrolysis. After incorporation of the same preparation into planar lipid bilayers Ca2+ elicits currents matching those of the MMC/PTP. Currents were fully reversible, were stabilized by benzodiazepine 423, a ligand of the OSCP subunit of F-ATP synthase that activates the MMC/PTP, and were inhibited by Mg2+ and adenine nucleotides, which also inhibit the PTP. Channel activity was insensitive to inhibitors of the adenine nucleotide translocase (ANT) and of the voltage-dependent anion channel (VDAC). Native gel-purified oligomers and dimers, but not monomers, gave rise to channel activity. These findings resolve the long-standing mystery of the MMC/PTP and demonstrate that Ca2+ can transform the energy-conserving F-ATP synthase into an energy-dissipating device.", *nature communication,* vol. 10.

Varanyuwatana, P. & Halestrap, A.P. 2012, "The roles of phosphate and the phosphate carrier in the mitochondrial permeability transition pore", *Mitochondrion,* vol. 12, no. 1, pp. 120-125.

Vassilopoulos, A., Pennington, J.D., Andresson, T., Rees, D.M., Bosley, A.D., Fearnley, I.M., Ham, A., Flynn, C.R., Hill, S., Rose, K.L., Kim, H.S., Deng, C.X., Walker, J.E. & Gius, D. 2014, "SIRT3 deacetylates ATP synthase F1 complex proteins in response to nutrient- and exercise-induced stress", *Antioxidants & redox signaling,* vol. 21, no. 4, pp. 551-564.

Velours, J., Dautant, A., Salin, B., Sagot, I. & Brethes, D. 2009, "Mitochondrial F1F0-ATP synthase and organellar internal architecture", *The international journal of biochemistry & cell biology,* vol. 41, no. 10, pp. 1783-1789.

Velours, J., Spannagel, C., Chaignepain, S., Vaillier, J., Arselin, G., Graves, P.V., Velours, G. & Camougrand, N. 1998, "Topography of the yeast ATP synthase F0 sector", *Biochimie,* vol. 80, no. 10, pp. 793-801.

von Stockum, S., Giorgio, V., Trevisan, E., Lippe, G., Glick, G.D., Forte, M.A., Da-Re, C., Checchetto, V., Mazzotta, G., Costa, R., Szabo, I. & Bernardi, P.

2015, "F-ATPase of Drosophila melanogaster forms 53-picosiemen (53-pS) channels responsible for mitochondrial Ca2+-induced Ca2+ release", *The Journal of biological chemistry,* vol. 290, no. 8, pp. 4537-4544.

Walker, J.E. 2013, "The ATP synthase: the understood, the uncertain and the unknown", *Biochemical Society transactions,* vol. 41, no. 1, pp. 1-16.

Walker, J.E., Fearnley, I.M., Gay, N.J., Gibson, B.W., Northrop, F.D., Powell, S.J., Runswick, M.J., Saraste, M. & Tybulewicz, V.L. 1985, "Primary structure and subunit stoichiometry of F1-ATPase from bovine mitochondria", *Journal of Molecular Biology,* vol. 184, no. 4, pp. 677-701.

Walker, J.E., Saraste, M., Runswick, M.J. & Gay, N.J. 1982, "Distantly related sequences in the alpha- and beta-subunits of ATP synthase, myosin, kinases and other ATP-requiring enzymes and a common nucleotide binding fold", *The EMBO journal,* vol. 1, no. 8, pp. 945-951.

Watanabe, R., Genda, M., Kato-Yamada, Y. & Noji, H. 2018, "Essential Role of the epsilon Subunit for Reversible Chemo-Mechanical Coupling in F1-ATPase", *Biophysical journal,* vol. 114, no. 1, pp. 178-187.

Waterhouse, A.M., Procter, J.B., Martin, D.M., Clamp, M. & Barton, G.J. 2009, "Jalview Version 2--a multiple sequence alignment editor and analysis workbench", *Bioinformatics (Oxford, England),* vol. 25, no. 9, pp. 1189-1191.

Weber, J. & Senior, A.E. 1996, "F1F0-ATP synthase: development of direct optical probes of the catalytic mechanism", *Biochimica et biophysica acta,* vol. 1275, no. 1-2, pp. 101-104.

Wen, S., Niedzwiecka, K., Zhao, W., Xu, S., Liang, S., Zhu, X., Xie, H., Tribouillard-Tanvier, D., Giraud, M.F., Zeng, C., Dautant, A., Kucharczyk, R., Liu, Z., di Rago, J.P. & Chen, H. 2016, "Identification of G8969>A in mitochondrial ATP6 gene that severely compromises ATP synthase function in a patient with IgA nephropathy", *Scientific reports,* vol. 6, pp. 36313.

Winklhofer, K.F. & Haass, C. 2010, "Mitochondrial dysfunction in Parkinson's disease", *Biochimica et biophysica acta,* vol. 1802, no. 1, pp. 29-44.

Wittig, I., Meyer, B., Heide, H., Steger, M., Bleier, L., Wumaier, Z., Karas, M. & Schagger, H. 2010, "Assembly and oligomerization of human ATP synthase lacking mitochondrial subunits a and A6L", *Biochimica et biophysica acta,* vol. 1797, no. 6-7, pp. 1004-1011.

Wittig, I. & Schagger, H. 2008, "Structural organization of mitochondrial ATP synthase", *Biochimica et biophysica acta,* vol. 1777, no. 7-8, pp. 592-598.

Wu, Y.T., Lee, H.C., Liao, C.C. & Wei, Y.H. 2013, "Regulation of mitochondrial F(o)F(1)ATPase activity by Sirt3-catalyzed deacetylation and its deficiency

in human cells harboring 4977bp deletion of mitochondrial DNA", *Biochimica et biophysica acta,* vol. 1832, no. 1, pp. 216-227.

Yang, W., Nagasawa, K., Munch, C., Xu, Y., Satterstrom, K., Jeong, S., Hayes, S.D., Jedrychowski, M.P., Vyas, F.S., Zaganjor, E., Guarani, V., Ringel, A.E., Gygi, S.P., Harper, J.W. & Haigis, M.C. 2016, "Mitochondrial Sirtuin Network Reveals Dynamic SIRT3-Dependent Deacetylation in Response to Membrane Depolarization", *Cell,* vol. 167, no. 4, pp. 985-1000.e21.

Yasuda, R., Noji, H., Kinosita, K.,Jr & Yoshida, M. 1998, "F1-ATPase is a highly efficient molecular motor that rotates with discrete 120 degree steps", *Cell,* vol. 93, no. 7, pp. 1117-1124.

Zhou, W., Marinelli, F., Nief, C. & Faraldo-Gomez, J.D. 2017, "Atomistic simulations indicate the c-subunit ring of the F1Fo ATP synthase is not the mitochondrial permeability transition pore", *eLife,* vol. 6, pp. 10.7554/eLife.23781.

Zulian, A., Schiavone, M., Giorgio, V. & Bernardi, P. 2016, "Forty years later: Mitochondria as therapeutic targets in muscle diseases", *Pharmacological research,* vol. 113, no. Pt A, pp. 563-573.